Illinois U Library

The American Mineralogist

Journal of the Mineralogical Society of America

Vol. 35 **MAY-JUNE 1950** **Nos. 5 and 6**

Contents

Contributions to Canadian Mineralogy

Volume 5, Part 2

Sponsored by The Walker Mineralogical Club

Edited by M. A. Peacock, *Toronto*

Description and synthesis of the selenide minerals............J. W. Earley 337
On pseudomalachite and cornetite..........................L. G. Berry 365
X-ray diffraction data on some radioactive oxide minerals...Ronald J. Arnott 386
Metamict pitchblende from Goldfields, Saskatchewan, and observations on some ignited pitchblendes.......C. E. B. Conybeare and R. B. Ferguson 401
An electron microscopic examination of synthetic tourmaline crystals..........William H. Barnes 407
A roentgenographic method for determining plagioclases.....Fernand Claisse 412
A new method for measuring the refractive indices in micaceous minerals..........J. P. Girault 421
On parkerite and shandite and the crystal structure of $Ni_3Pb_2S_2$..........M. A. Peacock and John McAndrew 425
Hauchecornite..........M. A. Peacock 440
Crystal properties of copper (II) and nickel (II) chloride coordination complexes with diethylenetriamine..........A. G. Brook 447
Notes and news:
  Mineral occurrences in western Canada..............R. M. Thompson 451
  The probable non-existence of alaskaite..............R. M. Thompson 456
  Hydrocarbon with cinnabar in British Columbia........K. DeP. Watson 457
  Red gold from the San Antonio gold mine, Bissett, Manitoba..........R. B. Ferguson 459
The Walker Mineralogical Club.. 461

EDITOR
WALTER F. HUNT
ASSOCIATE EDITORS
MICHAEL FLEISCHER, ESPER S. LARSEN,
AUSTIN F. ROGERS, M. N. SHORT AND GEORGE TUNELL

Published bi-monthly by the Society

Mineralogical Society of America

ASSOCIATED WITH THE GEOLOGICAL SOCIETY OF AMERICA

President: **George Tunell**, University of California at Los Angeles, California.
Vice President: **Ralph E. Grim**, Illinois Geological Survey, Urbana, Illinois.
Secretary: **C. S. Hurlbut, Jr.**, Harvard University, Cambridge, Massachusetts.
Treasurer: **Earl Ingerson**, U. S. Geological Survey, Washington 25, D.C.
Editor: **Walter F. Hunt**, University of Michigan, Ann Arbor, Michigan.
Councilors: **H. H. Hess**, Princeton University, Princeton, New Jersey.
Clifford Frondel, Harvard University, Cambridge, Massachusetts.
Lewis S. Ramsdell, University of Michigan, Ann Arbor, Michigan.
E. F. Osborn, School of Mineral Industries, Pennsylvania State College, Pennsylvania.
John W. Gruner, University of Minnesota, Minneapolis, Minnesota.

The enlarged issues of this journal for 1950 are made possible by a grant from the Penrose Fund of the Geological Society of America.

The American Mineralogist—Journal of the Mineralogical Society of America

A journal containing articles on mineralogy, crystallography, petrography, and allied sciences, issued every two months. Contributions are invited from everyone.

Office of Publication, Mineralogical Laboratory, Ann Arbor, Mich.

The general conduct of the journal is in the hands of the Editor, **Walter F. Hunt**, Ann Arbor, Michigan. The council of the Mineralogical Society has appointed the following board of associate editors, to whom should be sent articles dealing with the special subjects indicated:

Michael Fleischer, U. S. Geological Survey, Washington, D.C., *New minerals.*
Esper S. Larsen, U. S. Geological Survey, Washington, D.C., *Optical crystallography.*
Austin F. Rogers, Stanford University, California, *Geometrical crystallography.*
M. N. Short, University of Arizona, Tucson, Arizona, *Mineralography.*
George Tunell, University of California at Los Angeles, *Structural crystallography.*

Contributors of leading articles are given without charge 100 reprints (without covers) of their article. If additional reprints are desired these can be purchased at the following rates:

Pages	*1–4*	*5–8*	*9–12*	*13–16*	*17–20*	*21–24*	*25–28*	*29–32*	*Covers*
Copies									
25	$3.50	$5.00	$ 8.00	$ 9.50	$11.00	$13.00	$15.00	$16.00	$4.90
50	3.80	5.55	8.80	10.40	12.10	14.20	16.40	17.50	5.50
75	4.10	6.10	9.60	11.30	13.20	15.40	17.80	19.00	6.10
100	4.40	6.65	10.40	12.20	14.30	16.60	19.20	20.50	6.70
Addl. C's	1.20	2.20	3.20	3.60	4.40	4.80	5.60	6.00	2.40

Cover Composition $1.55.

Sent to all members and fellows of the Mineralogical Society of America. Subscription price, $4.00 per year (single copies of normal issues, $1.00 plus postage).

Entered as second class matter at the post office at Menasha, Wis., under Act of March 3, 1879. Acceptance for mailing at the special rate of postage provided for in section 1103, Act of Oct. 3, 1917, paragraph 4 section 429 P. L. & R. authorized March 13, 1922.

Notices of change of address, orders, and remittances should be sent to Dr. Earl Ingerson, U.S. Geological Survey, Washington 25, D. C.

Printed by the George Banta Publishing Company, Menasha, Wisconsin

THE AMERICAN MINERALOGIST
JOURNAL OF THE MINERALOGICAL SOCIETY OF AMERICA

Vol. 35 MAY–JUNE, 1950 Nos. 5 and 6

Contributions to Canadian Mineralogy

Volume 5, Part 2

Sponsored by **The Walker Mineralogical Club**
Edited by **M. A. Peacock,** *Toronto*

DESCRIPTION AND SYNTHESIS OF THE SELENIDE MINERALS*

J. W. EARLEY
Gulf Research & Development Company, Pittsburgh, Pennsylvania

CONTENTS

Abstract. 338
Introduction. 338
Methods of Study. 338
Material and Acknowledgments. 340
Mineral Descriptions and Syntheses. 340
  Naumannite. 340
  Aguilarite. 343
  Eucairite. 345
  Crookesite. 347
  Berzelianite. 351
  Umangite. 354
  Clausthalite. 356
  Tiemannite. 358
  Klockmannite. 360
  Penroseite. 360
    Other Selenides. 362
  Guanajuatite. 362
  Paraguanajuatite. 362
Classification. 362
References. 364

---

* Contributions to Mineralogy from the Department of Geological Sciences, University of Toronto, 1950, no. 1.

Extracted from a thesis to be submitted for the degree of Ph.D., *University of Toronto* (Toronto, Canada). Published with the permission of the Research Council of Ontario and the Gulf Research & Development Company.

ABSTRACT

A study of natural and artificial selenides, mainly by microscopic and x-ray methods, has led to revised descriptions of the selenide minerals. The mineral descriptions contain some new measurements of specific gravity, new unit cell dimensions (notably for eucairite, crookesite, and umangite), together with x-ray powder data for all the species and reproductions of the patterns. The classification of the selenides given in Dana (1944) is modified by the addition of a tetragonal group to the A_2X type, and the recognition of an $A_{2-x}X$ type.

INTRODUCTION

In 1818 Berzelius (Dana, 1944, p. 182) announced the discovery of the new element selenium simultaneously with the recognition of two selenide minerals now known as berzelianite and eucairite. Most of the additional selenide minerals known today were recognized and briefly described in the following three decades, and relatively little has been added to the knowledge of these minerals in the past century.

The telluride minerals, recently described by Thompson (1949), are rare and little known as compared to the sulphides, and the selenides bear a similar relation to the tellurides. As a group, the selenides are exceedingly uncommon in occurrence and they appear almost invariably in minute amounts, entirely lacking in crystal form, and intimately associated with various selenides and other ores. In consequence the crystallographic information is particularly incomplete on these minerals and their physical and chemical properties are not well known.

The known localities for the selenide minerals are primarily Skrikerum (Sweden), Harz Mountains (Germany), and Sierra de Umango (Argentina). Although the element selenium is recovered in notable quantities from the smelters at Sudbury and Noranda, the source of the selenium is not known. In 1949 Dr. E. W. Nuffield, University of Toronto, noted clausthalite, PbSe, in a suite of ore specimens from Theano Point (Ontario), and Mr. S. Kaiman, Bureau of Mines, Ottawa, has identified selenide minerals in ore specimens from Lake Athabaska (Northwest Territories); but beyond these occurrences nothing is known of the distribution of selenide minerals in Canada.

METHODS OF STUDY

The study of each mineral commenced with a macroscopic examination of hand specimens. This, coupled with a binocular-microscopic study, disclosed such physical properties as colour on fresh and tarnished surfaces, cleavage, fracture, hardness, and tenacity. Where possible, single crystal fragments were carefully chosen for specific gravity determinations using the Berman balance. A fragment or group of fragments weighing from 10–20 milligrams gave the most satisfactory results.

Since all selenide minerals are opaque, polished sections of each mineral were prepared for microscopic study in reflected light. This examination revealed such properties as colour, reflection pleochroism, polarization effects, and the Talmadge hardness estimated with a needle. In addition, the polished mineral surfaces were treated with standard etching reagents as used by Short (1940).

To obtain specific crystallographic information it was necessary, except with the cubic species, to use single crystal x-ray methods which yielded the symmetry and dimensions of the unit cell. With the selenides, which rarely show crystal form or display good cleavage, the search for a suitable single crystal is a long and tedious and sometimes fruitless procedure. Fragments showing only one or two poorly developed faces were oriented crystallographically as well as possible, firstly, using the optical goniometer and secondly by a series of rotation photographs coupled with minor adjustments of the x-ray goniometer head. The cell dimensions in kX units ($\lambda \text{Cu}K\alpha_1 = 1.5374$ kX) and the measured specific gravity of the mineral, with the mass factor 1.650, gave the molecular weight of the cell contents and in turn the calculated density. To complete the mineral description an x-ray powder pattern was taken as a "fingerprint" of the species. The tabulated powder data include the observed relative intensities and glancing angles for $\text{Cu}K\alpha_1$ radiation, together with the measured spacings, in kX, and when possible the indices of the powder lines and the calculated spacings, establishing a standard x-ray powder pattern with every line accounted for or proved to be extraneous. These standard patterns served to compare known and doubtful materials, and to identify unknown materials.

Since the selenides often occur in small amounts, closely associated with other selenides, sulphides, and their alteration products, it is often difficult to identify with certainty the rarer species using standard microscopic methods, and in such circumstances it is imperative to use the x-ray powder method. The procedure used to obtain x-ray powder photographs from small areas of a particular mineral in a polished section is essentially the same as that described by Thompson (1949, p. 344).

With a view to obtaining relatively abundant material of known composition on which to verify crystallographic, physical, and microscopical properties, an attempt was made to reproduce all the known selenide minerals and certain possible isostructural series by pyrosyntheses. For this purpose the pure powdered elements were weighed out in charges of 1–2 grams, intimately mixed, and introduced into silica glass tubes of about 2 cc. capacity, which had been closed at one end and drawn out to a narrow neck at the other. The tubes were evacuated, sealed off and heated with a Bunsen or hotter flame to produce fusion and combination of the elements. After cooling, the tubes were broken and the practically homogeneous plugs were broken into two, one part being mounted for a polished section, the other retained for x-ray and other observations and for reference. By this simple method artificial compounds were obtained, identical or sometimes only similar to the corresponding minerals.

MATERIAL AND ACKNOWLEDGMENTS

For the many excellent selenide specimens which were made available, my thanks are due to Dr. V. B. Meen, the Royal Ontario Museum of Geology and Mineralogy, Toronto, Ontario; to Dr. C. Frondel, Harvard Mineralogical Museum, Cambridge, Mass.; to Dr. E. P. Henderson, United States National Museum, Washington, D. C., and to Dr. L. G. Berry, Queen's University Museum, Kingston, Ontario. The author wishes to thank Professor M. A. Peacock for the use of several fine selenide specimens kindly provided by Dr. Frans Wickman, Stockholm, Sweden, and Professor P. Ramdohr, Berlin, Germany.

Professor Peacock gave generously of his time supervising this study and assisting in the preparation of this report. The writer is also indebted to Dr. F. G. Smith, Dr. E. W. Nuffield, and Mr. A. R. Graham for constructive discussion of various problems.

The Research Council of Ontario awarded generous scholarships to the author, making it possible to carry out this study in the Mineralogical Laboratories of the Department of Geological Sciences, University of Toronto.

MINERAL DESCRIPTIONS AND SYNTHESES

Naumannite—Ag_2Se

Naumannite with clausthalite and chalcopyrite in carbonate gangue, from Tilkerode, Harz, Germany; ore specimen and polished section provided by Professor P. Ramdohr (Berlin).

»»→

FIG. 1. Naumannite (medium grey) and clausthalite (light grey) in a veinlet partly rimmed by chalcopyrite in carbonate gangue; Tilkerode, Harz mountains, Germany.

FIG. 2. Aguilarite (medium grey) and pearceite (light grey) in calcite gangue; Guanajuato, Mexico.

FIG. 3. Umangite (dark grey) in groundmass of eucairite (medium grey); Sierra de Umango, Argentina.

FIG. 4. Eucairite (light grey) in carbonaceous and siliceous gangue, sieve-like texture; Skrikerum, Sweden.

FIG. 5. Penroseite (light grey) cut by veinlets of clausthalite (grey-white); Colquechaca, Bolivia.

FIG. 6. Eucairite (light grey) intimately intergrown with chalcomenite (dark grey); Sierra de Umango, Argentina.

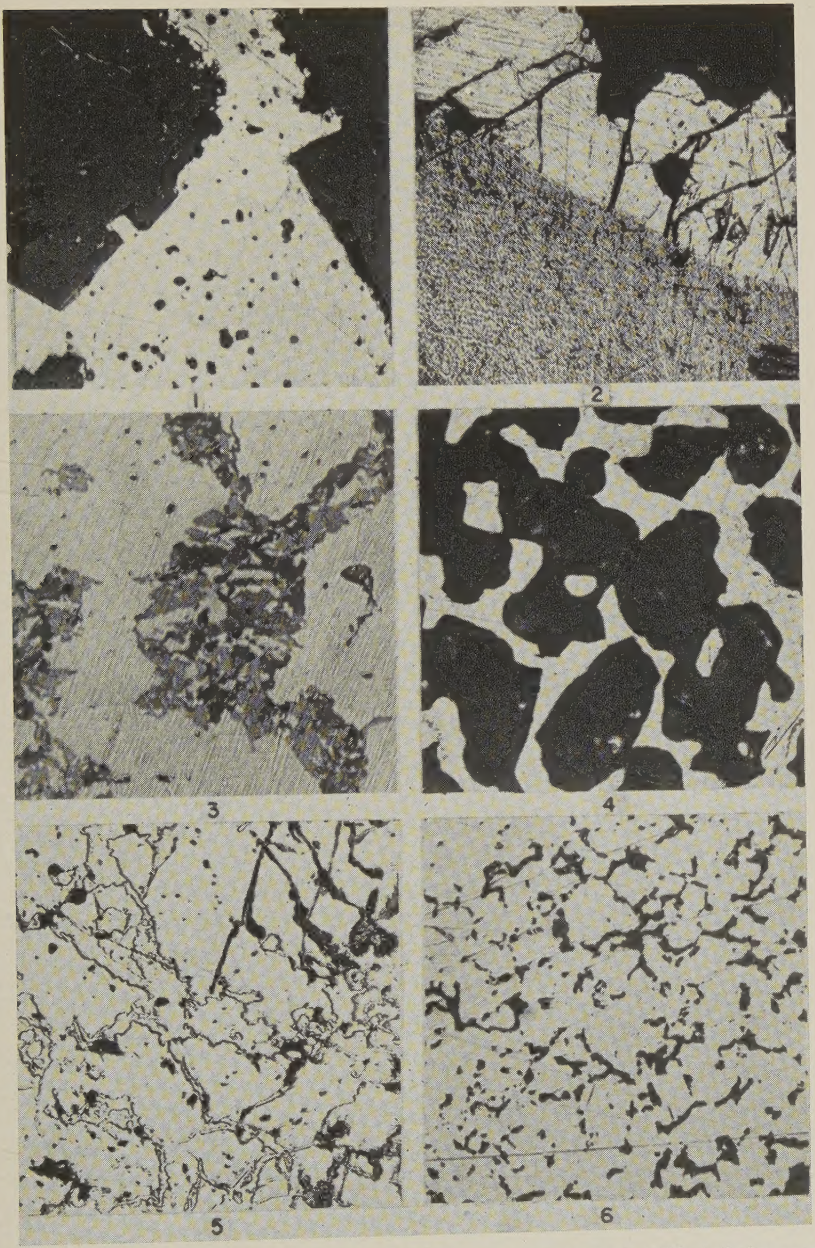

FIGS. 1–6. Photomicrographs of some selenide minerals. 1 nicol; ×70; full size reproductions of contact prints.

The selenides appear intimately intergrown in minute veinlets in the gangue, naumannite being hardly distinguishable from clausthalite even under the binocular. Naumannite is slightly more lustrous than clausthalite and its colour is greyish iron-black tarnishing in time to brownish iridescent, in contrast with the lead-grey of clausthalite. Naumannite is somewhat sectile with a poor hackly fracture. No cleavage was observed, and clean fragments of sufficient size for a specific gravity measurement could not be obtained.

In the polished section (Fig. 1) naumannite is grey (between argentite and tetrahedrite in colour), and darker than clausthalite, with no evidence of cleavage or parting. Anisotropism is distinct but weak (light grey to dark grey) and indications of mimetic twinning (Schneiderhöhn & Ramdohr, 1931) were not observed. Satisfactory etch tests could not be made. The Talmadge hardness is B.

Naumannite gave a complex *x*-ray powder pattern (Fig. 9 and Table 1) which cannot be indexed on a cubic lattice. The pattern compares in complexity with that of acanthite, which is monoclinic (pseudo-orthorhombic) according to Ramsdell (1943, p. 401), but the material offered no chance of single-crystal photographs for a determination of the unit cell. The cubic mineral identified as naumannite associated with penroseite from Colquechaca, Bolivia (Bannister & Hey, 1937, p. 319) is probably clausthalite.

The compound Ag_2Se was prepared by fusing the powdered elements in the proper atomic proportions in an evacuated silica glass tube. The charge fused readily to a bright metallic globule and cooled to a compact steel-grey regulus. Three fragments gave $G = 7.69–7.79$ which compares with 7.87 calculated for cubic Ag_2Se, 7.0–8.0 measured on naumannite (Dana, 1944, p. 179). In polished section the product is grey and homogeneous, with a few minute voids. It shows weak reflection pleochroism and moderate anisotropism (faint brown to pale blue) without indications of twinning or parting. Etch reactions: HNO_3 (1:1) stains light brown in 2 minutes; HCl (1:1) negative; KCN stains faint brown after 2 minutes; $FeCl_3$ instantly stains iridescent, bringing out texture; KOH negative, $HgCl_2$ quickly stains iridescent, bringing out scratches. These reactions are almost the same as those given for naumannite by Short (1940, p. 135). The *x*-ray powder pattern (Fig. 10) is substantially the same as that of naumannite.

These observations show that naumannite is natural β-Ag_2Se, the non-cubic phase which is stable below 122°–133° C. (Rahlfs, 1936, p. 157). It seems certain that the early reported good cubic cleavage (Rose, 1828) was actually that of the abundant associated and intergrown clausthalite, and the later allusions to cleavage traces might be due to parting associated with the α-β inversion. It remains to determine the unit cell of naumannite and eventually the structure.

Table 1. Naumannite, β-Ag_2Se: *X*-Ray Powder Pattern

I	θ(Cu)	*d*(meas.)	*I*	θ(Cu)	*d*(meas.)	*I*	θ(Cu)	*d*(meas.)
2	10.7°	4.14	½	29.6°	1.556	½	47.6°	1.041
½	11.8	3.76	1	30.8	1.501	½	49.6	1.009
1	13.5	3.29	½	31.5	1.471	½	50.3	0.999
1	15.5	2.88	2	32.35	1.437	½	52.05	0.975
1	16.5	2.71	½	33.6	1.389	½	53.85	0.952
10	16.8	2.66	1	34.95	1.342	½	55.2	0.936
10	17.45	2.56	1	35.6	1.321	½	55.75	0.930
2	18.55	2.42	½	36.2	1.302	½	57.35	0.913
6	20.15	2.23	½	37.45	1.264	½	57.85	0.908
2	21.4	2.11	2	38.3	1.240	½	59.05	0.896
2	21.75	2.07	½	39.4	1.211	½	59.9	0.889
4	22.6	2.00	½	40.2	1.191	½	61.0	0.879
½	23.4	1.936	½	41.05	1.171	½	63.1	0.862
2	24.3	1.868	½	42.35	1.141	½	69.15	0.823
1	25.05	1.816	½	43.25	1.122	½	71.05	0.813
1	26.65	1.714	½	44.55	1.096	½	71.85	0.809
1	27.5	1.665	½	45.85	1.071	½	75.15	0.795
2	28.6	1.606	½	46.65	1.057	½	77.75	0.787

Aguilarite—Ag_4SeS

Aguilarite, Guanajuato, Mexico (Royal Ontario Museum of Geology and Mineralogy, M3832); skeleton dodecahedrons embedded in transparent calcite, partially coated with clayey material.

In daylight with a hand lens, aguilarite appears in clumps of intergrown rudely dodecahedral crystals with pitted surfaces and mostly rounded edges, filled with calcite and a brittle metallic mineral which gave the *x*-ray pattern of pearceite (Peacock & Berry, 1947, p. 12). The aguilarite is a bright lead-grey on a fresh surface while exposed surfaces are dull iron-grey to black; it is sectile and yields a hackly fracture with no evidence of cleavage. Specific gravity determinations on three individual crystal fragments range from 7.40 to 7.53 with the Berman balance. A second sponge-like specimen coated with siderite and labelled "aguilarite" from Guanajuato, Mexico, gave the *x*-ray powder pattern of acanthite, although the metallic constituent was physically similar to aguilarite but lacked the usual crystal form.

Aguilarite polishes somewhat unevenly, giving a micro-pitted surface with no evidence of cleavage or parting. The section (Fig. 2) is light grey with a very faint greenish tinge, slightly darker than argentite.

Anisotropism is distinct but very weak (shades of grey). The etch reactions are similar to those given by Short (1940, p. 128): HNO_3 (1:1), light brown stain which is easily rubbed off, fumes tarnish a light brown; HCl (1:1), negative; $FeCl_3$, quickly stains iridescent; $HgCl_2$, quickly stains iridescent to black; KCN, leaves a light brown stain, easily rubbed off; KOH, negative. The Talmadge hardness is A.

Aguilarite gave a complex *x*-ray powder pattern (Fig. 7 & Table 2), distinctly different from those of naumannite and acanthite. The intensities and spacings agree substantially with those of Harcourt (1942, p. 69) and an attempt to index the pattern on a cubic lattice showed, as noted by Berman (Dana, 1944, p. 179), that this cannot be done. Since a single crystal fragment presumably represents the inversion product of a higher temperature cubic form, composed of individuals in random orientation, single crystal photographs for a unit cell determination seemed hopeless.

TABLE 2. AGUILARITE, β-Ag_4SeS: *X*-RAY POWDER PATTERN

I	θ(Cu)	*d*(meas.)	*I*	θ(Cu)	*d*(meas.)	*I*	θ(Cu)	*d*(meas.)
5	10.85°	4.09	1	24.1°	1.883	1	38.25°	1.242
1	12.0	3.70	1	26.55	1.720	1	39.05	1.220
2	15.8	2.83	1	29.15	1.578	$\frac{1}{2}$	44.85	1.090
2	17.05	2.62	1	29.85	1.545	$\frac{1}{2}$	47.75	1.038
2	17.3	2.58	1	31.55	1.470	$\frac{1}{2}$	48.25	1.030
10	18.5	2.42	1	32.65	1.425	$\frac{1}{2}$	53.25	0.959
6	20.5	2.19	1	34.65	1.353	$\frac{1}{2}$	54.05	0.950
2	21.8	2.07	1	36.1	1.305	$\frac{1}{2}$	60.35	0.855
2	22.95	1.971	1	36.7	1.286			

The compound Ag_4SeS was prepared by fusing the powdered elements in the proper proportions in an evacuated silica glass tube. The components fused readily to a bright metallic globule and cooled to a lead-gray regulus which had a very small amount of metallic silver in shiny particles adhering to the outer surface. A polished section of the product is homogeneous, grey, slightly porous and weakly anisotropic similar to aguilarite. The *x*-ray powder pattern of this compound (Fig. 8) is very similar to that of aguilarite.

These observations indicate that aguilarite corresponds to noncubic β-Ag_4SeS which is stable at room temperature. The dodecahedral crystal form suggests inversion from cubic high temperature α-Ag_4SeS. Since the *x*-ray powder patterns of aguilarite and Ag_4SeS show only faint resemblances to those of naumannite, Ag_2Se, and argentite, Ag_2S, aguilarite is a distinct species and not merely a member of a naumannite-acanthite series, as suggested in Schneiderhöhn & Ramdohr (1931, p. 222).

Eucairite—AgCuSe

Eucairite, Skrikerum, Sweden (Natural History Museum, Stockholm, yellow 2345); disseminated blebs with severely tarnished surfaces in a serpentinized gangue of quartz and calcite.

Eucairite, Sierra de Umango, Argentina (United States National Museum, 84457); associated with umangite, chalcomenite, and malachite in a highly altered copper ore specimen.

Viewed with a hand lens, eucairite is a brilliant creamy white on a fresh surface, whereas exposed surfaces are bright bronze due to a tarnish that develops quickly. The mineral is brittle and fractures unevenly to subconchoidally with no evidence of cleavage. None of the material was satisfactory for specific gravity measurements.

Eucairite polishes to a smooth surface with no evidence of cleavage or parting (Figs. 4, 6). The polished surface appears tin-white with a faint creamy tinge. Reflection pleochroism is very weak with no obvious colour change, but with variable relief along grain boundaries. Anisotropism is strong with polarization colours olive-brown to steel-blue with a purplish tinge, somewhat less vivid than those given by Schneiderhöhn & Ramdohr (1931, p. 306). The etch reactions are essentially the same as those of Short (1940, p. 135): HNO_3 (1:1), surface slowly stains greyish brown, fumes tarnish strongly brown to iridescent but rubs off; HCl (1:1), negative; $FeCl_3$, tarnishes iridescent to greyish blue; KCN, instantly stains brownish to black; $HgCl_2$, slowly yields a faint pinkish brown stain; KOH, negative. The Talmadge hardness is B.

A roughly equant fragment of eucairite was chosen from the Skrikerum specimen for single crystal measurements. The fragment was successfully oriented on the x-ray goniometer by a succession of rotation photographs and minor adjustments. Fairly good rotation and Weissenberg photographs gave the tetragonal cell dimensions:

$$a=4.075,\ c=6.29\ \text{kX}$$

Five very weak lines in the powder pattern (Table 3) can be explained by a triple c; but since there is no evidence for this on the rotation photograph, these weak lines are evidently extraneous.

The Laue symmetry is $4/mmm$ and the systematically missing spectra conform to the single condition: $(hk0)$ present only with $h+k=2n$. This condition is compatible with the space group $P4/nmm$. With the cell contents 2[AgCuSe] the calculated specific gravity is 7.91, as compared with the measured values 7.6–7.8 (Dana, 1944, p. 183).

Table 3 is based on the *x*-ray powder pattern (Fig. 11) of eucairite from Skrikerum, Sweden (NHM, Stockholm, yellow 2345). The measured spacings given by the ASTM (1945) cards do not agree well with those of our pattern.

A compound near AgCuSe in composition was prepared by fusing the elements in equal atomic proportions in a vacuum. The charge fused readily to a shiny somewhat porous regulus. A freshly broken surface revealed a bright metallic product which is white with a distinct reddish buff tinge. After a week an exposed surface acquired a distinctly bronzy tarnish, eventually turning iridescent. A polished section of the regulus shows two constituents, one similar to eucairite making up about 95 per cent of the section, the other an intensely anisotropic product, Cu_3Se_2 (umangite). An *x*-ray powder pattern of the dominant compound (Fig. 12) is similar to that of eucairite (Fig. 11).

TABLE 3. EUCAIRITE—AgCuSe: *X*-RAY POWDER PATTERN

Tetragonal, *P*4/*nmm*; $a=4.075$, $c=6.29$ kX; $Z=2$

I	θ(Cu)	*d*(meas.)	(*hkl*)	*d*(calc.)
½	11.8°	3.76	—	—
½	12.9	3.44	(011)	3.420
1	14.15	3.14	(002)	3.145
5	15.5	2.88	(110)	2.881
7	17.1	2.61	(111)	2.620
4	18.05	2.48	(012)	2.490
½	19.15	2.34	—	—
½	20.25	2.22	—	—
10	21.25	2.12	(112)	2.125
2	22.35	2.02	(020)	2.038
1	24.4	1.861	(013)	1.864
½	26.8	1.705	(022)	1.710
			(113)	1.695
½	28.25	1.624	—	—
1	29.2	1.576	(122)	1.577
			(004)	1.572
½	29.95	1.540	—	—
1	31.9	1.456	(023)	1.461
½	33.95	1.376	(114)	1.380
			(123)	1.375
½	35.0	1.340	(031)	1.328
½	35.75	1.316	(222)	1.310
½	36.6	1.289	(130)	1.289
½	37.35	1.267	(131)	1.262
½	38.25	1.242	(032)	1.247
			(024)	1.245
1	39.75°	1.202	(015)	1.202
1	40.15	1.192	(132)	1.192
			(124)	1.191
			(223)	1.187
½	42.65	1.135	(033)	1.140
1	48.0	1.034	(125)	1.035
			(034)	1.028
½	49.0	1.019	(040)	1.019
			(016)	1.015
½	56.6	0.921	(035)	0.923
			(332)	0.919
			(234)	0.918
½	57.55	0.911	(240)	0.911
			(126)	0.909
½	58.9	0.898	(135)	0.900
			(007)	0.899
			(143)	0.894
½	61.3	0.876	(017)	0.877
			(242)	0.875
			(333)	0.873
½	63.55	0.859	(117)	0.858
			(044)	0.855
½	72.55	0.806	(341)	0.808
			(051)	0.808
			(127)	0.806

These observations show that eucairite is tetragonal, in keeping with the strong anisotropism, and not isometric as suggested by Berzelius in 1818. The synthesis tends to confirm the accepted composition AgCuSe established from the analyses given in Hintze (1904).

Crookesite—$(Cu,Tl,Ag)_2Se$

Crookesite, Skrikerum, Sweden; finely disseminated specks and small veinlets in translucent calcite with minor quartz.

Finely disseminated crookesite is localized in small areas giving the specimen a slaty, bluish black, mottled appearance. Individual particles of the mineral are not visible to the naked eye but can be seen with a binocular microscope. Crookesite is lead-grey on a fresh surface, brittle when crushed with a needle and shows two fairly well developed cleavages at right angles. A sufficiently large, pure sample could not be obtained for specific gravity measurements.

Crookesite polishes to a smooth surface and is distinctly grey, somewhat darker than argentite but lighter than tetrahedrite. Reflection pleochroism is imperceptible and the anisotropism is weak but clearly discernible (shades of grey). Due to the reactive nature of the carbonate gangue the etch reactions for HNO_3, HCl, and $FeCl_3$ are unreliable. The observed etch reactions are in fair agreement with those of Murdoch (Schneiderhöhn & Ramdohr, 1931, p. 302): HNO_3 (1:1) fumes tarnish brown, rubs off; HCl (1:1) negative; $FeCl_3$ negative; KCN negative; $HgCl_2$ negative; KOH negative. The Talmadge hardness is C.

A fragment of crookesite (0.5×0.3 mm) showing two imperfect, mutually perpendicular cleavages was mounted for single crystal measurements. Good rotation and Weissenberg photographs gave tetragonal or pseudo-tetragonal unit cell dimensions:

$$a=10.38,\ c=3.92\ \text{kX}$$

Although the Weissenberg films show only monoclinic symmetry and the F-lattice type, with $a=b=10.38\sqrt{2}=14.68$ kX, $\beta=90°$, crookesite may be provisionally interpreted as pseudo-tetragonal with hkl present only with $h+k+l=2n$, leading to the possible space group $I4/mmm$. With reference to the pseudo-tetragonal unit cell the poorly developed cleavage is prismatic (020). The powder pattern of crookesite from Skrikerum (Sweden) (Fig. 13) has been indexed in this simpler manner (Table 4).

The composition of crookesite, known only through three early analyses by Nordenskiöld (1866, p. 366), is given as $(Cu, Tl, Ag)_2Se$. Microchemical tests confirmed the presence of Cu, Ag, Se. In addition a small amount of crookesite dissolved in HNO_3 yielded a character-

Table 4. Crookesite—(Cu,Tl,Ag)$_2$Se: *X*-Ray Powder Pattern

Pseudo-tetragonal, *I*4/*mmm*; $a=10.38$, $c=3.92$ kX; $Z=2$

I	θ(Cu)	*d*(meas.)	(*hkl*)	*d*(calc.)
1	8.5°	5.20	(020)	5.190
½	11.95	3.71	(220)	3.668
10	13.5	3.29	(130)	3.282
8	14.85	3.00	(121)	2.995
10	17.25	2.59	(040) (031)	2.595 2.594
1	18.4	2.44	(330)	2.447
3	19.35	2.32	(240) (231)	2.321 2.320
5	21.35	2.11	(141)	2.118
½	23.0	1.967	(002)	1.960
4	24.8	1.833	(440)	1.835
4	25.6	1.779	(350)	1.780
½	26.45	1.726	(222) (060) (251)	1.729 1.730 1.730
½	27.2	1.682	(132)	1.683
½	28.0	1.637	(260)	1.641
1	29.45	1.563	(161) (042)	1.565 1.564
½	30.15°	1.530	(332)	1.530
½	30.95	1.495	(451)	1.498
½	32.3	1.439	(361) (460)	1.439 1.439
1	35.65	1.319	(352) (080)	1.318 1.322
1	37.75	1.256	(561)	1.252
½	38.95	1.223	(660) (181) (471)	1.223 1.223 1.223
½	41.6	1.158	(480) (462)	1.160 1.160
1	44.05	1.106	(091)	1.106
½	45.3	1.081	(082) (671)	1.082 1.082
1	46.55	1.059	(282) (581)	1.059 1.059

istic thallium-green flame. With a unit cell containing 24 atoms in the proportions of the analyses, Cu:Tl:Ag$=0.4569:0.1669:0.0510$, or 8[Cu,Tl,Ag)$_2$Se], the calculated specific gravity is 7.71, somewhat greater than the value given by Nordenskiöld (1866).

An attempt was made to prepare an artificial compound similar to crookesite by fusing appropriate proportions of Cu, Tl, Ag and Se in a

---

→

Figs. 7–26. *X*-ray powder photographs with Cu/Ni radiation; Camera radius 90/π mm. (1°θ=1 mm. on film); full size reproductions of contact prints.

Fig. 7. Aguilarite, Guanajuato, Mexico.
Fig. 8. Compound Ag$_4$SeS formed by pyrosynthesis.
Fig. 9. Naumannite, Tilkerode, Harz Mountains, Germany.
Fig. 10. Compound Ag$_2$Se formed by pyrosynthesis.
Fig. 11. Eucairite, Skrikerum, Sweden.
Fig. 12. Compound AgCuSe formed by pyrosynthesis.
Fig. 13. Crookesite, Skrikerum, Sweden.
Fig. 14. Compound (Cu,Tl,Ag)$_2$Se formed by pyrosynthesis.
Fig. 15. Berzelianite, Skrikerum, Sweden.
Fig. 16. Compound Cu$_{2-x}$ formed by pyrosynthesis.

7

8

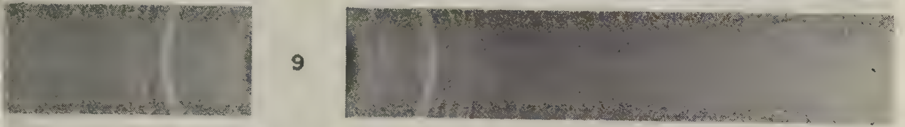
9

10

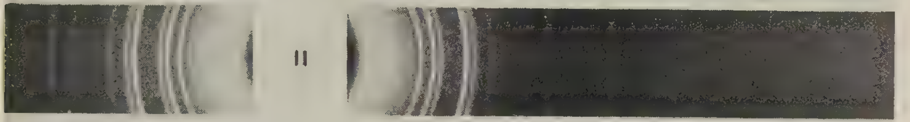
11

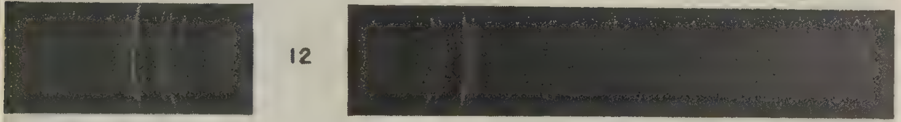
12

13

14

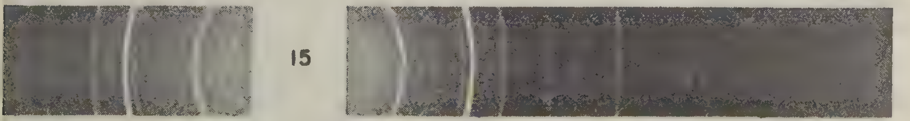
15

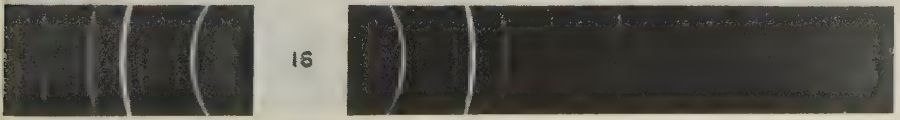
16

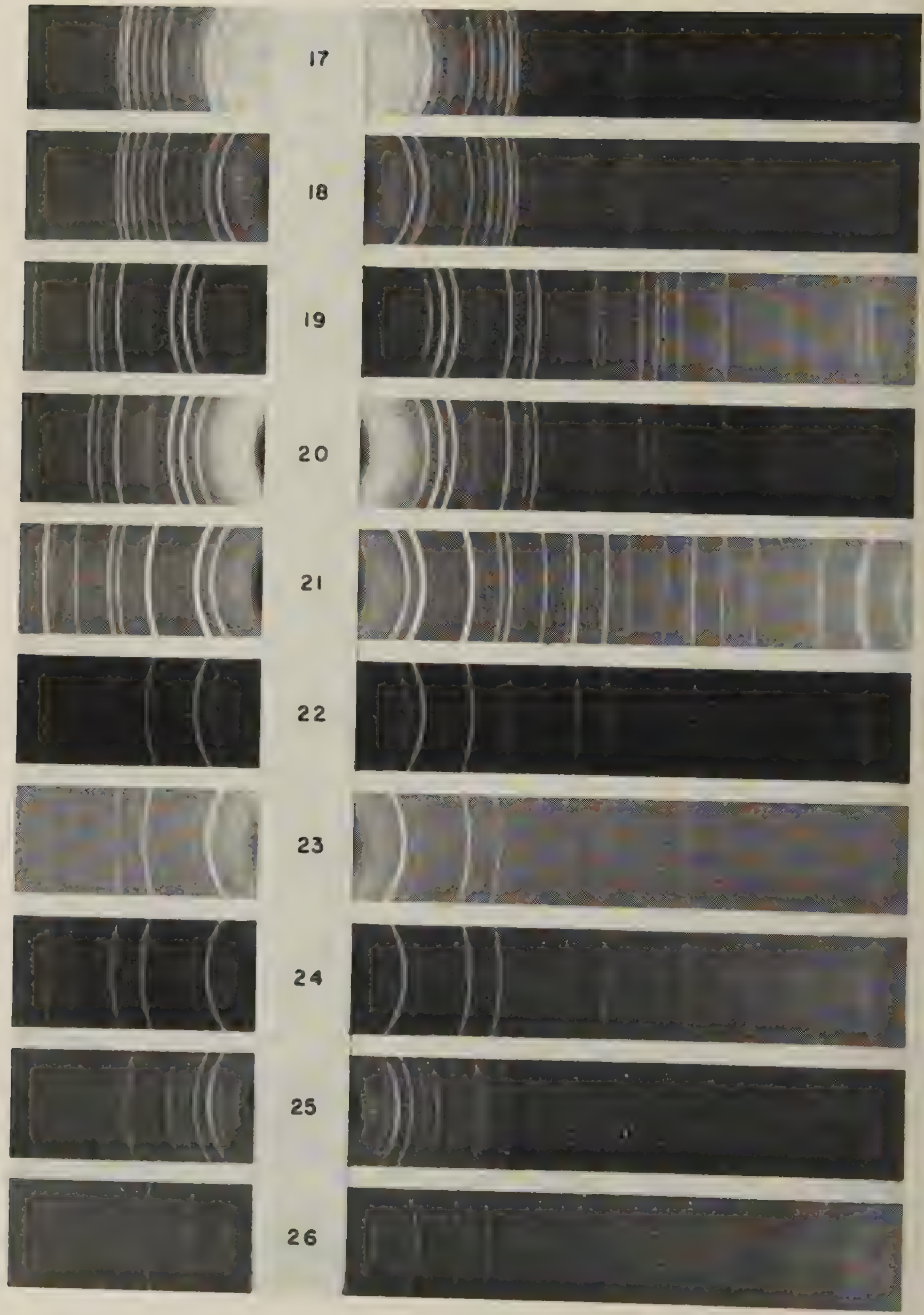
17
18
19
20
21
22
23
24
25
26

vacuum. The elements fused with difficulty and ebullition of gas to a porous inhomogeneous mass. A polished section shows two products, the one resembling crookesite and the other, berzelianite. An *x*-ray powder pattern of the aggregate (Fig. 14) is similar to crookesite except for two diffraction lines which correspond to the two strongest lines of berzelianite.

These results show that crookesite is not cubic as suggested by Hiller (1940, p. 138); but it is interesting to note that the true monoclinic $a = 14.68$ kX is almost identical with Hiller's cube edge 14.69 kX. The anisotropism and definite cleavage according to Ramdohr (in Hiller, 1940) are in good agreement with our observations.

Berzelianite—$Cu_{2-x}Se$

Berzelianite, Skrikerum, Sweden (Harvard Mineralogical Museum, 81739); finely disseminated in calcite gangue.

Berzelianite, Skrikerum, Sweden (ROM, M12324); finely disseminated in calcite gangue.

Berzelianite, locality unknown (Dept. of Geol., Univ. of Western Ontario); finely disseminated in calcite gangue.

Berzelianite, Aurora, Nevada, U.S.A.; disseminated in a highly weathered siliceous gangue associated with native gold and lead.

Berzelianite, Lake Athabaska, N.W.T., Canada (Bureau of Mines, Ottawa); blebs and veinlets in greyish pink calcite gangue associated with umangite and chalcocite.

Berzelianite appears as dusty black patches in otherwise translucent calcite associated with umangite, eucairite, and other selenides. With a binocular microscope, freshly fractured surfaces are shiny lead-grey with a faint bluish cast, somewhat less lustrous than clausthalite, while old surfaces are dusty metallic black. Berzelianite is brittle and fractures unevenly with no evidence of cleavage. Pure material could not be obtained in sufficient quantity for specific gravity measurements. However, specific gravity measurements of three independent fragments of pyrosynthetic material of composition $Cu_{1.85}Se$ yielded an average value 6.65.

←««««

FIG. 17. Umangite, Sierra de Umango, Argentina.
FIG. 18. Compound Cu_3Se_2 formed by pyrosynthesis.
FIG. 19. Penroseite, Colquechaca, Bolivia.
FIG. 20. Compound $(Ni,Cu)Se_2$ formed by pyrosynthesis.
FIG. 21. Clausthalite, Clausthal, Harz Mountains, Germany.
FIG. 22. Compound PbSe formed by pyrosynthesis.
FIG. 23. Tiemannite, Clausthal, Harz Mountains, Germany.
FIG. 24. Compound HgSe formed by pyrosynthesis.
FIG. 25. Guanajuatite, Guanajuato, Mexico.
FIG. 26. Compound Bi_2Se_3 formed by pyrosynthesis.

In polished section berzelianite is steel-greyish white, isotropic, and without obvious cleavage traces. A smooth polished surface, in time, tarnishes bronzy iridescent. The etch reactions are similar to those given by Schneiderhöhn & Ramdohr (1931, p. 301): HNO_3 (1:1), slowly stains iridescent with a reddish tinge; HCl (1:1), negative; $FeCl_3$, stains quickly light brown, rubs off; KCN, stains iridescent and finally black; $HgCl_2$ stains slowly greyish black; KOH, negative. The Talmadge hardness is B.

An *x*-ray powder pattern of berzelianite (Fig. 15 & Table 6) from Skrikerum, Sweden (HMM, 81739) has been indexed on a cubic lattice:

$$a = 5.728 \text{ kX}$$

The spacings and intensities are in good agreement with those of Harcourt (1942, p. 72), and the cell edge agrees closely with previous measurements on berzelianite and artificial $Cu_{2-x}Se$ (with $x=0.2$); the cube-edge of Cu_2Se is slightly higher at room temperature and distinctly higher at about 180° C. (Table 5).

TABLE 5. BERZELIANITE, $Cu_{2-x}Se$, AND Cu_2Se: CUBE-EDGES

Berzelianite	$Cu_{2-x}Se$	Cu_2Se
—	—	5.751 A (Davey, 1923)
5.731 A	—	5.748 A (Hartwig, 1926)
—	—	5.84 A at 180° C. (Rahlfs, 1936)
—	5.729 A ($x=0.2$)	— (Borchert, 1945)
5.728 kX	5.74 kX ($x=0.15$)	5.81 kX at about 55° C. (J.W.E.)

The systematically missing spectra are given by the conditions: *hkl* present only with *h*, *k*, *l*, all odd or all even, 0*kl* present only with $h+l=4n$, leading to the space group *Fd*3*m*. The calculated specific gravity with $4[Cu_{2-x}Se]$ ($x=0.15$) in the unit cell is 6.96, rather higher than the measured values, G=6.7, given by Berzelius (in Dana, 1892), and 6.65 on artificial material.

The following copper-selenium compounds were prepared by fusing known proprotions of the elements in a vacuum:

Cu:Se=32:16. The elements fuse with difficulty to a porous, steel-grey regulus which on breaking shows imperfect cubic cleavage. A section of the product is greyish white, homogeneous and isotropic. In a few weeks a polished surface develops a bronzy tarnish. An *x*-ray powder photograph of a random fragment yields a pattern similar to berzelianite but with each of the diffraction lines represented as doublets indicating a non-cubic lattice. However, an *x*-ray powder photograph taken at about 55° C. can be indexed as cubic with $a=5.81$ kX.

Cu:Se = 30:16. The product appears macroscopically and microscopically similar to Cu:Se = 32:16. The *x*-ray powder pattern of this material (Fig. 16) yields the berzelianite pattern with the exception of one very weak line which compares to one of the lines in the pattern of the former charge. The cube-edge is $a = 5.74$ kX.

Cu:Se = 28:16. The elements fuse with less difficulty to a purplish black slightly porous regulus. A polished section of this compound appears homogeneous, faintly purplish grey and is isotropic. An *x*-ray powder photograph of a random fragment shows the berzelianite pattern with six extra lines characteristic of the umangite pattern. This component, which is normally intensely anisotropic, must be distributed in extremely minute areas in the polished section, producing no distinct anisotropism.

TABLE 6. BERZELIANITE—$Cu_{2-x}Se$: *X*-RAY POWDER PATTERN

Cubic, *Fd3m*; $a = 5.728$ kX; $Z = 4$

I	θ(Cu)	*d*(meas.)	(*hkl*)	*d*(calc.)	*I*	θ(Cu)	*d*(meas.)	(*hkl*)	*d*(calc.)
½	12.65°	3.51	—	—	3	32.5°	1.431	(004)	1.432
9	13.4	3.32	(111)	3.308	2	35.8	1.314	(133)	1.315
1	15.55	2.87	(002)	2.864	4	41.1	1.169	(224)	1.170
*1	17.05	2.62	—	—	2	44.2	1.103	(115) (333)	1.103
*½	18.05	2.48	—	—					
*½	19.95	2.25	—	—	1	49.4	1.012	(044)	1.013
*1	21.15	2.13	—	—	1	52.65	0.967	(135)	0.968
10	22.35	2.02	(022)	2.026	2	58.05	0.906	(026)	0.906
*½	23.8	1.905	—	—	1	61.6	0.874	(335)	0.874
*½	24.95	1.822	—	—	½	68.5	0.826	(444)	0.827
*½	25.65	1.776	—	—	1	73.4	0.802	(117) (155)	0.802
8	26.45	1.726	(113)	1.728					

* Extra lines due mainly to umangite.

Cu:Se = 27:16. The elements fused similarly to the charge. Cu:Se = 28:16, producing a slightly porous, purplish regulus. A polished section of this material shows two phases, the one identical with Cu:Se = 28:16, the other with Cu:Se = 3:2 (umangite). The latter constituent occurs as elliptical inclusions in the groundmass. The *x*-ray powder pattern of a random fragment shows both umangite and berzelianite diffraction lines.

These observations show that berzelianite is cubic at ordinary temperatures and has a composition, $Cu_{2-x}Se$, representing a structure which is deficient in copper atoms as proposed by Borchert (1945). The homogeneous berzelianite phase appears to be slightly poorer in Cu than

Cu:Se = 30:16, indicating the composition with $x = 0.15$ (Cu:Se = 29.6:16), rather than $x = 0.2$ (Cu:Se = 28.8:16) given by Borchert. The compound Cu_2Se has a non-cubic low temperature phase, β-Cu_2Se, which inverts at elevated temperatures to α-Cu_2Se which is cubic, confirming the results of Rahlfs (1936).

Umangite—Cu_3Se_2

Umangite, Sierra de Umango, Argentina (ROM, E3249); massive ore specimen cut by veinlets of chalcomenite, malachite and calcite.

Umangite, Sierra de Umango, Argentina (Queen's University Museum of Geology and Mineralogy, A51a—1); massive ore specimen cut by veinlets of chalcomenite and malachite and having small inclusions of clausthalite.

"Berzelianite," Sierra de Cacheuta, Argentina (ROM, M12864); massive ore specimen cut by veinlets of chalcomenite and malachite.

"Berzelianite," Skrikerum, Sweden (QM, 491); finely disseminated specks in calcite, localized, giving a patchy appearance to the specimen, with minor chalcomenite and malachite.

"Klockmannite," Sierra de Umango, Argentina (USNM, R519); massive ore specimen cut by veinlets of clausthalite and chalcomenite.

"Berzelianite," Tilkerode, Germany (HMM, 81763); finely disseminated specks in a vein of calcite filling a fracture in dark siliceous rock.

On fresh surfaces umangite unlike any of the other selenides appears lustrous bluish black with a distinct reddish cast while weathered surfaces are a dull iridescent purplish colour. It is brittle and fractures unevenly or subconchoidally with evidence of two very poor rectangular cleavages, giving fragments which resemble small lumps of "hard" coal. Fragments of sufficient size and purity for specific gravity measurements were not available; however, measurements of three independent fragments of the artificial compound, Cu_3Se_2, gave values, $G = 6.44$–6.49, somewhat greater than the value, $G = 5.620$, given by Klockmann (1891, p. 269) for umangite.

Umangite polishes somewhat unevenly (Fig. 3) and has a characteristic reddish purple colour, not unlike rickardite, the analogous copper telluride described by Thompson (1949, p. 358). Grains of umangite show distinct rectangular outline. Reflection pleochroism is pronounced (reddish purple to greyish blue) somewhat less than that of klockmannite. Anisotropism is very strong (fiery orange to straw-yellow with a rose tint) with four positions of extinction parallel to the poor cleavages. The etch reactions are similar to those given by Short (1940, p. 127): HNO_3 (1:1) tarnishes to a deep bluish purple; HCl (1:1) stains bluish; $FeCl_3$, stains deep blue; $HgCl_2$ tarnishes bluish; KCN, tarnishes differentially blue to dark grey bringing out grain structure; KOH, tarnishes light blue. The Talmadge hardness is B.

Although many fragments with roughly rectangular outline were tested for single crystal properties, only one fragment with poorly developed cleavages proved in any way satisfactory for single crystal measurements. Fair rotation and Weissenberg photographs were obtained with Cu*K* radiation. Measurements on the films gave orthorhombic cell dimensions:

TABLE 7. UMANGITE—Cu_3Se_2: *X*-RAY POWDER PATTERN

Orthorhombic, $P22_12_1$; $a=4.27$, $b=6.39$, $c=12.44$ kX; $Z=4$

I	θ(Cu)	*d*(meas.)	(*hkl*)	*d*(calc.)
1	10.35°	4.28	(100)	4.270
10	12.45	3.57	(110) (102)	3.550 3.520
4	13.9	3.20	(020)	3.195
4	14.35	3.10	(004) (021) (112)	3.110 3.095 3.083
2	15.6	2.86	(022)	2.842
3	17.5	2.56	(120) (023)	2.558 2.531
1	18.9	2.37	(122)	2.366
4	19.9	2.26	(024)	2.229
2	21.15	2.13	(105) (200)	2.150 2.135
3	22.45	2.01	(210) (032)	2.025 2.015
3	23.8	1.905	(130)	1.906
9	25.0	1.819	(132) (213)	1.822 1.802
8	25.65°	1.776	(220)	1.775
½	26.7	1.711	(017) (222)	1.712 1.707
1	28.0	1.637	(223) (107)	1.632 1.641
½	28.8	1.596	(040)	1.597
1	29.65	1.554	(008) (027) (042)	1.555 1.553 1.547
½	31.65	1.465	(311) (232) (127)	1.465 1.465 1.460
1	32.75	1.421	(118) (300) (044) (233)	1.424 1.423 1.421 1.417

I	θ(Cu)	*d*(meas.)
½	33.6°	1.389
1	34.5	1.357
½	37.0	1.277
½	38.65	1.231
2	39.8	1.201
1	40.4	1.186
1	41.35	1.163
½	42.25	1.143
½	42.8	1.131
½	43.9°	1.109
½	44.5	1.097
½	46.15	1.066
½	46.95	1.052
½	47.9	1.036
½	49.45	1.012
½	50.35	0.998
½	51.35	0.984
½	52.75	0.966
1	54.75°	0.941
½	57.5	0.911
½	58.4	0.902
½	60.25	0.885
½	62.2	0.869
½	64.0	0.855
½	69.9	0.818
½	75.85	0.793
½	80.35	0.780

$$a=4.27,\ b=6.39,\ c=12.44 \text{ kX}$$

The systematically missing spectra conform to the conditions: *hkl* present in all orders, 0*k*0 present only with $k=2n$. The extinction condition in 00*l* was not determined from Weissenberg photographs but the indexed *x*-ray powder pattern suggests 00*l* present only with $l=2n$. These conditions are characteristic of the space group $P22_12_1$ (class 222).

The cell dimensions of umangite and the measured specific gravity of the compound Cu_3Se_2, combined with the analyses given by Klockmann (1891), indicate the cell content $Cu_{12}Se_8$. However, the specific gravity of umangite calculated for the unit cell containing $4[Cu_3Se_2]$ is 6.779, higher than the measured value, 6.44–6.49 for the artificial compound. This discrepancy may be due to the voids in the artificial material, but there is also the possibility that umangite, like rickardite (Forman & Peacock, 1949), is a grossly defective compound $Cu_{4-x}Se_2$ only approximating Cu_3Se_2 in composition.

Identical *x*-ray powder patterns are given by umangite (Fig. 17, Table 7) and pyrosynthetic Cu_3Se_2 (Fig. 18). The measured spacings given by Waldo (1935) and Harcourt (1942) agree fairly well with the strong lines of our pattern.

The compound Cu_3Se_2 was prepared by fusing copper and selenium metals in appropriate atomic proportions in a vacuum. The resulting regulus is bluish black with a reddish tint and homogeneous, except for a few minute voids. In polished section the product is reddish purple similar to umangite and yields an *x*-ray powder pattern identical with umangite.

These observations show that, although umangite (Cu_3Se_2) and rickardite (Cu_3Te_2) are physically, chemically and optically similar, they are not isostructural as might be expected. The empirical formula, Cu_3Se_2, suggested by Klockmann (1891) is confirmed by the fact that homogeneous artificial material identical with umangite was formed by fusion of the elements in these proportions.

Clausthalite—PbSe

Clausthalite, Clausthal, Harz mountains, Germany (ROM, E3120); granular and massive clausthalite embedded in a light silicified rock which contains a few grains of chalcopyrite.

Clausthalite and penroseite, Colquechaca, Bolivia (ROM, M19163); fine grained interstitial clausthalite in penroseite with siliceous veinlets and alteration products.

With a hand lens, clausthalite is lustrous lead-grey with a faint bluish cast on fresh surfaces, whereas old weathered surfaces are dull greyish black with occasional reddish brown spots. The mineral is brittle and fractures easily showing cubic cleavage, slightly less perfect than galena. Specific gravity measurements on clean, selected, cleavage fragments gave G=8.08–8.22 with the Berman balance.

Clausthalite polishes to a smooth surface broken only by a few triangular pits which are not as distinct as those in galena. The polished surface is galena-white with a greyish tinge but lighter than tetrahedrite. It is clearly isotropic. The etch reactions are similar to those given by Short (1940, p. 129): HNO_3 (1:1), tarnishes leaving a brick red coating of selenium; HCl (1:1), readily yields a greyish brown stain; $FeCl_3$, tarnishes iridescent; KCN, negative; $HgCl_2$, negative; KOH, negative. The Talmadge hardness is B.

Clausthalite (ROM, E3120) gave an *x*-ray powder pattern (Fig. 21) which is indexed on a cubic lattice with $a=6.110$ kX; this is distinctly lower than the values, $a=6.162$ A given by Olshausen (1925) for clausthalite and $a=6.14$ A given by Ramsdell (1925, p. 283) for the artificial compound PbSe. Table 8 gives the powder data with measured spacings which agree well with those of Harcourt (1942, p. 77). With 4[PbSe] in the unit cell the calculated specific gravity is G = 8.28, somewhat higher than the measured value, G = 8.08–8.22.

Table 8. Clausthalite—PbSe: *X*-Ray Powder Pattern

Cubic, *Fm3m*; $a=6.110$ kX; $Z=4$

I	*θ*(Cu)	*d*(meas.)	(*hkl*)	*d*(calc.)
2	12.6°	3.52	(111)	3.527
10	14.6	3.05	(002)	3.055
9	20.85	2.16	(022)	2.160
5	24.7	1.840	(113)	1.842
5	25.85	1.763	(222)	1.764
2	30.25	1.526	(004)	1.527
1	33.3	1.400	(133)	1.402
5	34.25	1.366	(024)	1.366
4	38.05	1.247	(224)	1.247
1	40.85	1.175	(115) (333)	1.176
1	45.45	1.079	(044)	1.080
½	48.15°	1.032	(135)	1.033
2	49.05	1.018	(006) (244)	1.018
2	52.8	0.965	(026)	0.966
2	56.65	0.920	(226)	0.921
½	60.65	0.882	(444)	0.882
½	63.95	0.856	(117) (155)	0.856
1	65.15	0.847	(046)	0.847
2	70.3	0.816	(246)	0.816
1	75.05	0.796	(137)	0.796

The compound PbSe was prepared by fusing the elements in equal atomic proportions in a vacuum. The components fused readily to a bright metallic globule and cooled to a compact shiny lead-grey regulus showing cubic cleavage. In polished section the product is grey, homogenous and isotropic, similar to clausthalite. An *x*-ray powder pattern (Fig. 22) from a random fragment of this material is identical to that of clausthalite (Fig. 21).

Clausthalite and galena are known to be isostructural, suggesting a solid solution series, PbSe—PbS. In order to test the existence of this series, fusions were made in the standard way at 20 atomic per cent intervals between the end members and the cube-edges of the products were measured exactly from the back reflection lines.

PbS	20 at. %	40	60	80	PbSe
a=5.923	5.959	6.002	6.038	6.076	6.110 kX

Fig. A gives a plot of the cube-edges and the compositions of the various fusion products. The smooth, almost linear, variation of cube-edge and composition shows that the isostructural compounds PbS and PbSe do in fact form a continuous solid solution series under fusion conditions.

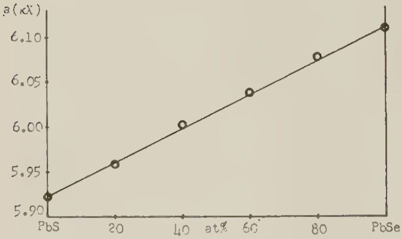

FIG. A. Plot of cube-edge and composition of artificial PbS-PbSe solid solutions.

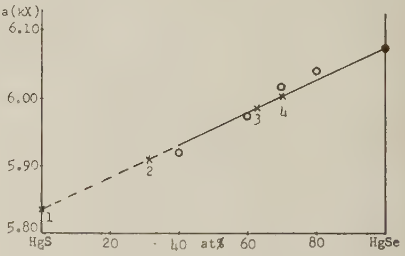

FIG. B. Plot of cube-edge and composition of artificial (circles) and natural (crosses) members of the HgS-HgSe series.

Tiemannite—HgSe

Tiemannite, Clausthal, Harz mountains, Germany (ROM, M20129); massive tiemannite separated from chalcopyrite by a calcite-vein, some of the tiemannite has a hard reddish brown coating (not identified).

Tiemannite, Clausthal, Harz mountains, Germany (ROM, M3872); a massive coating on siliceous carbonate rock.

"Onofrite," Pinte County, Utah, U.S.A. (ROM, M20131); a massive ore specimen with a small amount of clayey material.

"Onofrite," Pinte County, Utah, U.S.A. (ROM, M7376); massive in limestone.

In daylight, fresh surfaces of tiemannite are lead-grey with a purplish blue cast and have a metallic sheen not unlike some varieties of chalcocite, while weathered surfaces are dull reddish brown to black. Massive and compact granular tiemannite fractures unevenly to subconchoidally with no evidence of cleavage. Five determinations of the specific gravity, made with the Berman balance on clean fragments gave G=8.24–8.27.

In polished section tiemannite is greyish white, slightly darker than clausthalite, and isotropic. The etch reactions are similar to those given by Short (1940, p. 152): HNO_3 (1:1), negative; HCl (1:1), negative; KCN, negative; $FeCl_3$, strains greyish brown, rubs off easily; $HgCl_2$, negative; KOH, negative. The Talmadge hardness is B.

Tiemannite gave an *x*-ray powder pattern of the sphalerite type

(Fig. 23, Table 9), which is indexed on a cubic lattice with $a=6.072$ kX, in good agreement with the value $a=6.069$ A given by Hartwig (1926). With 4[HgSe] in the unit cell the calculated specific gravity is 8.24, confirming the measured values, G = 8.24–8.27.

The compound HgSe was prepared by fusing the elements in equal atomic proportions in a vacuum. The components fused readily to a bright metallic globule with violent evolution of vapour and cooled to a shiny regulus with some loss of Hg as a mirror sublimate on the wall of the tubes. A section of this material is porous, greyish white and has no evidence of cleavage. An *x*-ray powder pattern (Fig. 24) of the product is practically identical to that of tiemannite (Fig. 23).

TABLE 9. TIEMANNITE—HgSe: *X*-RAY POWDER PATTERN

Cubic, $F\bar{4}3m$; $a=6.072$ kX; $Z=4$

I	θ(Cu)	*d*(meas.)	(*hkl*)	*d*(calc.)
10	12.7°	3.50	(111)	3.506
2	14.65	3.04	(002)	3.036
*2	15.95	2.80	—	—
8	21.05	2.14	(022)	2.147
*2	22.75	1.988	—	—
8	24.85	1.829	(113)	1.831
½	26.0	1.754	(222)	1.753
1	30.5	1.515	(004)	1.518
2	33.45	1.394	(133)	1.393
½	34.55	1.355	(024)	1.358
2	38.4	1.238	(224)	1.239
1	41.1°	1.169	(115) (333)	1.169
1	45.7	1.074	(044)	1.073
2	48.6	1.025	(135)	1.026
½	53.25	0.959	(026)	0.960
½	56.1	0.926	(335)	0.926
½	61.5	0.875	(444)	0.876
½	64.85	0.849	(117) (155)	0.850
1	71.3	0.811	(246)	0.811
1	76.55	0.790	(137)	0.790

* Extra lines not identified.

Since metacinnabar (HgS) is isostructural with tiemannite (HgSe), and onofrite (Dana, 1944, p. 216) has been described as a selenian variety of metacinnabar, Hg(S,Se), a series of Hg—Se—S fusions was made in order to prove or disprove the existence of a solid solution series between the end members, HgSe and HgS. In all, six fusions were made at 20 atomic per cent intervals. *X*-ray powder patterns of the products gave the sphalerite type of pattern for those fusions with 40 atomic per cent HgSe or more while those with less than 40 atomic per cent gave the cinnabar type of pattern.

Fig. B is a plot of the cube-edges and compositions of the fusion products of sphalerite type (black points) establishing a roughly linear relation. The crossed points represent the cube-edges and compositions, actual or inferred from the curve, of minerals: (1) metacinnabar,

($a = 5.835$ kX, R. B. Ferguson); (2) onofrite ($a = 5.906$, Hartwig, 1926); (3) onofrite (ROM, M7376, $a = 5.980$ kX, J.W.E.); (4) onofrite (ROM, M20131, $a = 6.001$ kX, J.W.E.); (5) tiemannite (ROM, M3872, M20129, $a = 6.072$ kX, J.W.E.).

The plot indicates that there is a metacinnabar-tiemannite series which may be continuous in nature but ranges only from $HgS_{60}HgSe_{40}$ to HgSe under fusion conditions. Intermediate members of the series have been called onofrite. Onofrite from Pinte County, Utah, is evidently sulfurian tiemannite, while the mineral measured by Hartwig, in keeping with the analysis of onofrite from San Onofre, Mexico (Dana, 1944, p. 216), is properly called selenian metacinnabar.

Klockmannite—CuSe

For a full account of this species see the detailed study of natural and artificial klockmannite which appeared recently in this journal (Earley, 1949).

Penroseite—$(Ni,Cu)Se_2$

Penroseite, Colquechaca, Bolivia (ROM, M18460); massive ore specimen; botyroidal and radiating structures; old surfaces coated with limonite and other alteration products.

Penroseite and clausthalite, Colquechaca, Bolivia (ROM, M19163); granular to massive penroseite with interstitial clausthalite showing small siliceous veinlets and brick-red incrustations.

Fresh surfaces of penroseite are steel-grey tarnishing rapidly to a dull lead-grey. Weathered specimens show a brownish coating of limonite or goethite and a brick-red material which was not identified but is comparable to the incrustations of "ahlfeldite" mentioned by Bannister & Hey (1937). The mineral is brittle and fractures with imperfect cubic cleavage or subconchoidally. Although none of the material was entirely suitably for specific gravity measurements due to the many small veinlets of clausthalite, six measurements of carefully chosen cleavage fragments gave G = 6.58–6.74 with the Berman balance.

A section of penroseite polishes unevenly to a pitted surface and is creamy greyish white, somewhat less lustrous than the intergrown clausthalite. It is clearly isotropic. The etch reactions are substantially the same as those given by Gordon (1926): HNO_3 (1:1), stain iridescent subsequently etching a rough grey surface; HCl (1:1), negative; $FeCl_3$, negative; KCN, greyish brown stain; $HgCl_2$, negative; KOH, negative. The Talmadge hardness is C+, slightly harder than chalcopyrite.

Penroseite (ROM, M18460) gave an x-ray powder pattern (Fig. 19) of the pyrite type which can be indexed on a cubic lattice with $a = 5.979$ kX, in fair agreement with the value $a = 6.001$–6.017 A, given by Bannister & Hey (1937). The measured spacings in Table 11 are essentially the same as those given by Harcourt (1942, p. 93).

Compounds with the gross composition $(Ni,Cu,Pb)_2$ Se were prepared by fusing the elements in various atomic proportions in a vacuum. In general, the elements fused with difficulty at high temperatures (1000–1200° C.) to a sinter-like steel-grey mass. However, those fusions containing lead gave small globules of a bright metallic component which proved to be PbSe (clausthalite). A polished section of the sinter-like material is similar to penroseite. Table 10 gives the composition of the fusions, the products formed, and the cube-edge of the nickel bearing components.

TABLE 10. Ni-Cu-Pb-Se FUSIONS

Composition of Fusion	Products	Cube-edge of Ni-Component
$NiSe_2$	$NiSe_2$	5.945 kX
$(Ni,Pb)Se_2$(10% Pb)	$NiSe_2+PbSe$	5.945 kX
$(Ni,Pb, Cu)Se_2$(12% Pb, 5% Cu)	$(Ni,Cu)Si_2+PbSe$	5.962 kX
$(Ni,Cu)Se_2$(7% Cu)	$(Ni,Cu)Se_2$	5.979 kX

TABLE 11. PENROSEITE—$(Ni,Cu)Se_2$: X-RAY POWDER PATTERN

Cubic, *Pa*3; *a*=5.979 kX; *Z*=4

I	θ(Cu)	*d*(meas.)	(*hkl*)	*d*(calc.)
*1	12.5°	3.55	—	—
3	14.8	3.01	(002)	2.990
9	16.7	2.67	(021)	2.674
9	18.3	2.45	(112)	2.441
*1	20.85	2.16	—	—
1	21.3	2.12	(022)	2.114
½	22.7	1.992	(003)	1.991
*½	24.65	1.843	—	—
8	25.25	1.802	(113)	1.803
½	26.55	1.720	(222)	1.726
3	27.6	1.659	(023)	1.658
4	28.8	1.596	(123)	1.598
1	31.0	1.493	(004)	1.494
*1	34.4	1.361	—	—
½	35.25	1.332	(024)	1.337
2	36.2	1.301	(124)	1.395
1	37.1	1.274	(233)	1.275
½	39.05	1.220	(224)	1.220
3	42.0°	1.149	(115) (333)	1.150
2	43.9	1.109	(025) (234)	1.110
1	44.85	1.090	(125)	1.091
2	46.8	1.054	(044)	1.057
½	50.6	0.995	(006)	0.996
½	51.6	0.981	(016)	0.983
2	52.55	0.968	(116) (235)	0.970
1	57.6	0.910	(335)	0.912
1	59.6	0.891	(036)	0.891
1	60.7	0.881	(136)	0.881
½	68.0	0.829	(046)	0.829
1	69.4	0.821	(027) (146)	0.821
1	70.9	0.814	(255) (336)	0.814

* Extra lines due to clausthalite.

These cube-edge values are somewhat smaller than the values, $a=6.022$ A, given by de Jong & Willems (1928) for artificial $NiSe_2$. Since the addition of Pb produces no change in the cube-edge and results in visible PbSe (clausthalite), Pb apparently does not enter in the composition of penroseite. On the other hand the addition of Cu causes a progressive increase in cube-edge, the compound with 7% Cu (Fig. 20) giving exactly the cube-edge measured on natural penroseite.

From these observations penroseite is cubic as described by Bannister & Hey (1937) and not orthorhombic as suggested by Gordon (1926). The significant amounts of lead found in penroseite by Bannister & Hey (1937) are probably due to intergrown clausthalite.

Other Selenides

Guanajuatite—$Bi_2(S,Se)_3$

Two specimens of guanajuatite (ROM, M3773, M3826, Guanajuato, Mexico) are physically and optically similar to bismuthinite. An *x*-ray powder pattern (Fig. 25) of guanajuatite (ROM, M3773) shows that this specimen is isostructural with bismuthinite and by analogous indexing gives $a=11.35$, $b=11.48$, $c=4.04$ kX, as compared to $a=11.32$, $b=4.17$, $c=11.48$, all ± 0.02 A (Ramdohr, 1948*a*). A series of pyrosynthetic compounds, $Bi_2(S, Se)_3$, showed that Se can replace S up to $Se:S=1:1$ in the bismuthinite structure.

Paraguanajuatite—Bi_2Se_3(?)

No specimen of this mineral was available for study. Ramdohr (1948*a*, 1948*b*, p. 360) states that guanajuatite is paramorphosed in part to rhombohedral *paraguanajuatite* which corresponds to the artificial compound Bi_2Se_3 and has a structure similar to that of tellurbismuth Bi_2Te_3 and tetradymite Bi_2Te_2S. For paraguanajuatite Ramdohr gives hexagonal elements, $a=4.076$, $c=54.7$ A, which are not very close to $a=4.125$, $c=28.56$ (R. M. Thompson, *priv. comm.*) for artificial Bi_2Se_3. The *x*-ray powder pattern of this compound (Fig. 26) is distinctly different from that of guanajuatite (Fig. 25). Possibly paraguanajuatite with its smaller dimensions, *a* and *c*/2, carries S and has the composition $Bi(Se,S)_3$.

CLASSIFICATION

This study of the mineral selenides largely tends to confirm the classification of these minerals in Danna (1944, p. 157); at the same time it suggests certain modifications.

Under the chemical type A_2X naumannite and aguilarite are appropriately placed with argentite as the non-cubic low temperature β-phases which have inverted from cubic high temperature α-phases and have inherited pseudo-cubic crystal forms. The tetragonal or pesudo-tetragonal character of eucairite and crooksite suggest that these minerals might properly be placed in an appropriate sub-group of the A_2X type. The proof that berzelianite has a defective structure $Cu_{2-x}Se$ analogous to that of digenite $Cu_{2-x}S$, and that these minerals do not exist at the corresponding stoichiometric proportions, indicates the need of a separate $A_{2-x}X$ type (digenite group).

From the point of view of composition umangite falls in the A_3X_2 group but physically the mineral resembles rickardite whose structural formula is $Cu_{4-x}Te_2$ with x nearly 1. Even though umangite is not isostructural with rickardite it is possible that the selenide is a grossly defective compound $Cu_{4-x}Se_2$. In this connection it is noteworthy that the A_3X_2 type of Dana is represented only by maucherite with the probably defective structure $Ni_{11}As_8$, umangite, and bornite, Cu_5FeS_4, among which there are no structural relationships and the proportions A_3X_2 are not well shown. The classification of clausthalite, tiemannite, klockmannite and penroseite, is confirmed, and it is shown that onofrite is applicable to intermediate members of a metacinnabar-tiemannite series.

CLASSIFICATION OF THE SELENIDE MINERALS

A_2X type	
Non-cubic low temperature β-phases (argentite group)	
Naumannite	Ag_2Se
Aguilarite	Ag_4SeS
Tetragonal or pseudo-tetragonal	
Eucairite	$AgCuSe$
Crookesite	$(Cu,Tl,Ag)_2Se$
$A_{2-x}X$ type	
Cubic (digenite group)	
Berzelianite	$Cu_{2-x}Se$
A_3X_2 type	
Orthorhombic	
Umangite	Cu_3Se_2
AX type	
Cubic (galena group)	
Clausthalite	$PbSe$
Cubic (sphalerite group)	
Tiemannite	$HgSe$
Onofrite	$Hg(Se,S)$
Hexagonal (covellite group)	
Klockmannite	$CuSe$
AX_2 type	
Cubic (pyrite group)	
Penroseite	$(Ni,Cu)Se_2$

REFERENCES

ASTM (1945): X-ray diffraction patterns, first supplementary set of cards -*Am. Soc. Test. Mat.* (Philadelphia).

Bannister, F. A. & Hey, M. H. (1937): The identity of penroseite and blockite—*Am. Mineral.*, **22,** 319–324.

Borchert, W. (1945): Gitterumwandlungen im System $Cu_{2-x}Se$—*Zeits. Krist.*, **106,** 5–24.

Dana, E. S. (1892): *System of Mineralogy*, ed. 6—New York.

Dana, J. D. & E. S. (1944): *System of Mineralogy*, **1,** by C. Palache, H. Berman & C. Frondel—New York.

Davey, W. P. (1923): Berzelianit—*Phys. Rev.*, **21,** 380.

De Jong, W. F. & Willems, H. W. V. (1928): Die Verbindungen $FeSe_2$, $CoSe_2$ und $NiSe_2$—*Zeits. anorg. Chem.*, **170,** 241–245.

Earley, J. W. (1949): Studies of natural and artificial selenides: I—Klockmannite, CuSe—*Am. Mineral.*, **34,** 435–440.

Forman, S. A. & Peacock, M. A. (1949): Crystal structure of rickardite, $Cu_{4-x}Te_2$—*Am. Mineral.*, **34,** 441–451.

Gordon, S. G. (1926): Penroseite and trudellite: two new minerals—*Proc. Acad. Nat. Sci. Philadelphia*, **77,** 317–324.

Harcourt, G. A. (1942): Tables for the identification of ore minerals by *x*-ray powder patterns—*Am. Mineral.*, **27,** 63–113.

Hartwig, W. (1926): Die Kristallstruktur von Berzelianit—*Zeits. Kryst.*, **64,** 503–504.

Hiller, J. E. (1940): Die Gitterkonstanten von Crookesit, Argyrodit und Canfieldit - *ZBl. Min.*, A, 138–142.

Hintze, C. (1904): *Handbuch der Mineralogie*, **1**(1)—Leipzig.

Klockmann, F. (1891): Mineralogische Mittheilungen aus den Sammlungen der Bergakademie zu Clausthal—*Zeits. Kryst.*, **19,** 269–272.

Nordenskiöld, A. E. (1866): Undersokning of selenminerlaierna från Skrikerum *Svenska Acad. Öfv. Handl.*, **23,** 355–367.

Olshausen, S. v. (1925): Strukturuntersuchungen nach der Debye-Scherrer-Methode—*Zeits. Krist.*, **61,** 463–514.

Peacock, M. A. & Berry, L. G. (1947): Studies of mineral sulpho-salts; XIII—Polybasite and pearceite—*Min. Mag.*, **28,** 1–13.

Rahlfs, P. (1936): Über die kubischen Hochtemperaturmodifikationen der Sulfide, Selenide und Telluride des Silbers und des einwertigen Kupfers—*Zeits. phys. Chem.*, (B) **31,** 157–194.

Ramdohr, P. (1948*a*): The mineral species guanajuatite and paraguanajuatite (*trans.*)—*Comite direct invest recursos mineral. Méx.*, Bol., **20,** 1–15 [*Chem. Abs.*, **43,** 4979, 1949].

—— (1948*b*): *Klockmann's Lehrbuch der Mineralogie*, ed. 13—Stuttgart.

Ramsdell, L. S. (1943): The crystallography of acanthite, Ag_2S—*Am. Mineral.*, **28,** 401–425.

Rose, G. (1828): Selenmineralien—*Pogg. Ann.*, **14,** 471–473.

Schneiderhöhn, H. & Ramdohr, P. (1931): *Lehrbuch der Erzmikroskopie*, 2—Berlin.

Short, M. N. (1940): Microscopic determination of the ore minerals—*U.S.G.S.*, Bull. **914.**

Thompson, R. M. (1949): The telluride minerals and their occurrence in Canada—*Am. Mineral.*, **34,** 342–384.

Waldo, A. W. (1935): Identification of the copper ore minerals by means of *x*-ray powder diffraction patterns—*Am. Mineral.*, **20,** 575–597.

ON PSEUDOMALACHITE AND CORNETITE

L. G. BERRY*

Queen's University, Kingston, Ontario, Canada

ABSTRACT

New observations combined with existing chemical analyses on pseudomalachite and cornetite from several localities lead to the following description of the two minerals.

Pseudomalachite is monoclinic, prismatic, with space group $P2_1/a$; the unit cell with $a=17.06$, $b=5.76$, $c=4.49$A, $\beta=91°02'$, $a:b:c=2.962:1:0.7795$ contains $Cu_{10}(PO_4)_4(OH)_8 = 2[Cu_5(PO_4)_2(OH)_4]$; calculated specific gravity 4.34. Cleavage (100) perfect and difficult. Specific gravity 4.30–4.35 (coarse crystalline material), 4.08–4.21 (radiating and cryptocrystalline materials). Many specimens labelled pseudomalachite, dihydrite, ehlite, lunnite, tagilite, phosphorochalcite and prasine give the x-ray powder pattern of pseudomalachite.

Cornetite is orthorhombic, dipyramidal, with space group *Pbca*; the unit cell with $a=10.88$, $b=14.10$, $c=7.11$A, $a:b:c=0.772:1:0.504$. contains $Cu_{24}(PO_4)_8(OH)_{24} = 8[Cu_3PO_4(OH)_3]$; calculated specific gravity 4.10. Crystals commonly dipyramidal, showing forms $d(210)$, $v(121)$, $n(021)$, $p(221)$ with $(021):(0\bar{2}1)=90°33'$ (calc.) No cleavage observed. Specific gravity 4.10 (Hutchinson & MacGregor). Ungemach's elements (1929) transformed to the structural setting by 001/200/010 become 0.7715:1:0.5048.

PSEUDOMALACHITE—$Cu_5(PO_4)_2(OH)_4$

Pseudomalachite, dihydrite, ehlite, lunnite, phosphorochalcite, kupferdiaspore, prasine, and tagilite are among the names found in mineralogical literature for basic copper phosphates, generally similar to malachite in colour.

Wide variation in occurrence as distinct crystals, radiating aggregates and cryptocrystalline crusts together with variation in chemical composition is responsible for the variety of names. Schrauf (1879) proposed the name lunnite for a group including dihydrite, ehlite and phosphorochalcite as members of a series. Dihydrite was retained by Dana (1892) for the distinctly crystalline material and pseudomalachite for the radiating and cryptocrystalline materials.

In the course of this study a large number of museum specimens bearing the above names were examined. The great majority of these specimens yielded an identical x-ray powder pattern, a few proved to be malachite, and two gave patterns which have not been identified. The name psuedomalachite (Hausmann, 1813) which has priority, is retained for this mineral.

Materials and acknowledgements. Most of the specimens were loaned from Harvard Mineralogical Museum (HMM), United States National Museum (USNM), Royal Ontario Museum (ROM), and American Museum of Natural History (AMNH), through the courtesy of Dr. C.

---

* Associate Professor, Department of Mineralogy.

Frondel, Dr. W. F. Foshag and Mr. E. P. Henderson, Dr. V. B. Meen, and Dr. F. Pough respectively. The following specimens yielded the *x*-ray powder pattern of pseudomalachite:

1. Pseudomalachite (Queen's University A570) Rheinbreitinbach, Germany; dark green sub-spherical radiating aggregates on white and rusty quartz.
2. Dihydrite (ROM, M6762), Ehl, near Linz on the Rhine, Germany; green spherical aggregates in vugs in milky quartz.
3. "Lunnite near pseudomalachite" (HMM, Holden Coll., 100), Rheinbreitinbach, Rhenish Prussia; dark green crystals and sub-parallel aggregates with chalcedony in white and rusty fractured quartz.
4. Pseudomalachite (HMM, Holden Coll., 537), Rheinbreitinbach, Rhine Province, Germany; dark green aggregates and single crystals (0.5 mm. to 4 mm. long) on iron stained chert.
5. "Dihydrite" (USNM, R5381), Virneberg, Linz, Germany; dark green aggregate of crystals in opening in fractured white and rusty quartz.
6. Pseudomalachite *var.* lunnite (HMM, 61341), Rheinbreitinbach; dark green crust 2 mm. thick, coating milky quartz.
7. "Ehlite" (HMM, 90456), Ehl, Germany; rough dark green crystals on yellowish brown cherty matrix.
8. Pseudomalachite (HMM, 61351), Virneberg; radiating aggregates of dark green to black crystals on rusty chert and white milky quartz.
9. "Lunnite" (HMM), Nassau, Germany; dark green radiating aggregate.
10. Pseudomalachite (HMM), Bogoslovsk, Urals; bright green very fine grained radiating aggregate with concentric banding.
11. "Phosphorochalcite" (HMM), Rheinbreitinbach; bright green fine grained aggregate with concentric bands, smooth surface with fused appearance.
12. "Lunnite" (USNM, R5388), Rheinbreitinbach; dark green radiating groups.
13. "Ehlite" (USNM, R5387) Ehl, Germany; bright green radiating crust.
14. "Tagilite" (HMM, Holden coll., 2970), Nizhni Tagilsk, Ural; bright green and finely crystalline with smooth "fused" surface, with libethenite.
15. "Tagilite" (HMM, 61271), Nischne Tagilsk, Ural; bright green coating.
16. "Ehlite" (HMM, 61391), Ehl near Linz; dark green radiating spherical and sub-spherical aggregates up to 7 mm. diameter on rusty and milky chert.
17. "Prasin" (HMM, Pearce coll.), Libethen, Hungary; dark green botryoidal crust.
18. Pseudomalachite (AMNH, 15329), Rheinbreitinbach, Germany; dark green crystalline aggregates on chalcedony.
19. Pseudomalachite (AMNH, 15314), Ehl, Germany; bright green bladed rosettes coated by chalcedony.
20. Pseudomalachite (AMNH, 15325), Cornwall; bright green coating on quartz.
21. "Lunnite" (AMNH, 15322), Virneberg, Germany; dark green crystalline crust on quartz.
22. Pseudomalachite (AMNH, 15323), Libethen, Hungary; dark green compact knobs on quartz and limonite.
23. "Ehlite" (USNM, R5386), Liskeard, Cornwall; bright green coating on quartz.
24. "Dihydrite (USNM, 103826), Emme Mine, Deserta, Chile; dull green cryptocrystalline material with finely crystalline coating.
25. "Dihydrite" (USNM, C4202), Linz, Prussia; dark green radiating aggregate, 1¼″ radius in milky quartz.
26. "Ehlite" (ROM, M15549), Nizhni Tagilsk; bright green radiating aggregate with shiny botryoidal surface and concentric layers, partial outer coating of malachite.

27. "Dihydrite" (AMNH, 15327), Rheinbreitinbach; dark green crust coating and coated by quartz.

28. "Tagilite" (HMM, 61281), Tagilsk, Urals; dark green crystalline crust with libethenite and malachite.

29. Pseudomalachite (HMM), Empire-Nevada mine, Yerrington, Nevada; bright green crust.

30. "Dihydrite" (USNM, R5382), Bogollo Portugal; green crust on dark limonitic rock with libethenite.

31. Pseudomalachite, *var.* ehlite (HMM, 61321), Ehl near Linz; bright green crystalline crust on dense milky quartz.

32. "Dihydrite" (USNM, C4201), Rhenish, Prussia; green radiating crust with botryoidal surface and concentric banding.

33. Pseudomalachite, *var.* prasine (HMM, 61371), Libethen, Hungary, green botryoidal crust.

34. "Cornwallite with olivenite" (ROM, M11677), Wheal Unity, St. Day, Cornwall; dark green shiny cryptocrystalline crust with libethenite.

35. "Cornwallite" (HMM, 96231) Wheal Unity, Cornwall, England; green cryptocrystalline crust with libethenite.

36. On cornetite (USNM, R5345), Étoile du Congo, Katanga, bright green spherical aggregates on cornetite.

Physical Properties. Specific gravity determinations, made with the Berman balance, yielded the values given in Table 1. The specific gravity obtained for single crystals or coarse crystalline aggregates (materials 1, 3 and 8) agree closely with values given by Schrauf. The values obtained for finely crystalline radiating aggregates are distinctly lower, suggesting the presence of impurities.

The values for specific gravity given in the literature for analyzed materials are arranged in Table 1 in order of increasing water content. They show a similar variation, many of the higher values are for coarsely crystalline materials while most of the low values are for fine radiating aggregates and cryptocrystalline materials. The specific gravities corresponding to analyses 6, 7, 8 and 13 are not corrected for the malachite shown in the analyses. The colour is lighter for the finer grained materials which usually show a higher water content.

Structural Crystallography. The specimen of pseudomalachite (material 1) at first available to the writer did not show single crystals but yielded a cleavage fragment suitable for single crystal study. This fragment was difficult to orient and did not yield films from which β could be determined. Weissenberg resolutions about a and c indicated a sensibly rectangular lattice but with distinct monoclinic symmetry. Rotation and Weissenberg films about b on materials 2 and 3 readily yielded all the lattice dimensions. Since most crystals on our specimens are quite rough and the β angle is close to 90°, precession camera films about b are particularly valuable for identification of the forms, particularly in distinguishing between (hkl) and $(\bar{h}kl)$. Typical precession films of the zero layer ($h0l$) and the first layer ($h1l$) are shown in Figs. 1 and 2. The lattice dimensions determined from these films are given in Table 2. The rotation and Weissenberg films were taken with CuK and FeK radiation; CuK and MoK radiations were used for the precession films. The

TABLE 1.—PSEUDOMALACHITE: SPECIFIC GRAVITY

New Measurements	
Pseudomalachite, Rheinbreitinbach, Germany (material 1)	4.33
"Dihydrite," Ehl, Germany (material 2)	4.15
"Lunnite," Rheinbreitinbach (material 3)	4.35
Pseudomalachite, Virneberg (material 8)	4.30
"Lunnite," Nassau, Germany (material 9)	4.21
Pseudomalachite, Bogoslovsk, Urals (material 10)	4.17
"Phosphorochalcite," Rheinbreitinbach (material 11)	4.18
"Ehlite," Nizhni Tagilsk, Urals (material 26)	4.08
Old Measurements from Literature	
"Dihydrite," Nizhni Tagilsk (anal. 4)	4.4
"Dihydrite," Rheinbreitinbach (anal. 5)	4.309
Pseudomalachite, Nizhni Tagilsk (anal. 6 and 7)	4.24
Pseudomalachite, Nizhni Tagilsk (anal. 8)	4.06
"Phosphorochalcite" Nizhni Tagilsk (anal. 10)	4.25
Pseudomalachite, Katanga (anal. 11)	3.58
Pseudomalachite, Nizhni Tagilsk (anal. 13)	4.13
"Ehlite," Ehl (anal. 3 and 15)	4.1024
Pseudomalachite, Nizhni Tagilsk (anal. 17)	4.175
"Phosphorochalcite," Virneberg (anal. 18)	4.40
Pseudomalachite, Libethen (anal. 19)	4.1556
"Prasine" (anal. 22)	3.98
"Lunnite," Cornwall (anal. 23)	4.25
"Ehlite," Cornwall (anal. 24, 33, 35)	3.911 to 4.23
"Phosphorochalcite," Virneberg (anal. 26)	4.2 to 4.4
"Phosphorochalcite," Nizhni Tagilsk (anal. 27)	4.0
"Ehlite," Ehl (anal. 31 or 32)	4.198
"Ehlite," Nizhni Tagilsk (anal. 38)	3.80
"Tagilite," Nizhni Tagilsk (anal. 39)	3.50

β angle was deduced from the measured spacings of (100), (001), (401), $(\bar{4}01)$, (601), and $(\bar{6}01)$, as well as from direct measurement on Weissenberg and precession resolutions of the zero layer ($h0l$).

The values obtained for the lattice dimensions agree well with the average values:

$$a = 17.06,\ b = 5.76,\ c = 4.49 \text{ A},\ \beta = 91°02$$

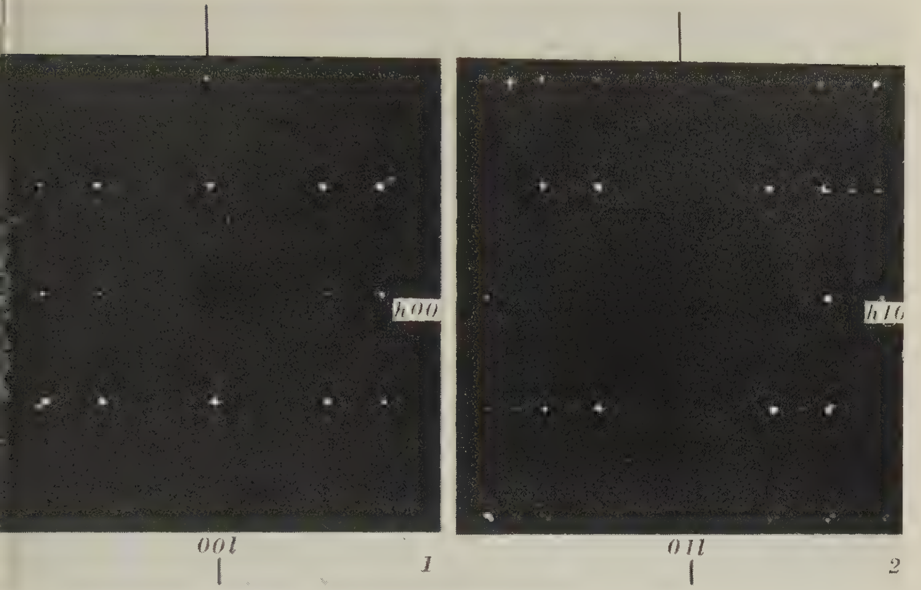

FIGS. 1, 2. Pseudomalachite, Rheinbreitinbach, Germany (material 3): *x*-ray precession photographs with Cu$K\alpha$ radiation; film to specimen distance 60 mm. reproduced $\frac{2}{3}$ actual size. FIG. 1. The zero level ($h0l$) showing diffractions present only with $h=2n$ characteristic of the space group $P2_1/a$. FIG. 2. The first level ($h1l$) with all diffractions present. Both films show the near orthorhombic character of the lattice with $\mu = 88°58'$.

TABLE 2. PSEUDOMALACHITE: LATTICE DIMENSIONS[1]

Material	Type of Films	a	b	c	β
1	Rotation, Weissenberg about a and b	17.03 A	5.76 A	4.49 A	90°±1°
2	Rotation, Weissenberg about b and c	17.10	5.76	4.49	90°57′
3	Rotation, Weissenberg about b	17.04	5.75	4.48	91 01
	Precession about b	17.08	—	4.49	91 00
4	Precession about b	17.02	—	4.50	[91 32]
5	Precession about b & c	17.08	5.75	4.47	91 07
8	Precession about b & c	[17.16]	5.77	4.49	[91 22]
31	Precession about b & c	[17.14]	5.76	4.49	91 05
	Average*	17.06	5.76	4.49	90°02′

[1] Using Cu$K\alpha$ 1.5418, Fe$K\alpha$ 1.9373, Mo$K\alpha$ 0.7107 A, mass factor 1.6602.

* Omitting bracketed values.

The observed diffractions conform to the conditions: (hkl) present in all orders, $(h0l)$ present only with $h=2n$, $(0k0)$ present with $k=2n$; these criteria are characteristic for the space group. $C_{2h}^5-P2_1/a$.

Geometrical Crystallography. Single crystals occur on several of the available specimens of pseudomalachite and a number of these were mounted for measurement on the two-circle goniometer. On most crystals only the faces of the pinacoid $a(100)$ give good reflections, other faces are usually rough, rounded, or rarely striated. Most of these crystals were adjusted on the goniometer with (100) polar and measured in that position. The measured angles for materials 4, 5, 27 and 31, clearly very poor, were converted to ϕ, ρ angles graphically on a stereographic net. The indexing of the terminal faces was clearly established by a zero layer precession photograph about the b-axis of one of the measured crystals of materials 4, 5 and 31. The crystals from material 3, although usually fragments from subparallel aggregates, are quite sharp and most faces give fair signals, $a(100)$ and $T(\bar{2}01)$ give excellent signals. Fully developed crystals are not present on material 3, all the measured crystals show only $(\bar{h}0l)$ and $(\bar{h}kl)$ terminal faces and no crystals show the faces (001) and (100) intersecting. Fig. 3 illustrates a typical crystal of material 4 and Fig. 4 a typical crystal of materials 5 and 8. In Table 3, the measured ϕ_2 and ρ_2 angles for material 3 are given together with

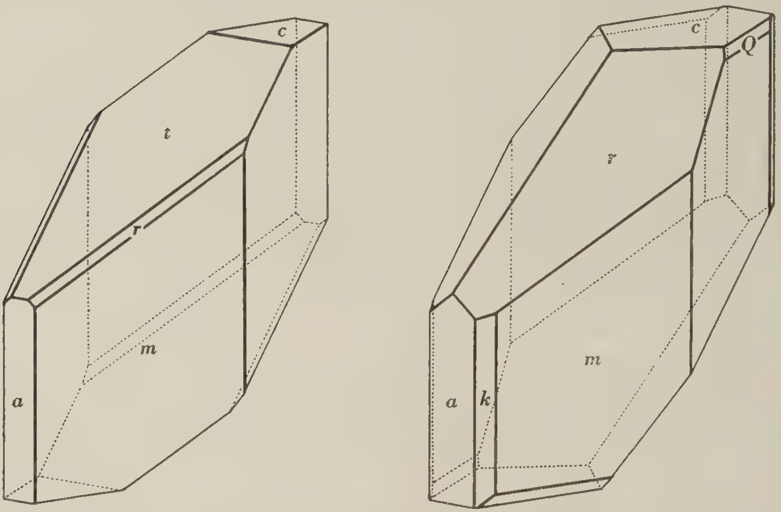

FIGS. 3, 4. Pseudomalachite, crystal drawings. FIG. 3 (left). Rheinbreitinbach, Germany (material 4), showing the forms $c(001)$, $a(100)$, $m(110)$, $t(201)$ and $r(311)$. FIG. 4 (right). Virneberg, Linz, Germany (materials 5 and 8), showing the forms $c(001)$, $a(100)$, $m(110)$, $k(210)$, $r(311)$ and $Q(\bar{3}31)$ or $(\overline{10}.8.3)$.

ϕ and ρ angles obtained stereographically from angles measured with (100) polar for crystals of other materials. With the latter crystals, the original measurements are so poor that no loss of accuracy results from this procedure. The ($hk0$) faces, which are very rough and rounded, have been indexed as $m(110)$ although the measured ϕ angles differ by 4° to 6° from the calculated angles. The indexing of these forms is therefore quite rough.

The measured angles for material 3 give rather widely divergent values for the polar elements; which in turn yield the average values:

$$r_2:p_2:q_2=1.239:0.3422:1;\ \mu=87°58'$$

The axial ratio, obtained from these polar elements, agrees poorly with the triclinic elements given by Schrauf (1879) and the structural lattice axial ratio:

$a:b:c\ =2.924\ :1:0.808\quad \beta=92°02'$ (goniometric)
$a:b:c/2=2.8252:1:0.7669\quad \alpha=89°29\tfrac{1}{2}'\ \beta=91°00\tfrac{1}{2}'\ \gamma=90°39\tfrac{1}{2}'$ (Schrauf)
$a:b:c\ =2.962\ :1:0.7795\quad \beta=91°02'$ (x-ray)

The majority of published drawings of pseudomalachite crystals together with the crystals studied here clearly suggest monoclinic symmetry; this is now confirmed by the x-ray films. The measured interfacial angles given by Schrauf when considered in the light of known monoclinic symmetry, show inconsistencies similar to those in the measured angles given here. Schrauf took the inconsistencies seriously and deduced triclinic elements with interaxial angles close to 90°; he also gave rather improbably indices to some faces. It is, therefore, proposed that the structural lattice axial ratio best represents crystals of pseudomalachite. These elements have been used to calculate the following angle table (Table 4).

A comparison of the measured angles with the calculated angles reveals fair agreement for a few forms but generally poor for most forms. Schrauf's symbols are converted to the structural setting by dividing the l index by 2.

Composition and cell content. The structural lattice dimensions combined with the measured specific gravity (4.309) and chemical analysis of the crystalline material ("dihydrite") from Rheinbreitinbach, Germany (Schrauf, 1879) gives the numbers of atoms in the unit cell (Table 5). The number of atoms (3) clearly indicate the structural formula:

$$Cu_{10}(PO_4)_4(OH)_8=2[Cu_4(PO_4)_2(OH)_4]$$

with the ideal numbers of atoms in column 4. The specific gravity calculated for this structural formula is 4.34 in close agreement with the measured values for well crystallized specimens (Table 1).

TABLE 3. PSEUDOMALACHITE: CRYSTAL MEASUREMENTS

Rheinbreitinbach (material 3)—8 crystals

Form	Number of Faces	Quality	Average		Range	
			ϕ_2	ρ_2	ϕ_2	ρ_2
c(001)	5	good	89° 27′	90° 00′	89° 04′–89° 43′	—
a(100)	5	good	0 00	90 00	—	—
m(110)	5	rough	0 00	19 23	—	18° 55′–20° 49′
k(210)	4	striated	0 00	33 47	—	33 14 –34 11
j(310)	1	striated	0 00	40 00	—	—
T($\bar{2}$01)	7	good	116 50	90 00	116 43 –116 59	—
D($\bar{4}$43)	3	rough	108 40	48 05	108 06 –108 48	46 40 –49 20
S($\bar{3}$12)	1	rough	110 57	72 05	—	—
R($\bar{3}$11)	6	rough	127 39	57 18	126 21 –129 44	56 18 –58 08
($\overline{12}$.3.2)	3	rough	146 04	55 44	145 44 –146 29	54 39 –56 19

Rheinbreitinbach (material 4)—2 crystals

Form	Number of Faces	Quality	ϕ	ρ
c(001)	2	very rough	90°	1° 26′
a(100)	2	good	90	90
m(110)	4	rough, rounded	24¼	90
t(201)	2	rough	90	29
r(311)	4	rough	46	48¼

Virneberg, Linz, Germany (material 5)—2 crystals

Form	Number of Faces	Quality	ϕ	ρ
c(001)	2	very rough	90	3°
b(010)	1	narrow	0	90
a(100)	2	good	90	90
m(110)	6	large, rough	22	90
k(210)	4	narrow	36	90
r(311)	3	large, rough	42	53
($\overline{10}$.8.3)	4	narrow line	−23	65

Rheinbreitinbach (material 27)—1 crystal

a(100)	1	good	90	90
m(110)	2	rough, rounded	18½	90
t(201)	1	large, rough	90	31½
u(601)	1	small, rough	90	59½
r(311)	1	rough	46½	48½

TABLE 3—*continued*

Ehl, Linz, Germany (material 31)—3 crystals

c(001)	2	very rough	90	1½
a(100)	4	fair	90	90
m(110)	9	rough	21½	90
e(021)	4	narrow	6	53
r(311)	6	rough	47½	4
D($\bar{4}43$)	3	rough	−21	48

TABLE 4. PSEUDOMALACHITE: $Cu_5(PO_4)_2(OH)_4$

Monoclinic, $P2_1/a$

$a:b:c = 2.962:1:0.7795$; β 91° 02′, $r_2:p_2:q_2 = 1.283:0.3376:1$

$p_0:q_0:r_0 = 0.2632:0.7795:1$; $\mu = 88° 58'$, $p_0' = 0.2632$, $q_0' = 0.7795$, $x_0' = 0.0180$

Form	ϕ	ρ	ϕ_2	$\rho_2 = B$	C	A
c(001)	90° 00′	1° 02′	88° 58′	90° 00′	0° 00′	88° 58′
b(010)	0 00	90 00	—	0 00	90 00	90 00
a(100)	90 00	90 00	0 00	90 00	88 58	0 00
m(110)	18 39½	90 00	0 00	18 39½	89 40	71 20½
n(540)	22 53	90 00	0 00	22 53	89 36	67 07
l(430)	24 14½	90 00	0 00	24 14½	89 34½	65 45½
k(210)	34 02	90 00	0 00	34 02	89 25½	55 58
j(310)	45 22	90 00	0 00	45 22	89 16	44 38
e(021)	0 40	57 19½	88 58	32 41	57 19	89 26½
t(201)	90 00	28 34	61 26	90 00	27 32	61 26
u(601)	90 00	57 57	32 03	90 00	56 55	32 03
T($\bar{2}01$)	−90 00	26 57	116 57	90 00	27 59	116 57
f(332)	19 27	51 07	67 34	42 46½	50 46½	74 59
P($\bar{1}11$)	−17 27½	39 15½	103 46½	52 52	39 34½	100 57
D($\bar{4}43$)	−17 45½	47 30	108 25	45 24	47 49½	103 00
Q($\bar{3}31$)	−18 15½	67 54	127 39	28 22½	68 13½	106 52½
h(432)	24 58	52 12½	61 26	44 14½	51 47	70 31
r(311)	46 01	48 18	51 04½	58 46	47 34	57 30½
S($\bar{3}12$)	−44 02	28 27½	110 39	69 58	29 11	109 21½
H($\bar{4}32$)	−23 30	51 53½	116 57	43 49	52 18½	108 17
R($\bar{3}11$)	−44 42½	47 38½	127 39	58 19	48 22½	121 19½
($\overline{10}.8.3$)	−22 53	66 06	131 16½	32 37	66 30½	110 49½
($\overline{12}.3.2$)	−53 10	62 51½	147 21½	57 46	63 41	135 25

Table 5. Pseudomalachite: Composition and Cell Content

M = 1145

	1	2		3	4	5
CuO	69.25	9.96	Cu	9.96	10	69.09
FeO	0.19	0.03	Fe	0.03		
P_2O_5	23.86	1.93	P	3.86	4	24.65
H_2O	6.76	4.30	H	8.60	8	6.26
	100.06		0	23.94	24	100.00

1. Rheinbreitinbach, Germany; anal. Schrauf (1879) 2. Unit cell content. 3. Number of atoms in unit cell. 4. Ideal cell content $2[Cu_5(PO_4)_2(OH)_4]$. B. Composition for ideal cell content.

Table 6. Pseudomalachite: Analyses Reduced to 24 Atoms of Oxygen

	1	2	3	4	5	6	7	8
Cu	10.00	10.13	10.02	9.75	10.00	9.94	9.92	9.72
Fe	—	—	0.06	—	0.03	—	—	—
P	4.06	3.94	3.94	4.06	3.88	3.86	3.85	3.90
H	7.72	8.04	8.12	8.20	8.64	8.82	8.90	9.08
O	24.00	24.00	24.00	24.00	24.00	24.00	24.00	24.00

	9	10	11	12	13	14	15	16
Cu	9.78	9.80	10.43	10.57	9.61	9.48	9.88	9.71
Fe	—	—	—	—	—	—	0.05	—
P	3.87	3.80	3.52	3.44	3.81	3.84	3.65	3.09
As	—	—	—	—	—	—	—	0.17
H	9.11	9.40	9.52	9.64	9.76	9.86	9.88	10.06
O	24.00	24.00	24.00	24.00	24.00	24.00	24.00	24.00

	17	18	19	20	21	22	23	24
Cu	9.77	9.37	9.94	8.99	10.48	9.08	9.65	9.70
Fe	—	—	0.03	—	—	—	—	—
P	3.68	3.83	3.58	3.94	3.29	3.70	3.60	3.34
As	—	—	—	—	—	0.14	—	0.25
H	10.10	10.10	10.18	10.33	10.60	10.64	10.64	10.68
O	24.00	24.00	24.00	24.00	24.00	24.00	24.00	24.00

	25	26	27	28	29	30	31	32
Cu	8.76	10.27	9.43	9.43	9.01	9.86	9.25	9.46
Fe	—	—	—	—	—	—	0.29	—
P	3.97	3.33	3.66	3.65	3.81	3.47	3.51	3.80
H	10.73	10.80	10.82	10.90	10.92	10.94	11.08	11.10
O	24.00	24.00	24.00	24.00	24.00	24.00	24.00	24.00

Table 6—*continued*

	33	34	35	36	37	38	39	A	B
Cu	9.21	9.09	9.21	10.22	8.06	9.12	8.09	9.61	10
P	3.70	2.84	3.67	3.21	4.01	3.54	3.91	3.72	4
V	—	0.90	—	—	—	—	—		
H	11.12	11.12	11.24	11.32	11.82	12.05	12.26	10.16	8
O	24.00	24.00	24.00	24.00	24.00	24.00	24.00	24.00	24

1. "Dihydrite," Rheinbreitinbach, Germany; anal. Arfvedson (1825), in Dana (1892, p. 794, no. 2). 2. Pseudomalachite ("Kupferdiaspore"), Libethen, Hungary, fibrous, radiating; anal. Kühn (1844) (Dana, no. 22). 3. "Dihydrite," Eh., Germany; anal. Schrauf (1879, p. 14) from analysis 10 after deducting chrysocolla (Schrauf, 1879). 4. "Dihydrite," Nizhni Tagilsk, Russia, crystals; anal. Hermann (1846), (Dana, no. 1). 5. "Dihydrite," Rheinbreitinbach, hemispherical aggregates, crystals; anal. Schrauf (1879) (Dana, no. 3). 6, 7, 8 and 9. Nischni Tagilsk; anal. Nordenskiöld (1858), less malachite on basis of CO_2 given in analysis; 6 & 7. not distinctly crystallized; 8. compact massive; 9. nearly amorphous; in part in Dana (1882). 10. "Phosphorochalcite," Nizhni Tagilsk, nodules and tubular masses with fibrous structure; anal. Hermann (1846) (Dana, no. 9). 11. Pseudomalachite, Katanga, Belgian Congo, banded, fibrous masses; anal. Cesàro & Bellière (1922). 12. Pseudomalachite, Herschberg, spherical and radiating groups, anal. Kühn (1840) (Dana, no. 16). 13. Nizhni Tagilsk, fine fibrous; anal. Nordenskiöld (1858) in Dana (1882), after deducting 4.07% malachite. 14. Pseudomalachite, Rheinbreitinbach, fibrous; anal. Bergemann (1828). 15. "Ehlite," Ehl; anal. Schrauf (1879) (Dana, no. 15). 16. Phosphorochalcite, Linz; anal. Bergemann (1858) (Dana, no. 19). 17. Pseudomalachite, Nizhni Tagilsk, concentric layer structure; anal. Schrauf (1879) (Dana no. 20). 18. "Phosphorochalcite," Virneberg, spherical radiating masses; anal. Hermann (1846) (Dana, no. 4). 19. Pseudomalachite, Libethen, radiating concentric aggregates; anal. Schrauf (1879) (Dana, no. 21). 20. "Ehlite," Rheinbreitinbach, dark green spherical masses; anal. Bergemann (1828). 21. Pseudomalachite, Las Coste, fibrous reniform concretions; anal La Croix (1910). 22. "Prasine," radiating botryoidal shells; anal. Maskelyne & Flight (1872) (Dana, no. 11). 23. "Lunnite," Cornwall; minute radiating spheres; anal. Heddle (1855) (Dana, no. 8). 24. "Ehlite," Cornwall, radiating globules; anal. Church (1873) (Dana, no. 12). 25. "Ehlite," Rheinbreitinbach, spherical masses; anal. Bergemann (1828). 26. "Phosphorochalcite," Virneberg, near Rheinbreitinbach; anal. Rhodius (1847). 27. "Phosphorochalcite," Nizhni Tagilsk, lamellar masses with curved radiating structure; anal. Hermann (1846). 28. "Ehlite," Nizhni Tagilsk; anal. Wendel in Rammelsberg (1875) (Dana no. 10). 29. "Ehlite," Ehl; anal. Bergemann (1828) (Dana, no. 6). 30. "Phosphorochalcite," Rheinbreitinbach, dense masses; average of 3 analyses, Kühn (1844) (Dana, no. 17). 31. "Ehlite," Ehl; anal. Nordenskiöld (1858) (Dana, 1882, no. 4). 32. "Ehlite," Ehl; anal. Nordenskiöld in Rammelsberg (1860) (Dana, no. 5). 33. "Ehlite," Cornwall; anal. Church (1873) (Dana no. 14). 34. "Ehlite," Ehl; anal. Bergemann (1858) (Dana, no. 7). 35. "Ehlite," Cornwall; anal. Church (1873) (Dana, no. 13). 36. "Prasine," Libethen; anal. Church (1864) (Dana, no. 18). 37. "Tagilite," Mercedes mine, Coquimbo, Chile, stellated and fibrous masses on limonite; anal. Field (1859) in Dana (1892). 38. "Ehlite," Nizhni Tagilsk; anal. Hermann (1846). 39. "Tagilite," Nizhni Tagilsk; anal. Hermann (1846) in Dana (1892), less 1.75% limonite. A. Average cell content from 39 analyses. B. Ideal cell content for $2[Cu_5(PO_4)_2(OH)_4]$.

The numerous published analyses of pseudomalachite show considerable variation and have led to several empirical formulae. The empirical formula $Cu_5P_2H_4O_{12}$ proposed by Schrauf for dihydrite is confirmed by the unit cell content. Other formulae have been deduced from analyses showing higher water content.

The available analyses of pseudomalachite in Table 6 which have been reduced to atomic proportions on the basis of 24 oxygen atoms are arranged in order of increasing H content. The average numbers of atoms (column A) agree reasonably well with the ideal cell content except in the number for H which is close to 10. In many cases the apparent high water content is probably due to admixed malachite which is a very common associate especially at Nizhni Tagilsk, Siberia. Nordenskiöld's analyses (6, 7, 8, 9, 13) of this material, which all show CO_2, fit the ideal cell content fairly well when malachite is deducted. Chrysocolla, deducted by Schrauf from analysis 10 resulting in analysis 3, may be present in other analysed materials. The cryptocrystalline materials appeared homogeneous and identical with the crystalline upon examination by *x*-ray powder patterns.

Optical Properties. Optical data for pseudomalachite have been published by Larsen (1921) and by Barth & Berman (1930). The Harvard Museum specimens for which Barth & Berman (1930) give optical data were fortunately available for *x*-ray study. Three of these specimens (materials 6, 7, 8 in Table 7) with closely similar optical properties gave the characteristic powder pattern of pseudomalachite. The fourth (HMM 90455) gave the pattern of malachite; the optical data also agree closely with those for malachite. The optical data given by Larsen (1921) differ rather markedly from the others. Unfortunately Larsen's specimens were not available for *x*-ray study. Crystals of materials 3 and 5 which had been oriented on the precession camera were mounted on the universal stage for measurement of the extinction angle. The *X* direction lies in the obtuse angle β in both cases.

X-ray Powder Pattern. All the materials listed in the first part of this paper yield an identical *x*-ray powder pattern (Figs. 5, 6). The films of materials 2, 3 and 9 were carefully measured. Materials 2 and 3 were coarsely crystalline and yielded material for single crystal study while material 9 is a fibrous radiating aggregate. The estimated intensities, measured θ and *d* values given in Table 8 were averaged from closely similar measurements on the three films. The films for materials 2 and 9 showed many back reflection rings providing a check on film shrinkage. The recorded diffractions for θ greater than 37° occurred only on these two films. A few weak diffractions which were only observed on one of the two films were omitted from the table. The pattern has been indexed

TABLE 7. PSEUDOMALACHITE: OPTICAL DATA, $Z=b$

α	β	γ	2V	$c\wedge X$	Material and Observer
—	—	—	—	21°	material 3, L.G.B.
—	—	—	—	26°	material 5, L.G.B.
1.789	1.835	1.845	50°±	21°	material 6, Barth & Berman (1930)
1.785	1.850	1.862	50°±	21°	material 7, Barth & Berman (1930)
1.80	1.86	1.88	46°	23°	material 8, Barth & Berman (1930)
1.719	1.763	1.805	90°±	—	Bogolo, Portugal, Larsen (1921)
1.73	—	1.807		—	Hungary, Larsen (1921)

TABLE 8. PSEUDOMALACHITE—$Cu_5(PO_4)_2(OH)_4$: X-RAY POWDER PATTERN

Monoclinic, $P2_1/a$; $a=17.06$, $b=5.76$, $c=4.49$ A, $\beta=91°\,02'$; $Z=2$

I	θ(Cu)	d(meas.)	(hkl)	d(calc.)
½	9.33°	4.75 A	(210)	4.770 A
10	9.92	4.48	(001)	4.489
5	12.87	3.46	$(\bar{1}11)$	3.477
			(410)	3.425
½	13.64	3.27	(211)	3.254
2	14.29	3.12	$(\bar{4}01)$	3.120
4	14.43	3.09	(401)	3.064
2	14.69	3.04	$(\bar{3}11)$	3.025
4	15.03	2.97	(311)	2.987
3	15.24	2.93	(510)	2.933
1	15.71	2.85	(600)	2.843
			(120)	2.838
3	16.43	2.72	(220)	2.729
			(411)	2.705
1	17.55°	2.56 A	(320)	2.569 A
			(610)	2.543
6	18.55	2.42	(021)	2.424
			$(\bar{6}01)$	2.421
8	18.85	2.39	(121)	2.397
			(420)	2.388
			(601)	2.382
5	19.38	2.32	$(\bar{2}21)$	2.337
			(221)	2.325
5	20.19	2.23	(002)	2.245
			(710)	2.243
			$(\bar{3}21)$	2.237
			$(\bar{6}11)$	2.232
			(321)	2.221

I	θ(Cu)	d(meas.)
1	20.61°	2.19 A
1	21.31	2.12
3	21.66	2.09
1	22.56	2.01
2	23.13	1.963
1	23.42	1.939
2	24.56	1.854
4	25.93	1.763
5	26.5	1.728
2	27.47	1.670
1	28.33	1.624
2	28.87	1.597
4	29.64	1.559
2	30.32	1.527
2	30.96	1.498
2	31.14°	1.491 A
1	31.81	1.462
3	32.57	1.431
3	32.91	1.419
4	33.64	1.392
1	34.37	1.365
2	34.81	1.350
3	35.28	1.335
2	35.75	1.319
3	36.02	1.310
1	39.48	1.212
1	40.13	1.196
½	45.75	1.076
3	47.91	1.039
3	49.46	1.014
1	51.51°	0.985 A
1	53.52	0.958
1	55.42	0.936
2	58.63	0.903
1	61.09	0.880
2	62.25	0.871
1	64.27	0.856
1	67.61	0.834
1	69.26	0.824
1	71.52	0.813
1	72.18	0.810
2	72.77	0.807
1	73.28	0.804
1	73.87	0.802
3	76.34	0.794

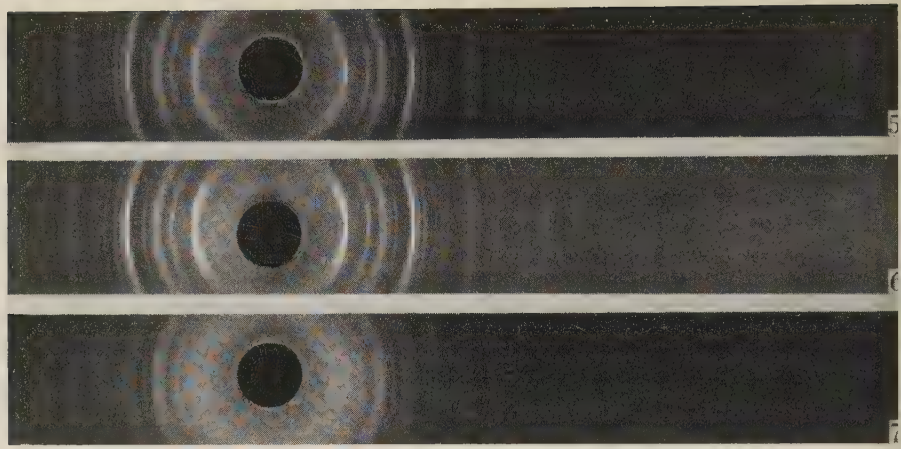

FIGS. 5, 6, 7. *X*-ray powder photographs with Cu/Ni radiation; camera radius $90/\pi$ mm. ($1°\theta = 1$ mm. on film); full size reproduction of contact prints. FIG. 5. Pseudomalachite, Rheinbreitinbach, Germany; coarse crystalline (material 1). FIG. 6. Pseudomalachite, Nassau, Germany; radiating fibrous aggregate (material 9). FIG. 7. Cornetite, Bwana Mkubwa, Northern Rhodesia.

as far as $\theta = 20.19°$ and the measured spacings agree closely with one or more calculated values.

CORNETITE—$Cu_3PO_4(OH)_3$

Cornetite was first described by Cesàro (1912*a*, *b*) from the copper mine L'Étoile du Congo, Katanga, Belgian Congo and by Hutchinson & MacGregor (1913, 1921) from Bwana Mkubwa, Northern Rhodesia. Cesàro (1912*b*) described the chemical composition as "essentiellement d'un phosphate de cuivre et de cobalt"; the name cornetite was given by Buttgenbach (1916) to the material described by Cesàro. Hutchinson & MacGregor (1913, 1921) give a chemical analysis of their material yielding the emprirical formula $2Cu_3(PO_4)_2 \cdot 7Cu(OH)_2$. In the later communication these authors (1921) recognize their material as cornetite and conclude that the material described by Cesàro differs only in a small content of cobalt. Schoep (1922) re-examined cornetite from L'Étoile du Congo, Katanga and proved conclusively that cobalt is not a constituent of the cornetite crystals.

The observations given in this paper were obtained from crystals on a typical specimen from Bwana Mkubwa, Northern Rhodesia, from the mineralogical collections of Queen's University. The mineral occurs as an incrustation of peacock blue crystals up to $0.3 \times 0.3 \times 0.2$ mm. underlain by a thin layer of brownish black material on compact, grey argillaceous sandstone. The specimen is similar in nearly every respect to one specimen described by Hutchinson & MacGregor (1921) from the same locality.

Two additional specimens (USNM R5345 and ROM M13540) from Étoile du Congo, Katanga, Belgian Congo, were also examined. These specimens consisted of small blue crystals and crystal aggregates partially embedded in fine grained argillaceous sandstone. On one specimen a few small spherical aggregates of pseudomalachite are implanted on top of the cornetite crystals.

Structural Crystallography. Crystals of cornetite on our specimen from Bwana Mkubwa are ideally suited for single crystal x-ray studies. Rotation, zero and first layer Weissenberg photographs about $c[001]$ and $a[100]$ and a rotation film about $b[010]$ indicate orthorhombic symmetry in the Laue class D_{2h}-mmm and lead to an orthorhombic cell:

$$a=10.88,\ b=14.10,\ c=7.11\ \text{A}.$$

The observed diffractions conform to the conditions: (hkl) present in all orders; $(0kl)$ present only with $k=2n$; $(h0l)$ present only with $l=2n$; $(hk0)$ present only with $h=2n$. These conditions are characteristic of the space group $D_{2h}^{15}-Pbca$.

Rotation and zero-layer Weissenberg films about $[0\bar{1}2]$ on one crystal of cornetite from Katanga give $a=10.85$ A and other values in close agreement with values calculated from the above structural elements.

Geometrical Crystallography. Cesàro (1912*b*), Hutchinson & MacGregor (1913, 1921), Schoep (1927) and Ungemach (1929) give crystal measurements for cornetite and deduce orthorhombic elements in three different settings. Hutchinson & MacGregor (1921) and Schoep (1927) retain Cesàro's setting and elements. Ungemach lists the same forms recorded by Cesàro together with 6 new forms. From excellent measured angles $(110)\wedge(1\bar{1}0)$ and $(021)\wedge(02\bar{1})$ he obtains the axial ratio:

$$a:b:c=0.99045:1:1.5282$$

in Cesàro's setting but with the c-axis doubled to give more normal symbols. The morphological lattices are related to the structural lattice by the reversible transformation formulae:

Cesàro (1912*b*), Hutchinson & MacGregor (1921) to Berry	001/100/0½0
Berry to Cesàro (1912*b*), Hutchinson & MacGregor (1921)	010/002/100
Hutchinson & MacGregor (1913) to Berry	100/0½0/00¼
Berry to Hutchinson & MacGregor (1913)	100/020/004
Ungemach to Berry	001/200/010
Berry to Ungemach	0½0/001/100

The geometrical axial ratios transformed into the structural setting compare closely with the structural lattice axial ratio:

$a:b:c=0.773\ :1:0.504$ (structural lattice)
$c:a:b/2=0.7801:1:0.5079$ (Cesàro, 1912*b*)
$2a:b:c/2=0.788\ :1:0.505$ (Hutchinson & MacGregor, 1913)
$c:a:b/2=0.7703:1:0.5074$ (Hutchinson & MacGregor, 1921)
$c/2:a:b/2=0.7715:1:0.5048$ (Ungemach, 1929)

The close agreement between the structural lattice elements and the elements deduced by Ungemach from careful measurements on a number of crystals indicates that the latter elements best represent crystals of cornetite. Table 9 gives the observed forms of cornetite with their indices in the structural setting. In Table 10 the two circle angles, calculated from Ungemach's elements in the structural setting, are given for all the forms observed on cornetite crystals.

TABLE 9. CORNETITE: OBSERVED FORMS

Cesàro (1912*b*)	Hutchinson & MacGregor (1913)	(1921)	Ungemach (1929)	Berry
—	—	—	*g′* (010)	*c* (001)
a (100)†	—	—	—	*b* (010)
—	—	—	*p* (001)	*a* (100)
—	—	—	a^2 (102)	*m*(110)
a^2 (102)	(110)	*d* (102)	a^4 (104)	*d* (210)
m (110)	(011)	*m*(110)	*m* (110)	*n* (021)
—	—	—	$e^{1/2}$(021)	*e* (102)
$b^{1/4}$(221)	—	*v* (221)	$b^{1/2}$(111)	*v* (121)
$b^{1/2}$(111)	—	*p* (111)	b^1 (112)	*p* (221)
—	—	—	$b^{3/2}$(113)	*r* (321)
—	—	—	b^2 (114)	*s* (421)
—	—	—	—	*t* (521)*

* New form observed on one crystal from Katanga.
† Observed by Schoep (1927).

The crystals of cornetite from Northern Rhodesia, used in this study, show the forms *d*(210), *n*(021), *v*(121) and *p*(221). A typical crystal is illustrated in Fig. 8. Measured angles on these crystals agree closely with Ungemach's calculated angles. One crystal fragment of cornetite from Katanga (ROM M13540) which was mounted for *x*-ray measurements shows the forms *n*(021), *v*(121), *p*(221) and one face with indices (521). The measured angles for this face, compared with the angles calculated from Ungemach's elements, are given in Table 11.

TABLE 10. CORNETITE: $Cu_3PO_4(OH)_3$

Orthorhombic, *Pbca*

$a:b:c=0.7715:1:0.5048$; $p_0:q_0:r_0=0.6544:0.5048:1$

Form	ϕ	$\rho=C$	ϕ_1	$\rho_1=A$	ϕ_2	$\rho_2=B$
c (001)	—	0° 00′	0° 00′	90° 00′	90° 00′	90° 00′
b (010)	0° 00′	90 00	90 00	90 00	—	0 00
a (100)	90 00	90 00	—	0 00	0 00	90 00
m(110)	52 21	90 00	90 00	37 39	0 00	52 21
d (210)	68 54½	90 00	90 00	21 05½	0 00	68 54½
n (021)	0 00	45 16½	45 16½	90 00	90 00	44 43½
e (102)	90 00	18 07	0 00	71 53	71 53	90 00
v (121)	32 57	50 16	45 16½	65 16½	56 48	49 48½
p (221)	52 21	58 49½	45 16½	47 21½	37 23	58 29½
r (321)	62 47	65 38	45 16½	35 54	26 59½	65 22½
s (421)	68 54½	70 23	45 16½	28 30	20 54½	70 11
t (521)	72 51	73 43	45 16½	23 28½	16 59½	73 33½

Ungemach's observed forms listed approximately in order of decreasing importance are:

Ungemach	(110), (111), (104), (102), (112), (001), (021), (100), (010), (113), (114)
Structure	(021), (121), (210), (110), (221), (100), (102), (010), (001), (321), (421)

The first three are also the most important observed by Cesàro, Hutchinson & MacGregor and Schoep. Donnay[1] states that the morphological analysis confirms Ungemach's unit and predicts the space group *Pbcn* with one anomaly; namely, (104) more important than (102). This is an

TABLE 11. CORNETITE, KATANGA

Comparison of Measured and Calculated angles

	Measured	Calculated
n(021):*n*(0$\bar{2}$1)	90° 43′	90° 33′
n(021):*v* (121)	24 53	24 43½
n(021):*p*(221)	41 36	42 38½
n(021):*t* (521)	67 20	66 31½
v (121):*t* (521)	41 55	41 48
p(221):*t* (521)	26 10	23 53

---

[1] Personal communication April 8, 1948.

established fact as (104) (Ungemach) was observed by earlier authors and is more important on the crystals used in this study, while (102) has been observed only by Ungemach as a less important form. Transformed to the structural setting this space group becomes *Pbca* as determined by *x*-ray methods and (104) becomes (210) which is more important than (110) as expected in this space group. However, the important form (111) Ungemach becomes (121) and is anomalous in the structural setting.

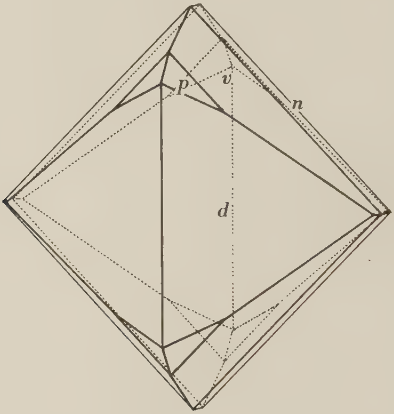

FIG. 8. Cornetite, Bwana Mkubwa, Northern Rhodesia; crystal showing the forms *s*(210), *n*(021), *v*(121) and *p*(221).

Composition and Cell Content. The structural lattice dimensions together with the measured specific gravity of cornetite, 4.10 (Hutchinson & MacGregor, 1913, 1921) give the molecular weight of the cell contents, M = 2693.6. In Table 12 this value has been used to obtain the atomic contents of the unit cell from the one published analysis of cornetite.

TABLE 12. CORNETITE: ANALYSIS AND CELL CONTENT

M = 2693.6

	1	2		3	4
CuO	71.30	24.15	Cu	24.15	24
P_2O_5	19.96	3.79	P	7.58	8
H_2O	8.73	13.04	H	26.08	24
	99.99		O	56.14	56

1. Bwana Mkubwa, Northern Rhodesia; anal. Hutchinson & MacGregor (1921). 2. Unit cell content. 3. Atoms in the unit cell. 4. Ideal cell content for $8[Cu_3PO_4(OH)_3]$.

TABLE 13. CORNETITE—$Cu_3PO_4(OH_3)$: X-RAY POWDER PATTERN

Orthorhombic, *Pbca*; $a=10.88$, $b=14.10$, $c=7.11$ A; $Z=8$

I	θ(Cu)	*d*(meas.)	(*hkl*)	*d*(calc.)
5	8.07°	5.48 A	(111)	5.483 A
			(200)	5.440
6	8.74	5.07	(210)	5.075
			(021)	5.006
3	9.74	4.55	(121)	4.548
9	10.34	4.29	(220)	4.307
7	12.09	3.68	(131)	3.689
			(221)	3.684
1	12.64	3.53	(230)	3.556
			(002)	3.555
			(040)	3.525
8	14.09	3.17	(231)	3.181
			(022)	3.174
			(041)	3.158
			(311)	3.149
10	14.69	3.04	(122)	3.047
			(141)	3.033
5	15.15	2.95	(240)	2.958
			(321)	2.937
3	16.30°	2.74 A	(131)	2.744 A
			(222)	2.742
			(241)	2.731
3	17.65	2.54	(302)	2.539
			(420)	2.538
2	17.95	2.50	(250)	2.504
			(042)	2.503
			(411)	2.500
			(312)	2.499
3	18.45	2.44	(142)	2.439
2	20.22	2.23	(431)	2.235
			(332)	2.234
			(061)	2.231
3	21.0	2.15	(402)	2.160
			(260)	2.157
			(440)	2.153
			(213)	2.147
7	22.0	2.06	(261)	2.064
			(342)	2.060
			(441)	2.061
			(511)	2.058

I	θ(Cu)	*d*(meas.)
2	23.15°	1.959 A
1	23.96	1.897
½	24.86	1.833
2	25.47	1.791
2	26.27	1.740
1	26.88	1.703
4	29.29	1.574
4	29.90	1.545
3	30.70	1.509
1	31.51	1.471
1	32.21°	1.445 A
2	32.92	1.418
1	34.23	1.369
1	35.43	1.329
1	37.45	1.266
1	38.25	1.244
2	39.16	1.219
½	40.17	1.193
1	47.01	1.053
1	48.12	1.034
1	50.33°	1.001 A
½	52.15	0.975
½	52.75	0.968
2	53.66	0.956
½	55.77	0.932
2	63.72	0.859
2	69.86	0.821
½	76.20	0.794
1	83.75	0.775

The total number of oxygen atoms is clearly 56, thus the true cell content may be represented by the structural formula

$$24CuO \cdot 4P_2O_5 \cdot 12H_2O = 8[Cu_3PO_4(OH)_3].$$

Column 2 indicates the cell content of H_2O to be 13, however this would require a total oxygen content of 57 which is incompatible with the symmetry of the space group D_{2h}^{15}—*Pbca*. The cell content given in column 4 above gives the calculated specific gravity, 4.100, in agreement with the measured value. This affords complete confirmation of the structural formula given here and the simpler empirical formula suggested by Hutchinson & MacGregor (1921) rather than the more complex formula, $2Cu_3(PO_4)_2 \cdot 7Cu(OH)_2$.

X-ray Powder Pattern. Table 13 gives the observed relative intensities and measured spacings of the observed diffractions for the *x*-ray powder spectrum of cornetite (Fig. 7). The pattern has been indexed as far as $\theta = 22.0°$; the measured spacings agree satisfactorily with one or more spacings calculated from the lattice dimensions and thus the pattern is adequately verified.

Optical Properties. The optical data on cornetite given by Cesàro (1912) and Hutchinson & MacGregor (1921) have been supplemented by new observations by Larsen & Berman (1934). A re-statement of the optical properties with reference to the new structural setting of cornetite may properly be given here. Observations on a typical crystal from Northern Rhodesia, mounted on a universal stage, confirmed this orientation of the ellipsoid in the structural setting.

$X = b[010]$	$\alpha = 1.765$ (green)	negative
$Y = a[100]$	$\beta = 1.81$	$2V = 33°$ (Tl)
$Z = c[001]$	$\gamma = 1.82$	$r < v$ strong

REFERENCES

Arfvedson (1825): Mineralogie—*Berzelius' Jahresber.*, **4**, 140–175.

Barth, T. & Berman, H. (1930): Neue optische Daten wenig bekannter Minerale. (Die Einbettungsmethode).—*Chemie der Erde*, **5**, 22–42.

Bergemann, C. (1828): Chemische Untersuchungen und mineralogische Bemerkungen über verschiedene phosphorsaure Kupfer—*Schweigg. Jour.*, **54**, 305–324.

—— (1858): Bemerkungen über phosphorsaures Kupferoxyd—*Ann. Phys. Chem.*, **104**, 190–192.

—— (1858): Über den Ehlit—*N. Jb. Min.*, 191–195.

Buttgenbach, H. (1916): *Les minéraux et les roches*—Liége.

Cesàro, G. (1912*a*): Sur un nouveau mineral du Katanga—*Ann. Soc. géol. Belgique*, **39**, pp. B241–B242.

—— (1912*b*): Sur un nouveau mineral du Katanga—*Ann. Soc. géol. Belgique*, annexe to **39**, pp. 41–48 (Publ. rel. Congo Belge).

—— & Bellière, M. (1922): Sur le diaspore, la libéthenite et quelques autres minéraux du Katanga—*Ann. Soc. géol. Belgique*, **45**, 172–182 [*M.A.*, **2**, 226].

Church, A. H. (1864): Revision of the mineral phsophates—*Chem. News*, **10**, 217.

—— (1873): New analyses of certain mineral arseniates and phosphates—*Jour. Chem. Soc.*, **26**, 101–111.

Dana, J. D. (1882): *System of Mineralogy*—ed. 5—New York.

Dana, J. D. & E. S. (1892): *System of Mineralogy*—ed. 6—New York.

Field, F. (1859): On the occurrence of tagilite and libethenite, as well as some combinations of lime, copper, and phosphoric acid, in a mine near Coquimbo, Chile—*Chem. Gaz.*, **17**, 225.

HAUSMANN, J. F. L. (1813): *Handbuch der Mineralogie*, 3 vols.—Gottingen.

HEDDLE (1855): Analysis of lunnite from Cornwall—*Phil. Mag.*, **10,** 39.

HERMANN, R. (1846): Untersuchungen russischer Mineralien—*J. Prakt. Chem.*, **37,** 175–193.

HUTCHINSON, A. & MACGREGOR, A. M. (1913): A crystalline basic copper phosphate from Rhodesia—*Nature*, **92,** 364.

—— (1921): On cornetite from Bwana Mkubwa, Northern Rhodesia—*Min. Mag.*, **19,** 225–232.

KÜHN, O. B. (1840): Phosphorsaures Kupferoxyd—*Ann. Chem. Pharm.*, **34,** 218–220.

—— (1844): Ueber einige natürliche phosphosaure und arsensaure Kupfersalze—*Ann. Chem. Pharm.*, **51,** 123–132.

LACROIX, A. (1910): *Minéralogie de la France et de ses colonies*, vol. 4—Paris.

LARSEN, E. S. (1921): The microscopic determination of the nonopaque minerals—*U. S. Geol. Surv.*, Bull. **679**.

LARSEN, E. S. & BERMAN, H. (1934): The microscopic determination of the nonopaque minerals—*U. S. Geol. Surv.*, Bull. **848**.

MASKELYNE, S. & FLIGHT (1872): Mineralogical notices—*Jour. Chem. Soc.*, **25,** 1057.

NORDENSKIÖLD, A. E. (1858): Undersökning af några vid Nischni-Tagil förekommande kopparfosfater—*Acta Soc. Scient. Fenn.*, **5,** 335–341.

RAMMELSBERG, C. (1860): *Handbuch der Mineralchemie*, ed. 1—Leipzig.

—— (1875): *Handbuch der Mineralchemie*, ed. 2—Leipzig.

RHODIUS, R. (1847): Untersuchung des Phosphorochalcits, Ehlits und eines natürlichen Bleioxyd-Chlorbleis—*Ann. Chem. Pharm.*, **62,** 369–374.

SCHOEP, A. (1922): On the absence of cobalt in cornetite from Katanga, Belgian Congo—*Min. Mag.*, **19,** 301–302.

—— (1927): Kristallen van Cornetiet en hunne brekingsindices—*Naturuwetenschappelijk Tijdschrift, Antwerpen*, **9,** 125–128.

SCHRAUF, A. (1879): Ueber Phosphorkupfererze—*Zeits. Kryst.*, **4,** 1–33.

UNGEMACH, H. (1929): Precisions crystallographiques sur quelques minéraux du Congo Belge—*Ann. Soc. géol. Belgique* (*Publ. rel. Congo Belge*), **52,** c75–c85.

X-RAY DIFFRACTION DATA ON SOME RADIOACTIVE OXIDE MINERALS*

RONALD J. ARNOTT
American Cyanamid Company, Stamford, Connecticut

ABSTRACT

X-ray powder photographs and specific gravity determinations of specimens belonging to the uraninite-thorianite series and the pyrochlore-microlite series gave, for the former, $a = 5.403$–5.575 A (19 specimens), $G = 6.43$–9.55 (9), and for pyrochlore-microlite, $a = 10.296$–10.441 A (5). Indexed powder data are given for uraninite and for ignited microlite. The powder pattern of orthorhombic euxenite (ignited at 1000° C), interpreted with the aid of established morphological descriptions, gave for this mineral, $a = 5.520$, $b = 14.57$, $c = 5.166$ A, most probable space-group *Pcmn*, $Z = 4$, G (meas.) $= 5.23$, ρ (calc for Y:Er $= 2:1$) $= 5.58$. An indexed powder pattern is given. Two specimens of "tanteuxenite" gave patterns of the uraninite type with $a \sim 5.10$ A thus casting doubt on their identity with euxenite.

Radioactive minerals are currently of general interest because they frequently contain uranium and related elements, but they hold a special interest mineralogically because they include most of the minerals classed as "metamict." The possession of this characteristic is probably the main reason why certain of these minerals have not previously been studied by *x*-ray diffraction methods. The author of this paper became interested in radioactive minerals during the summer of 1948 while working in the radioactive laboratory of the Mineralogical Section of the Geological Survey of Canada, at Ottawa. Dr. H. V. Ellsworth, mineralogist in charge of that laboratory, kindly donated a representative collection of these minerals, mostly from Canadian localities, many of which he had analyzed chemically (Ellsworth, 1932). Other specimens of radioactive minerals were obtained from the Mineralogical Museum of the Department of Geology, University of Manitoba, in which Department the present research was carried out under the direction of Dr. R. B. Ferguson, Assistant Professor of Mineralogy, whose guidance is gratefully acknowledged.

This paper deals with the members of three series of radioactive minerals, uraninite-thorianite, pyrochlore-microlite, and euxenite-polycrase. The investigation of representatives of the first two of these groups, both of which are isometric, was confined to indexing the *x*-ray powder photographs and to tabulating new cell edges with old and new specific gravities for specimens from various localities. In the case of the orthorhombic mineral euxenite, however, cell dimensions, possible space-groups, and probable cell content were deduced for the first time from power data.

---

* Extracted from an unpublished M.Sc. thesis: A study of some radioactive minerals by *x*-ray diffraction—*University of Manitoba*, 1949. This work was carried out with the aid of a bursary from the National Research Council (Canada), and is published with the permission of the Council.

The metamict state. A considerable number of minerals are known which show external crystal form but are amorphous to *x*-rays—they are noncrystalline pseudomorphs of originally crystalline material and are termed "metamict." Although amorphous, these minerals can be restored to crystallinity by heating them until they glow, their original structure presumably being regained. The resultant material, however, is cryptocrystalline and not suitable for single-crystal study.

All minerals that are commonly metamict have fairly complex compositions, involving a large amount of isomorphous substitution. They usually contain, among other elements, metals of the rare-earth group, and uranium and thorium, and it is the presence of these elements which accounts for the characteristic radioactivity of these minerals. There has been some speculation in the past as to the reason for the breakdown of the crystal structure in metamict minerals, but no definite conclusions have been reached. Proposed explanations have attributed it to hydration (Brögger, 1893), radioactivity (Mügge, 1922), the type of lattice and valence-change (Goldschmidt & Thomassen, 1924), and pressure (Vegard, 1927).

Methods. Standard *x*-ray powder diffraction techniques were employed. All lattice spacings and cell dimensions are given in Ångström units ($CuK\alpha_1 = 1.5405$ A) except where stated otherwise. Data obtained from outside sources either are given in kX units ($CuK\alpha_1 = 1.5374$ kX) or have been converted to A units. Specific gravities were measured on a Berman microbalance. For the heating experiments on euxenite, a rheostat-controlled electric furnace was used and the accuracy is probably about ±25°C.

URANINITE-THORIANITE SERIES

In addition to the two end-members, uraninite UO_2 and thorianite ThO_2, this series includes several varieties, the best known of which is pitchblende, a massive or colloform uraninite. The members of this series are isometric with cell edges of about 5.47 kX for uraninite and 5.57 kX for thorianite (Goldschmidt & Thomassen, 1923). Neither of these minerals has been reported as metamict.

X-ray powder photographs were taken of nineteen specimens belonging to this series. Table 1 gives, for a typical uraninite, the indexed powder data, in A units, which are in reasonable agreement with those published in the ASTM card index (1945), and Figs. 1 and 2 show powder photographs of two different members of this series. Table 2 gives a list of the specimens examined, the cell edge derived from a powder photograph of each one, and the measured specific gravities for most of them.

TABLE 1. URANINITE—$(U,Th)O_2$: *X*-RAY POWDER PATTERN

Locality: Lot 31, Range 1, Ottawa county, P.Q.

Cubic, *Fm3m*; $a=5.468$ A, $Z=4$

I	θ(Cu)	*d*(meas.)	(*hkl*)	*d*(calc.)
10	14.10°	3.16	(111)	3.157
5	16.38	2.73	(002)	2.734
8	23.45	1.935	(022)	1.935
8	27.85	1.648	(113)	1.648
2	29.23	1.576	(222)	1.578
1	34.30	1.366	(004)	1.367
3	37.95	1.252	(133)	1.254
3	39.10	1.221	(024)	1.222
3	43.65	1.116	(224)	1.116
3	47.05°	1.052	(333) (115)	1.052
1	52.95	0.965	(044)	0.967
4	56.35	0.925	(135)	0.924
2	57.65	0.912	(006) (244)	0.912
2	63.05	0.864	(026)	0.865
2	67.35	0.835	(335)	0.834
2	69.15	0.824	(226)	0.825
$\frac{1}{4}$	77.85	0.788	(444)	0.790

TABLE 2. URANINITE-THORIANITE SERIES: DENSITY AND CELL EDGE OF SPECIMENS FROM VARIOUS LOCALITIES

Mineral	Locality	Measured Sp. Gr.	*a* (A)
Thorianite	Artificial ThO_2	9.87*	5.62*
Thorianite	Galle, Ceylon	9.43	5.575
Thorianite	Ceylon	—	5.563
Thorianite	Sherrer Quarry, Eastern Penn.	—	5.505
Uraninite	Artificial UO_2	10.95*	5.48*
Uraninite	Branchville, Conn.	9.73*	5.486
Uraninite	Raade, Norway (*var.* Bröggerite)	—	5.485
Uraninite	Wilberforce, Ontario	7.05	5.469
Uraninite	Lot 31, Range 1, Ottawa Co., P.Q.	6.50	5.468
Uraninite	Belgian Congo	—	5.458
Uraninite	Besner Mine, Henvey twp., Ont.	—	5.454
Uraninite	Yancey Co., North Carolina	9.55	5.449
Uraninite	Deer Park Mine, N. Carolina	6.52	5.446
Uraninite	Lanark Co., Ontario	—	5.436
Uraninite	Lot 9, Range 2, Mattawan twp., Ont.	8.64	5.433
Uraninite	Reboleira property, Portugal	—	5.409
Pitchblende	Various	6.5–8.5*	5.43–5.46*
Pitchblende	Great Bear Lake, N.W.T.	6.43	5.475
Pitchblende	Great Bear Lake, N.W.T.	6.51	5.472
Pitchblende	Great Bear Lake, N.W.T.	—	5.461
Pitchblende	Hottah Lake, N.W.T.	6.46	5.441
Pitchblende	Black Lake, Sask.	—	5.403

* From Palache, Berman & Frondel (1944). *a* values have been converted from kX to A units.

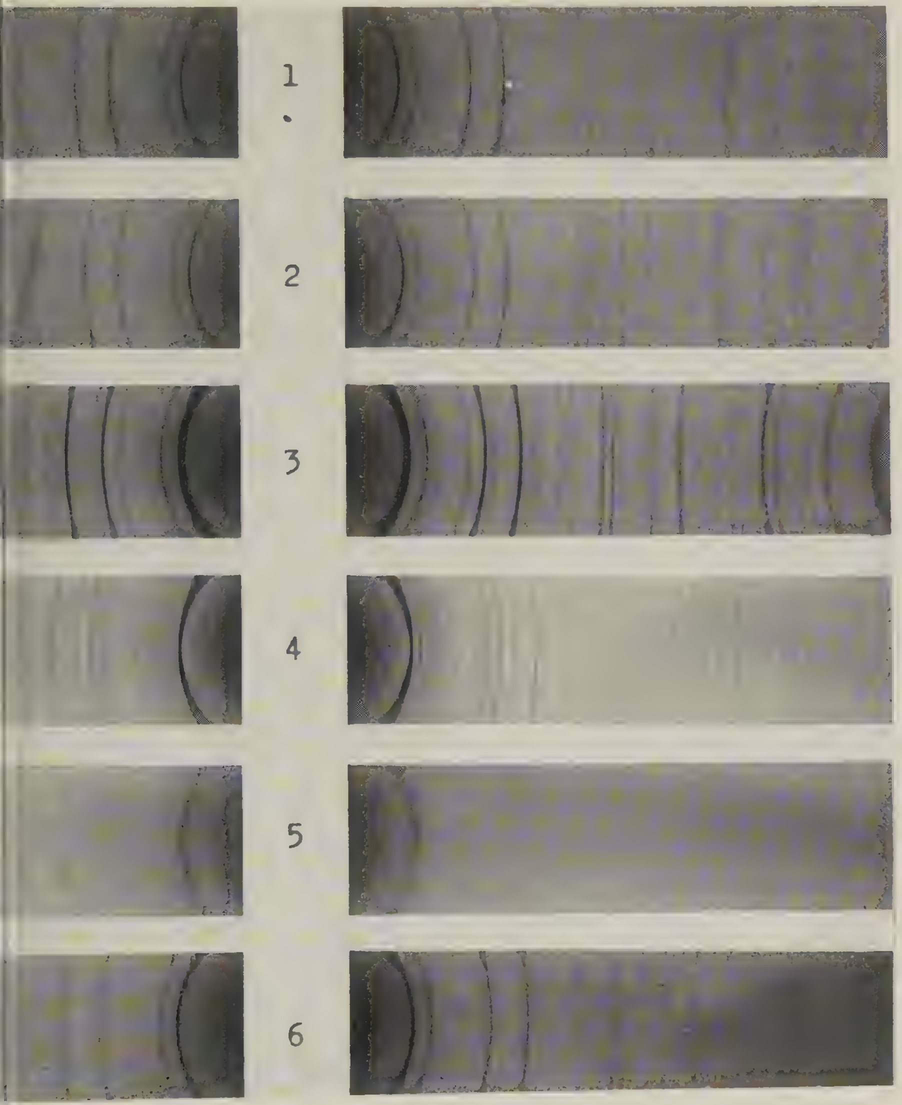

FIGS. 1–6. X-ray powder photographs with Cu/Ni radiation; camera radius 360/4π mm. (1 mm. on film = 1° θ); full size reproductions of double-printed negatives. FIG. 1. Pitchblende, Great Bear Lake, Northwest Territories, $a=5.472$ A. FIG. 2. Thorianite, Galle, Ceylon, $a=5.575$ A. FIG. 3. Microlite, Amelia Court House, Virginia, $a=10.424$ A. FIG. 4. Euxenite, Mattawan twp., Ontario, heated at 1000° C. for 100 hours. FIG. 5. Euxenite, Sabine twp., Ontario, heated at 400° C. for 5 minutes. Fig. 6. "Tanteuxenite," Eleys, West Australia, $a=5.10$ A.

Several of the specimens were largely altered, and fragments suitable for specific gravity determinations could not be obtained from them. Where the specific gravities were measured, a range of values was obtained for each sample. In all cases, the specific gravity quoted is the largest, since the variation is due to different degrees of alteration, and the unaltered mineral has the greatest specific gravity.

Table 2 shows that apparently no correlation exists between cell edge and specific gravity, nor between the latter and the mineral variety. The range of cell edges for thorianite (5.505 to 5.62 A), however, is above the range for uraninite-pitchblende (5.403 to 5.486 A) so that these two members of the series can be distinguished by powder photographs. The table also shows a wider range of cell edges for pitchblende (5.403 to 5.475 A) than that given by Palache, Berman & Frondel (1944), 5.43 to 5.46 A.

PYROCHLORE-MICROLITE SERIES

Although many elements are found in small amount in these minerals, the essential composition of pyrochlore may be expressed as $NaCaCb_2O_6F$, and of microlite as $(Na,Ca)_2Ta_2O_6(O,OH,F)$. The variable composition has given rise to numerous varietal names according to the predominant replacing element. The members of this series are cubic with symmetry of the space-group *Fd3m*, and with cell edges of about 10.37 A for pyrochlore and about 10.40 A for microlite. Almost all specimens of pyrochlore and microlite are metamict, this characteristic varying from slight to complete.

X-ray powder diffraction photographs were taken of one specimen of microlite, one of pyrochlore, and two of "ellsworthite" (uranian pyrochlore). All of these were metamict, and were ignited and rephotographed, although the microlite gave an indistinct pattern without heating indicating that it was only partially metamict. The patterns obtained in this manner were read and indexed using the cubic crystal analyzer. The indexed powder data for microlite (ignited) from Amelia Court House, Virginia, are given in Table 3 and the photograph appears as Fig. 3.

The cell edges obtained from the five photographs are in good agreement with those in Palache, Berman & Frondel (1944), and are as follows: microlite from Amelia Court House, Virginia, before ignition 10.441 A, after ignition 10.424 A; ignited pyrochlore from Brevik, Norway, 10.404 A; ignited ellsworthite from Hybla, Ontario 10.318 A, and from Cardiff township, Ontario 10.296 A.

EUXENITE-POLYCRASE SERIES

In addition to euxenite and polycrase, this series includes lyndochite, which is a member having less than one per cent uranium (Ellsworth,

Table 3. Microlite (Ignited)—$(Na,Ca)_2Ta_2O_6(O,OH,F)$: *X*-ray Powder Pattern

Locality: Amelia Court House, Virginia

Cubic, *Fd3m*; $a=10.424$ A; $Z=8$

I	θ(Cu)	*d*(meas.)	(*hkl*)	*d*(calc.)
6	7.40°	5.98	(111)	6.01
¼	12.05	3.69	(022)	3.69
4	14.35	3.11	(113)	3.14
10	15.00	2.98	(222)	3.00
3	17.38	2.58	(004)	2.61
1	18.85	2.38	(133)	2.39
¼	21.45	2.11	(224)	2.13
2	22.65	1.999	(333) (115)	2.01
8	24.80	1.836	(044)	1.843
2	26.00	1.757	(135)	1.762
½	26.85	1.705	(244)	1.735
¼	29.05	1.585	(335)	1.589
8	29.50	1.563	(226)	1.571
2	30.88	1.500	(444)	1.504
2	31.95	1.455	(117) (155)	1.460
2	34.70	1.352	(137) (355)	1.357
2	36.25	1.302	(008)	1.303
½	37.25	1.272	(337)	1.274
¼	38.95	1.225	(066) (228)	1.228
¼	39.85	1.202	(555)	1.203
3	40.15	1.194	(266)	1.195
3	41.35	1.165	(048)	1.165
1	42.45	1.141	(119) (357)	1.144
¼	42.95	1.130	(248)	1.137
½	43.85	1.112	(466)	1.111
1	44.80	1.093	(139)	1.093
3	46.35	1.064	(448)	1.064
1	47.35	1.047	(177) (339) (557)	1.047
½	49.15°	1.018	(0.2.10) (268)	1.022
½	49.75	1.009	(377) (159)	1.008
3	50.20	1.003	(666)	1.003
½	52.40	0.972	(359)	0.972
1	55.15	0.939	(1.1.11) (577)	0.938
2	56.75	0.921	(088)	0.921
2	57.75	0.911	(1.3.11) (179) (559)	0.911
4	60.90	0.881	(2.6.10) (668)	0.881
3	62.45	0.869	(0.0.12) (488)	0.869
1	63.75	0.859	(1.5.11) (777)	0.860
¼	65.25	0.848	(2.2.12) (4.6.10)	0.846
2	66.95	0.837	(3.5.11) (579)	0.837
3	69.20	0.824	(0.4.12)	0.824
1	69.55	0.822	(199)	0.817
1	75.15	0.797	(1.1.13) (1.7.11) (5.5.11) (399)	0.798
3	75.70	0.795	(6.6.10)	0.795
2	78.85	0.785	(4.4.12)	0.786
1	81.75	0.778	(1.3.13) (3.7.11) (779)	0.779
½	82.45	0.777	(0.6.12) (4.8.10)	0.777

1932, p. 49). Tanteuxenite, a supposed high-tantalum member of this series, is discussed briefly at the end of this paper. The composition of these minerals may be expressed as AB_2O_6 where A = Y, Ce, Ca, U, Th; and B = Ti, Cb, Ta, and Fe‴. The high-Ti end-member is polycrase and the high-(Cb+Ta) member is euxenite.

According to morphological evidence, these minerals crystallize in the dipyramidal class of the orthorhombic system and have an axial ratio of $a{:}b{:}c = 0.3789{:}1{:}0.3527$ (Palache, Berman & Frondel, 1944). They are all metamict and, to date, their unit cell dimensions and space-group have not been published.

It was possible to obtain x-ray diffraction patterns from these minerals by igniting them but since the ignited fragments were cryptocrystalline, it was not possible to use them for single-crystal x-ray analysis. Attempts were made, however, to produce single crystals sufficiently large for this purpose by heating the fragments for long periods at high temperatures.

Heating Experiments and Variations in the Powder Pattern. To investigate this possibility, a sample of euxenite (from Lot 28, Con. 1, Sabine twp., Nippissing District, Ontario) was selected, and portions of it were heated for varying lengths of time at different temperatures. The first sample was heated at 400° C. for 5 minutes, the second at 800° C. for 10 minutes, the third at 800° C. for 6 hours, and others at 1000° C. for 1, 2, 13, 26, 32, 40, and 100 hours. Although a slight increase in crystal size was noted with the first three samples, all those heated to 1000° C. appeared cryptocrystalline under the petrographic microscope and work along this line was discontinued.

Powder pictures were taken of all fragments ignited and it was noted that, whereas all the powder patterns were generally similar, only those of samples which had been heated to 1000° C. were identical. Those samples heated to 400° and 800° C. showed considerable variations, chiefly in the presence or absence of certain lines. This same type of variation was found in a set of six powder pictures of euxenites from different Canadian localities, these specimens having been heated over a Tyrrel burner to render them crystalline.

The work of Faessler (1942) on gadolinite seems relevant to the present problem. He found that the crystalline structure of that mineral is regained rapidly by heating to 800° C. (the recovery is accompanied by glowing), and is regained more slowly by heating to lower temperatures. This suggests a possible explanation of the variations with heat treatment of the euxenite powder pattern. If, as the constancy of the 1000° C. pattern suggests, the temperature of rapid recovery of the crystal structure lies between 800° C. and 1000° C., then these variations could be the result of incomplete recovery of the crystalline structure when the sample is heated to only 800° C. or less. The variations in the patterns of euxenites from different localities is probably also due to this, since these specimens were heated for about one minute in a Tyrrel burner which gives a range of temperatures up to 1000° C. Fig. 4 reproduces the powder pattern which is believed to be the "true" euxenite pattern (sample heated at 1000° C. for 100 hours), and Fig. 5 reproduces, for comparison, one of the variable euxenite patterns which illustrates the chief difference from the true pattern—a doubling of the strongest line.

The "Euxenite Analyzer" and Extraction of Cell Dimensions. In an effort to index the powder patterns, an analyzer of the type used for cubic crystals was constructed for euxenite. To take account of the three orthorhombic cell dimensions, the axial ratio $a:b:c=0.3789:1:0.3527$ was used to calculate 40 or so of the largest "spacings" with $b=1$. These values and a corresponding set for $b=10$ provided the data necessary for plotting the curves of d against b for numerous lattice planes. The completed analyzer appears as Fig. 7.

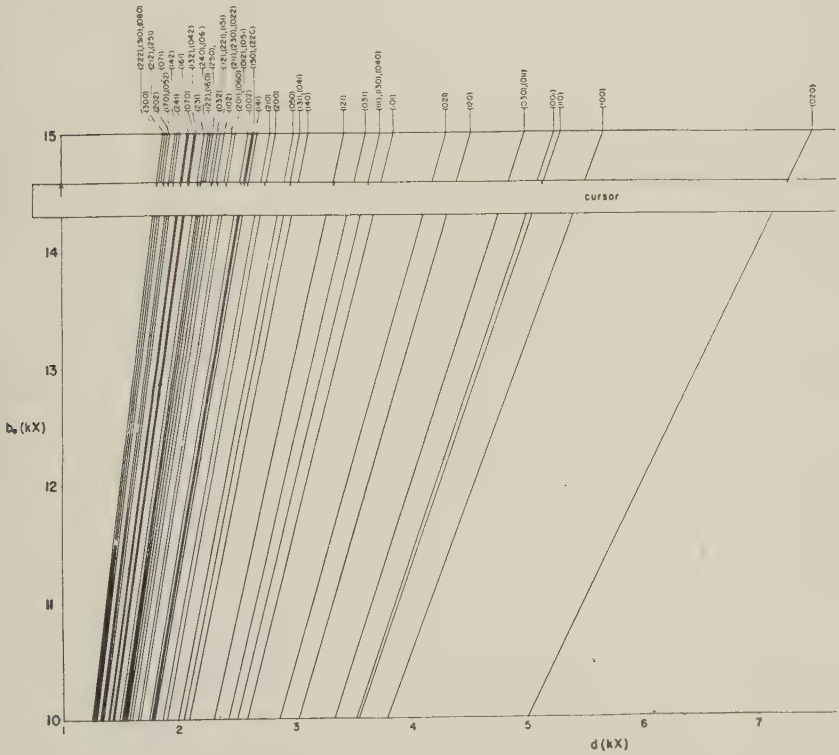

FIG. 7. Analyzer for euxenite giving the variations of $d(hkl)$ with b for the morphological ratio $a:b:c=0.3789:1:0.3527$.

Attempts were made to index the lines on four of the variable patterns using this analyzer, but these were unsuccessful, probably because these patterns were not, as described above, the true euxenite pattern. Then, since the samples of euxenite which had been heated to 1000° C. gave a constant x-ray pattern, one of these patterns (of a specimen from

Mattawan township, Ontario) was chosen for detailed analysis. It was examined for a series of spacings which might represent the various orders of reflection from one set of lattice planes. One such series was readily found, being 7.30, 3.66, 2.43, 1.823, 1.457, and 1.216 A. Since the 7.30 A spacing is that of the innermost line on the film, this was assumed to be a pinakoidal spacing and, adopting the accepted orthorhombic orientation $c<a<b$, this was further assumed to be the first order of the side pinakoidal reflection, i.e. $d(010)$. On these assumptions, the smaller values above would be the second to sixth order reflections of $(0k0)$. When applied to the analyzer, this value of 7.30 A for b left many strong lines not indexed. However, when double this value of b was used (14.60 A), it was found that all but a few very weak lines could be satisfactorily indexed. In this way, the approximate cell dimensions were deduced as $a=5.53$, $b=14.60$, $c=5.17$ A.

Derivation of the Space-Group. Using the above values for the unit cell dimensions, the spacings of all possible planes were calculated down to a spacing of 2.00 A. By comparing these possible reflections with those actually observed in the powder pattern, a set of possible space-groups for euxenite was derived. The method was as follows: (110) and (001) are the only planes which would give the second line on the powder pattern, and these reflections would be extinguished by all (hkl) conditions except (hkl) present only with $(h+k)=2n$ and (hkl) present only with $(h+k+l)=2n$. Of these, the former is excluded by the unique reflection (121) and the latter by another unique reflection (102). Thus, no condition is possible in (hkl) which must therefore be present in all orders, and euxenite must have a primitive lattice. By similar reasoning applied to a number of reflections given by unique special planes, the space-group of euxenite was reduced to the possibilities *P*(*mnc*) (*mc*) (*mnab*).

Now, if the intensity effect of the structure factor is disregarded, and it is assumed that possible planes which are *not* represented by observed lines have been cancelled by some extinction condition, the number of possible space-groups can be reduced much further. For instance, the line (021) does not appear, and therefore either of the extinction conditions $(0kl)$ present only with $(k+l)=2n$, or $(0kl)$ present with $l=2n$ must hold since only these will extinguish reflections from this plane. Carried further, this method will reduce the number of probable space-groups for euxenite to only one, *Pccn*. However, *Pcmn* is eliminated by the condition $(h0l)$ present only with $l=2n$ based solely on the absence of the (101) reflection, and the occurrence of both (101) and (201) as common crystal forms, as explained in the next paragraph, makes it appear more likely that *Pcmn* is a possibility. Thus we arrive at the most probable space-group of euxenite as either *Pccn* or *Pcmn*.

At this point it was found profitable to consider by application of the Donnay-Harker law, which of these two space-groups, if either, is favored by the morphology of the mineral. Donnay and Harker (1937) give as their modification of the Bravais law:

> "The morphological importance of a crystal face is inversely proportional to its reticular area S if the lattice is of the hexahedral mode (no centering) and the space group symmetry does not contain any screw axis or glide plane. The effect of lattice centering, screw axes, and glide planes is corrected for if the face indices are replaced, in the S formula, by the "multiple indices" of the lowest order of *x*-ray reflection compatible with the space group symmetry."

Since the reticular area of a lattice plane is inversely proportional to the spacing of its set of planes, the Donnay-Harker principle implies that the decreasing order of importance of the faces on a crystal is exactly that of the order of appearance of the lines on the *x*-ray powder pattern of that crystal, provided none of the possible lines is extinguished by a very low structure factor value. Consequently, the presence or absence of certain crystal forms can be used as an aid in deducing the space-group of a given crystal. Donnay and his students have, in fact, used the morphology alone to deduce the unique space-group of certain well-developed crystals such as scheelite (Donnay, 1942), but with euxenite the comparatively poor face development can only assist in determining the space-group. Dana's *System of Mineralogy* (Palache, Berman & Frondel,

TABLE 4. EUXENITE: COMPARISON OF THEORETICAL AND ACTUAL FORM IMPORTANCE

d(*hkl*) A	*Pccn*	*Pcmn*	Observed
7.28	(020)	(020)	(010)
5.16	(110)	(110)	(101)
3.77	—	(101)*	(110)
3.65	(130)	(130)	—
3.65	(111)	(111)	(111)
3.36	(121)	(121)	(121)†
2.98	(131)	(131)	(131)†
2.77	(200)	(200)	(100)
2.62	(141)	(141)	—
2.58	(002)	(002)	(001)†
2.57	(150)	(150)	—
2.54	(012)	(012)	—
2.44	(022)	(022)	(011)†
2.44	—	(201)*	(201)†

* Not observed on powder pattern.

† Infrequent forms whose order of importance cannot be given.

1944) gives, as the commonest crystal forms for the euxenite-polycrase series, (010), (101), (110), (111), and (100); and, as other forms, (001), (011), (201), (121), and (131). Since good crystals of these minerals are uncommon, the above order which is approximately that of decreasing importance, may not be too reliable. Table 4 shows the order of appearance of the lines on an *x*-ray powder pattern of euxenite which would be given by each of the two possible space-groups deduced above, and in comparison, the observed order of form importance. In this table, the

TABLE 5. EUXENITE—(Y, Ce, Ca, U, Th) (Cb, Ta, Ti)$_2$O$_6$: *X*-RAY POWDER PATTERN

Locality: Lot 29, Con. 3, Mattawan twp., Nippissing dist., Ont.

Orthorhombic, *Pcmn*; $a=5.520$, $b=14.57$, $c=5.166$ A, $Z=4$

I	θ(Cu)	*d*(meas.)	(*hkl*)	*d*(calc.)	*I*	θ(Cu)	*d*(meas.)	(*hkl*)	*d*(calc.)
1	6.05°	7.30	(020)	7.28	4	24.98°	1.823	(222)	1.826
2	8.58	5.16	(110)	5.16				(310)	1.826
3	12.15	3.66	(130)	3.65				(152)	1.825
			(111)	3.65				(260)	1.823
			(040)	3.65				(171)	1.823
2	13.28	3.36	(121)	3.36				(080)	1.822
10	15.00	2.98	(131)	2.98	3	25.80	1.769	(062)	1.770
2	16.18	2.77	(200)	2.77	4	26.55	1.723	(311)	1.721
¼	17.15	2.61	(141)	2.62				(330)	1.720
2	17.35	2.58	(002)	2.58				(261)	1.719
			(220)	2.58	½	27.30	1.679	(242)	1.675
			(150)	2.57	3	28.08	1.635	(181)	1.640
½	17.63	2.54	(012)	2.54				(113)	1.633
3	18.48	2.43	(022)	2.44				(331)	1.632
			(201)	2.44	1	28.65	1.605	(123)	1.604
			(060)	2.43	½	29.10	1.583	(252)	1.583
1	19.53	2.30	(112)	2.31				(271)	1.582
			(221)	2.31	1	29.55	1.560	(341)	1.565
			(151)	2.31				(133)	1.557
¼	20.00	2.252	(032)	2.280	¼	30.38	1.522	(280)	1.520
			(122)	2.227	¼	30.85	1.501	(302)	1.499
1	20.50	2.199	(240)	2.200				(143)	1.498
1	20.68	2.182	(231)	2.176	4	31.18	1.487	(312)	1.490
2	21.45	2.106	(132)	2.108				(351)	1.490
¼	21.83	2.071	(161)	2.042				(262)	1.490
½	22.35	2.025	(241)	2.024				(082)	1.489
½	23.00	1.970	(142)	1.969				(191)	1.488
1	23.45	1.935	(170)	1.948	1	31.90	1.457	(322)	1.462
			(052)	1.933				(203)	1.461
2	24.05	1.889	(202)	1.886				(281)	1.458
								(0.10.0)	1.457

TABLE 5—*continued*

I	θ(Cu)	d(meas.)	I	θ(Cu)	d(meas.)	I	θ(Cu)	d(meas.)	I	θ(Cu)	d(meas.)
2	32.43°	1.436	1	39.80°	1.203	½	48.40°	1.030	1	58.80°	0.901
½	33.35	1.400	2	40.65	1.182	2	48.90	1.024	1	59.95	0.890
½	33.60	1.391	2	41.05	1.173	1	49.35	1.015	1	60.95	0.881
1	34.50	1.359	3	41.75	1.156	½	49.80	1.008	1	63.10	0.864
2	35.20	1.336	½	42.35	1.143	1	50.65	0.996	1	64.00	0.857
1	35.95	1.311	½	43.50	1.119	1	51.35	0.986	½	64.70	0.852
1	36.55	1.292	1	43.95	1.110	½	51.75	0.981	1	65.35	0.848
½	37.20	1.273	1	44.45	1.100	½	52.75	0.968	2	66.70	0.839
¼	37.80	1.256	½	44.90	1.091	1	53.15	0.963	1	69.85	0.820
½	38.35	1.241	2	45.50	1.080	1	53.35	0.960	2	72.35	0.808
2	39.05	1.222	1	46.80	1.057	2	54.90	0.941	½	74.75	0.798
1	39.30	1.216	1	47.40	1.046	3	57.25	0.916	1	80.05	0.782

least important form (100), of those whose order of importance is given in Dana, has been placed after (121) and (131) whose order is not given. With this minor change, the table shows very good agreement between the actual order of importance and those orders predicted by the two space-groups, especially by *Pcmn*. The order given by *Pccn* is the same as that given by *Pcmn* apart from the omission of (101) and (201) both of which are observed forms. This difference suggests strongly that *Pccn* is the less likely of the two, and consequently, the *most probable* space-group for euxenite is *Pcmn* (or *Pc2n* if euxenite is hemihedral).

The cell dimensions were finally recalculated from the indexed powder pattern using only those lines which index uniquely. This was done for two euxenite specimens. Euxenite from Mattawan twp., Nippissing District, Ontario gave the values:

$$a=5.520,\ b=14.57,\ c=5.166\ \text{A}.$$

This x-ray axial ratio, $a:b:c=0.3789:1:0.3546$, is in excellent agreement with the morphological ratio, $a:b:c=0.3789:1:0.3527$. Table 5 gives the powder data for euxenite indexed to $d=1.457$ A on the above cell dimensions. Euxenite from Sabine twp., Nippissing district, Ontario, gave $a=5.552$, $b=14.16$, $c=5.194$ A, and the ratio $a:b:c=0.3800:1:0.3556$.

Specific Gravity and Cell Content. In order to study the effects of heating on the density of euxenite, the Berman microbalance was used to measure the specific gravity of several fragments of the unheated euxenite from Sabine township, Nippissing district, Ontario, and of several fragments from each sample of the same euxenite specimen which had been ignited at 1000° C. for varying lengths of time. The specific gravity varied considerably for different fragments of the same sample and in each case the highest value is the one reported. The results, given in Table 6, show that the specific gravity increases with heating to a maximum at about two hours, and decreases with longer heating. Since alteration lowers the specific gravity, the highest values are considered the best. From the above table, these are: before heating, G=4.98; after heating, G=5.23. These results agree well with the range of values given in Palache, Berman & Frondel (1944, p. 788): "G. 5.00±0.10 (for Cb:Ta>2:1, . . .); . . . the G. decreases with alteration and increases after ignition."

TABLE 6. EUXENITE: VARIATION IN SPECIFIC GRAVITY WITH HEAT TREATMENT

Treatment	Specific Gravity	Treatment	Specific Gravity
Unheated	4.98	25 hrs. at 1000° C.	5.15
1 hr. at 1000° C.	5.18	32 hrs. at 1000° C.	5.02
2 hrs. at 1000° C.	5.23	40 hrs. at 1000° C.	5.07
13 hrs. at 1000° C.	5.14	100 hrs. at 1000° C.	4.98

Using the value 5.23 for the measured specific gravity of euxenite, the molecular weight M of the unit cell was calculated to be 1327. Table 7 gives, for euxenite from Sabine township, the analysis by Ellsworth (1932), and the number of the various types of atoms in the unit cell,

TABLE 7. EUXENITE: ANALYSIS AND CELL CONTENT

	1	2	3	4
TiO_2	22.96	—	3.985	7.969
Fe_2O_3	2.07	—	0.359	0.539
Cb_2O_5	28.62	—	2.986	7.465
Ta_2O_5	2.65	—	0.166	0.416
CaO	1.92	0.475	—	0.475
UO_2	8.61	0.442	—	0.884
UO_3	0.20	0.010	—	0.019
ThO_2	3.94	0.207	—	0.414
$(Y, Er)_2O_3$	24.31	2.985	—	4.478
$(Ce, etc.)_2O_3$	0.44	0.037	—	0.056
	95.72	4.156	7.496	22.715

1. Euxenite, Sabine twp., Nippissing Dist., Ont.; anal. Ellsworth (1932).
2. Atoms of type A in the unit cell.
3. Atoms of type B in the unit cell.
4. Oxygen atoms in the unit cell.

calculated for the above value of M. The letters A and B in the table have the same meaning as in the formula for euxenite, AB_2O_6, where A=(Y, Er, Ce, etc.), Ca, U, Th; and B=Cb, Ta, Ti, Fe'''. From this table it will be seen that the cell content of euxenite is $A_{4.16}B_{7.50}O_{22.72}$, which is close to $A_4B_8O_{24}$. Therefore, Z is probably 4. The value of Z for the A part of the molecule (4.16) is close to this figure but, since the proportional values for the B elements (3.75) and the oxygen atoms (3.78) check well between themselves, it is likely that their proportions represent the true relative value of Z and that the density should be increased to bring them to 4. The consequent error in the A part of the molecule probably arises from the calculation of the number of Y+Er atoms in the unit cell, which was done on the assumption that this combination is all yttrium. If part of this is erbium, the number of these combined atoms in the unit cell will be lower, since the atomic weight of erbium, 167.2, is nearly double that of yttrium, 88.92. The Y:Er ratio necessary to give Z for the A part of the molecule a value of 3.75 calculates to about 2:1. The low value of Z (3.75 instead of 4) obtained above is probably due to a low measured specific gravity. Evidently the density of euxenite is not completely regained on heating. Assuming the value of Z to be 4, the molecular weight of the unit cell was recalculated to be 1416, giving a calculated density of 5.58.

Tanteuxenite. During the investigation of euxenite, *x*-ray powder photographs were taken of two specimens donated by Dr. Ellsworth, labelled "tanteuxenite," one from Woodstock, West Australia, and the other from Eleys, West Australia. Both specimens lack crystal form and both have low densities (4.9), but otherwise they correspond to the physical description of tanteuxenite given in Palache, Berman & Frondel (1944, p. 791): "Fracture subconchoidal. H. 5–6. G. 5.4–5.9. Luster resinous with brownish black color." Both specimens are metamict but on ignition they gave patterns which are similar to those of the uraninite-thorianite series. They were readily indexed on a cubic lattice, the cell edge of the specimen from Woodstock being 5.12 A and of the specimen from Eleys 5.10 A. The powder photograph of the specimen from Eleys is reproduced as Fig. 6. In addition to the strong pattern described above, this specimen gave a considerable number of very weak lines which could not be indexed on the above cell edge. These two photographs suggest that "tanteuxenite" is not a member of the euxenite-polycrase series as presently assumed, and that a more detailed investigation is necessary to identify it correctly.

REFERENCES

ASTM (1945): *X*-ray diffraction patterns, first supplementary set of cards—*Am. Soc. Test. Mat.* (Philadelphia).

Brögger, W. C. (1893): Amorph—*Salmonsen's Conversationlexicon*—Copenhagen [*Zeits. Krist.*, **25**, 427, 1896].

Donnay, J. D. H. (1942): Morphologie cristalline du groupe de la schéelite—*Mém. Soc. Roy. Canada*, 36(4), 37–57.

Donnay, J. D. H. & Harker, D. (1937): A new law of crystal morphology extending the law of Bravais—*Am. Mineral.*, **22**, 446–467.

Ellsworth, H. V. (1932): Rare-element minerals of Canada—*Geol. Surv. Canada*, Econ. Geol. Series, **11**.

Faessler, A. (1942): Untersuchungen zum Problem des metamikten Zustandes—*Zeits. Krist.*, **104**, 81–113 [*Min. Abs.*, **8**, 337].

Goldschmidt, V. M. & Thomassen, L. (1924): Geochemische Verteilungsgesetze der Elemente. III—*Vidensk. Sk.*, I. Mat.-nat. Kl., **5**.

Mügge, O. (1922): Über isotrop gewordene Kristalle—*CBl. Min.*, 721–739, 753–765.

Palache, C., Berman, H. & Frondel, C. (1944): *Dana's system of mineralogy*, ed. 7, **1**—New York.

Vegard, L. (1927): The structure of xenotime and the relation between chemical composition and crystal structure—*Phil. Mag.*, **4**, 511–525.

Wells, R. C., Fairchild, J. G. & Ross, C. S. (1933): Thorianite from Easton, Pa.—*Am. J. Sc.*, **26**, 45–54.

METAMICT PITCHBLENDE FROM GOLDFIELDS, SASKATCHEWAN AND OBSERVATIONS ON SOME IGNITED PITCHBLENDES

C. E. B. CONYBEARE* AND R. B. FERGUSON†
University of Manitoba, Winnipeg, Canada.

ABSTRACT

Seven metamict pitchblendes, apparently the first to be reported, are described from three localities in the Goldfields area of Saskatchewan. The changes in *x*-ray powder pattern and color of the powder after ignition are tabulated for these and two other pitchblendes; the principal changes are the restoration of the structure of metamict specimens and the occasional development of U_3O_8 with, or in place of UO_2. On the basis of these changes the nine pitchblendes examined are classified into five distinct types.

During the summers of 1947 and 1948, while employed by the Crown Company, Eldorado Mining and Refining (1944) Ltd., the first author collected a suite of pitcheblende specimens from the Ace and Christie Lake localities in the Goldfields area of northern Saskatchewan, mapped by Christie & Kesten (1949). With a view to determining roughly the U:Th ratio, the writers took *x*-ray powder photographs of two representative specimens of this suite, and were surprised to find that the patterns were very weak, suggesting that the uraninite is to a considerable degree metamict. As metamict uraninite has not, as far as the writers know, been previously described, it was decided to investigate these and other specimens further.

LABORATORY PROCEDURE

Small chips were broken from those portions of the pitchblende samples which showed the least amount of impurities, and the purest pieces selected under a binocular microscope. In some cases it was impossible to separate pieces entirely free from the associated carbonate, hematite, pyrite, and pyrrhotite. The selected pieces were then crushed and powdered in a mullite mortar, and the powder was divided into two portions. One portion was heated for five minutes in a covered crucible over a Bunsen flame (roughly 800° C.), and parts of each portion were then mounted on separate glass rods and photographed using Cu radiation and a Ni filter (Cu $K\alpha_1 = 1.5405$ A). Pitchblendes treated in this way included not only those from Ace and Christie Lakes, but also one from adjacent Beaverlodge Lake (all in the Goldfields area), one from Black Lake (Saskatchewan) situated approximately 100 miles east of Goldfields, and one from Great Bear Lake, Northwest Territories. Dr.

---

* Assistant Professor of Geology.

† Assistant Professor of Mineralogy.

G. M. Brownell Chairman of the Department of Geology, University of Manitoba, kindly provided the specimens from Beaverlodge and Black Lakes.

OBSERVATIONS AND CONCLUSIONS

The results of this investigation appear in the accompanying table. The most striking observations are first, that certain specimens give a weak UO_2 pattern before ignition and a strong UO_2 pattern after, and second, that other specimens give a weak or a strong UO_2 pattern before ignition but a combination of a UO_2 and a U_3O_8 pattern after, these two patterns varying in relative strength with different specimens. From chemical analyses it is well known that pitchblende consists of a mixture of variable amounts of UO_2, U_3O_8, and UO_3, and Goldschmidt & Thomassen (1923) have related the degree of oxidation with the x-ray powder pattern. Their conclusions, which offer an explanation for the present results, are summarized in Palache, Berman & Frondel (1944, p. 619):

> "Natural uraninite containing much UO_3 through oxidation is apparently structurally identical with UO_2, . . . but on ignition out of contact with oxygen it may recrystallize in part or entirely to U_3O_8, while pure UO_2 remains unchanged. The excess O in the oxidized uraninites may be in solid solution in the structure. Since UO_3 is apparently amorphous the x-ray evidence for excess O in the structure is not conclusive. Pitchblende is structurally identical with uraninite, but has a very small particle size (10^{-4} to 10^{-7} cm.) and somewhat smaller cell dimensions ($a_0 = 5.42 - 5.45$[kX])."

On the basis of Goldschmidt & Thomassen's work, and taking into account the observed metamict character of most of our specimens, it is convenient to classify them according to the x-ray patterns of the unheated and of the ignited powders. An extension of such a classification might well prove useful in describing the character of uraninites and pitchblendes in general. Following is our classification with the sample numbers which exemplify each type:

1. Crystalline UO_2, not oxidized; strong UO_2 pattern before and after ignition; sample 9 (Figs. 1a, 1b).

2A. Metamict UO_2, not oxidized; faint UO_2 pattern before ignition, strong UO_2 pattern after; samples 1 (Figs. 2a, 2b), 3, and 6.

FIGS. 1–4. X-ray powder photographs with Cu/Ni radiation; camera radius $360/4\pi$ mm. (1 mm. on film$=1°\theta$); full size reproductions of contact prints. FIGS. 1a, b. Pitchblende, Great Bear Lake, Northwest Territories, representing type 1. 1a, before ignition: UO_2; 1b, after ignition: UO_2. FIGS. 2a, b. Pitchblende, Ace Lake, Saskatchewan, representing type 2A. 2a, before ignition: metamict UO_2; 2b, after ignition: crystalline UO_2. FIGS. 3a, b. Pitchblende, Black Lake, Saskatchewan, representing type 3, 3a, before ignition: UO_2; 3b, after ignition: U_3O_8. FIG. 4. Synthetic U_3O_8.

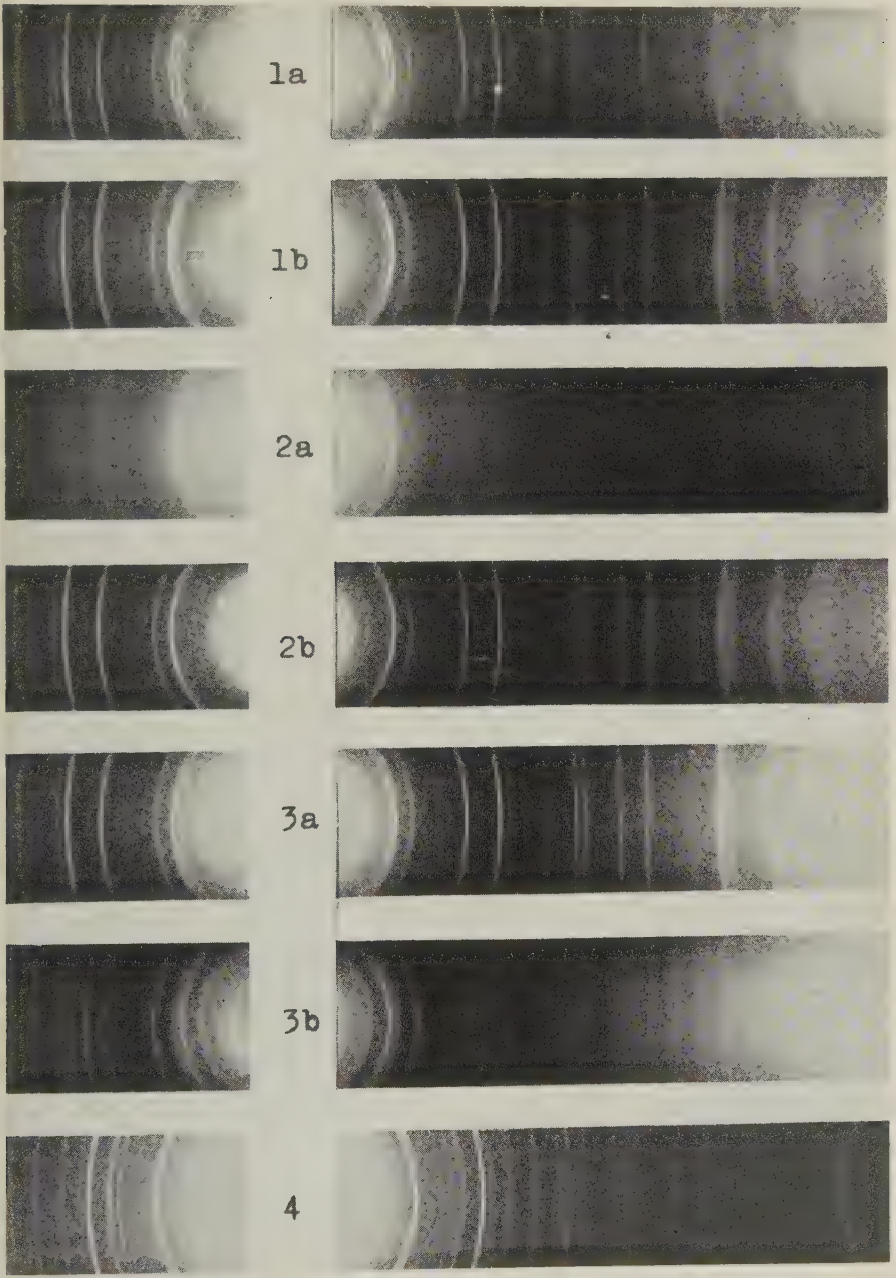
1a
1b
2a
2b
3a
3b
4

2B. Metamict UO_2, partly oxidized; faint UO_2 pattern before ignition, moderately strong UO_2 and U_3O_8 patterns after; samples 4 and 7.

2C. Metamict UO_2, largely oxidized; faint UO_2 pattern before ignition, moderately strong U_3O_8 and faint UO_2 pattern after; samples 2 and 5.

3. Crystalline UO_2, largely oxidized; strong UO_2 pattern before ignition, strong U_3O_8 pattern after with no appreciable UO_2; sample 8 (Figs. 3a, 3b).

The powder patterns representative of types 1, 2A, 3 are reproduced as Figs. 1, 2, 3 respectively, and for comparison, Fig. 4 shows the pattern of synthetic U_3O_8 prepared by R. J. Arnott by heating $UO_2(NO_3)_2 \cdot 6H_2O$ and then reducing the product with lampblack. The spacings and intensities of this pattern and those of the pitchblendes which gave U_3O_8 lines, are in substantial agreement with the data for U_3O_8 in the ASTM Card Index (1945, II-585). Some of the photographs which are reproduced show, in addition to the uranium oxide patterns, a few very weak lines due to impurities.

The question arises as to whether the oxidation from UO_2 to U_3O_8 is due to oxygen within the pitchblende, or to the addition of oxygen during heating. As all specimens were heated under uniform conditions it would be expected, if oxygen were added during heating, that all specimens would have changed in part to U_3O_8. As this is not the case it is inferred that the chemical changes are due to the state of oxidation of the pitchblende itself, prior to heating, or to the presence of oxygen in solid solution.

With the small number of specimens examined, it is difficult to make generalizations relating the degree of oxidation and the metamict character to any one of the cell edge, the locality, or the color of the streak. The cell edges, ranging from 5.39 to 5.45 A, fall a little outside the range given by Goldschmidt & Thomassen, 5.43 to 5.46 A, but almost within the range given by Arnott in a paper elsewhere in this issue, 5.403 to 5.475 A. Regarding locality, all the metamict pitchblendes come from the Goldfields area and show varying degrees of oxidation, whereas the specimens from both Black Lake and Great Bear Lake are crystalline and differ strongly in their degrees of oxidation.

Most of the samples showed a noticeable change in the color of the powder after ignition and, as indicated at the foot of the table, the colors were matched with those in the *Rock Color Chart*. The *Handbook of Chemistry and Physics* (1948, p. 514) gives the following colors for the uranium oxides; UO_2, brownish-black; U_3O_8, olive-green; and UO_3, yellowish-red. Our observed colors show limited correlation with these. The unoxidized pitchblendes (1, 3, 6, and 9) are mainly brownish-gray, most of them turning to a dark gray after ignition. The olive-green color of pure U_3O_8 is suggested by only one of the specimens containing

TABLE 1

No.	Locality	*Color of Unheated Powder	*Color of Ignited Powder	Strength of Pattern	a, A (± 0.01) of UO_2	Remarks
1a	Ace Lake	Brownish-gray	....	Faint	....	Metamict UO_2
1b	Ace Lake	....	Dark gray	Moderately strong	5.43	UO_2 structure restored
2a	Ace Lake	Brownish-gray	....	Very faint	....	Metamict UO_2
2b	Ace Lake	....	Dark Yellowish-brown	Moderately strong	....	Mainly U_3O_8, some UO_2
3a	Ace Lake	Dark greenish-gray	....	Faint	....	Metamict UO_2
3b	Ace Lake	....	Dark gray	Strong	5.39	UO_2 structure restored
4a	Christie Lake	Olive-gray	....	Very faint	....	Metamict UO_2
4b	Christie Lake	....	Dusky Yellowish-brown	Moderately strong	5.42	UO_2 and U_3O_8
5a	Christie Lake	Brownish-gray	....	Faint	....	UO_2
5b	Christie Lake	....	Grayish-brown	Faint	....	Mainly U_3O_8, some UO_2
6a	Christie Lake	Brownish-gray	....	Faint	....	Metamict UO_2
6b	Christie Lake	....	Grayish-brown	Strong	5.41	UO_2 structure restored
7a	Beaverlodge Lake	Brownish-gray	....	Faint	....	Metamict UO_2
7b	Beaverlodge Lake	....	Dusky brown	Moderately strong	5.42	UO_2 and U_3O_8
8a	Black Lake	Dark greenish-gray	....	Strong	5.45	UO_2
8b	Black Lake	....	Dark greenish-gray	Strong	....	Mainly U_3O_8
9a	Great Bear Lake	Med. dark gray	....	Strong	5.45	UO_2
9b	Great Bear Lake	....	Dark gray	Strong	5.41	UO_2

* Colors of the powders are close to those given in the *Rock Color Chart* (National Research Council, Washington, D. C.).

it, number 8, although the brownish shade assumed by 2, 4, 5, and 7 after ignition may be due to the development of U_3O_8 in these powders. In general, however, our observations indicate that no definite deductions regarding the state of oxidation of the uranium in a given pitchblende can be made from the color of its powder either before or after ignition.

SUMMARY

(1) The work of Goldschmidt & Thomassen (1923) and the present study indicate that a convenient way of determining the approximate degree of oxidation of the uranium in a given pitchblende is to

make *x*-ray patterns of the powder before ignition and after ignition in a closed crucible. Specimens not oxidized give a UO_2 pattern in both cases; specimens highly oxidized give a UO_2 pattern before ignition and a U_3O_8 pattern after; and specimens partly oxidized give UO_2 before and both UO_2 and U_3O_8 after.

(2) Nine specimens of pitchblende studied in this way showed examples representing all stages of oxidation.

(3) Seven pitchblendes from the Goldfields area, Saskatchewan, are shown to be metamict, apparently the first metamict pitchblendes to be described. These varied widely in their degree of oxidation.

(4) On the basis of their crystalline or metamict character, and their degree of oxidation as described under (1), the nine specimens examined have been classified into five types. An extension of this classification might prove useful in describing all uraninites and pitchblendes.

(5) The streak of a given pitchblende does not, in general, give definite evidence concerning the state(s) of oxidation of the constituent, uranium.

REFERENCES

ASTM (1945): X-ray diffraction patterns, first supplementary set of cards—*Am. Soc· Test. Mat.* (Philadelphia).

Goldschmidt, V. M. & Thomassen, L. (1923): Die Krystallstruktur natürlicher und synthetischer Oxyde von Uran, Thorium und Cerium—*Vidensk. Selsk. Skr.*, Mat.-nat. Kl., **2.** [*Min. Abs.* **2**—206.]

Palache, C., Berman, H. & Frondel, C. (1944): *Dana's system of mineralogy*, ed 7, **1**—New York.

Christie, A. M. & Kesten S. N. (1949): Goldfields and Martin lake map-areas, Saskatchewan—*Geol. Surv. Canada*, paper 49-17.

AN ELECTRON MICROSCOPIC EXAMINATION OF SYNTHETIC TOURMALINE CRYSTALS

William H. Barnes
National Research Council, Ottawa, Ontario.

Abstract

Representative electron micrographs illustrating the forms of tourmaline crystals synthesized by Frondel, Hurlbut & Collette are reproduced. A few measurements on the sizes of the crystals are given and the behavior of the crystals during fusion in the electron beam is illustrated.

Tourmaline crystals have been synthesized by Frondel, Hurlbut & Collette (1947) using a hydrothermal method involving the recrystallization of powdered tourmaline glass heated with water solutions of magnesium and alkali borates. Since the crystals are very small (of the order of 0.5 μ) it was considered of interest to examine them in the electron microscope. Two samples (numbers 278 and 348) were kindly supplied by Dr. Clifford Frondel and were studied in an R.C.A. electron microscope, model EMU, equipped with a biased electron gun. Each sample was in the form of a fine powder having a light buff tint.

Preparation of Specimens

Suspensions of the crystals in distilled water were prepared by hand shaking, with the aid of a spatula and under the influence of a Tesla coil. No marked difference in dispersal was observed as a result of the different methods so that simple shaking of a small amount of the powder in distilled water contained in a closed vial was adopted as a general procedure. In some cases the larger particles were allowed to settle before removing a drop of the suspension to the specimen screen; in others, the suspension was shaken immediately before removal of the drop. Larger aggregates were observed in the latter case but individual crystals appeared to be of the same average size and to show the same forms as those in drops taken from the supernatant suspension after allowing the larger aggregates to settle. In all cases a drop of the aqueous suspension was placed on a thin film of formvar covering the stainless steel specimen screen and was allowed to dry in air (protected from dust contamination) before placing in the specimen holder of the microscope. In some cases two or three drops of the suspension were placed on the formvar, the water being allowed to evaporate completely after the addition of each drop.

OBSERVATIONS AND RESULTS

A general survey of preparations made up from the two samples showed (a) that the tourmaline is very well crystallized in both and (b) that there is no noticeable difference either in the habits or size range of the crystals in the two samples. Typical electron micrographs are shown in Fig. 1 where the scale line in each photograph represents a length of one micron.

Isolated single crystals are relatively rare and some of those observed probably were detached from the more common spherulitic clusters such as that shown in Fig. 1 A. Fan-shaped groups, as illustrated in Fig. 1 B, C, D, are very prevalent and may also be fragments of larger spherical aggregates. The majority of the crystals have an elongated prismatic habit. Dimensions, as measured on optical enlargements of the photographs, which actually are plane projections of the crystals, are as follows: length, 0.2μ to 2.5μ (24 crystals measured); breadth, 0.03μ to 0.4μ (79 crystals measured); ratio, length to breadth, 2.6 to 14 (22 crystals measured).

Virtually all the prisms in the photographs appear to be terminated by pyramidal faces on the ends away from the centers of the aggregates, *i.e.*, in the direction of growth. Although the opposite ends are visible only in a very few cases they appear to be terminated by the basal pinacoid, or by less steep oblique faces. These observations suggest that the outer ends of the prisms, in the direction of growth, are the antilogous poles (Frondel, 1948, p. 9). It should be noted, however, that the electron micrographs are plane projections and that the depth of focus of the electron microscope is relatively large. Thus a prism terminated by a pinacoid but inclined to the observer in a direction normal to the field of view may project as a rectangle terminated by a triangle. Stereoscopic photographs indicate that the depths of the crystal groups are from one-quarter to as much as the width of the field or more. The pyramidal terminations of some of the prisms in the plane photographs appear in a stereoscopic view to be due to the inclination of the crystals to the plane of projection. This is often difficult to decide because the crystals are so opaque in the photographs that only the silhouette edges are visible. Not all the crystals, however, have simple prismatic forms; more complex ones are shown in Fig. 1 E, F, G, H. The largest dimension of these more compact forms was found to vary from about 0.8μ to about 2.5μ. Several examples of parallel growth were observed. One of these is illustrated in Fig. 1 I; in others the central hole was enclosed completely.

Characteristic of these tourmaline samples is the presence of a thin micaceous by-product of which small sheets are attached to the edges of the crystals in Fig. 1 C, D. Better examples will be found in Fig. 1 J,

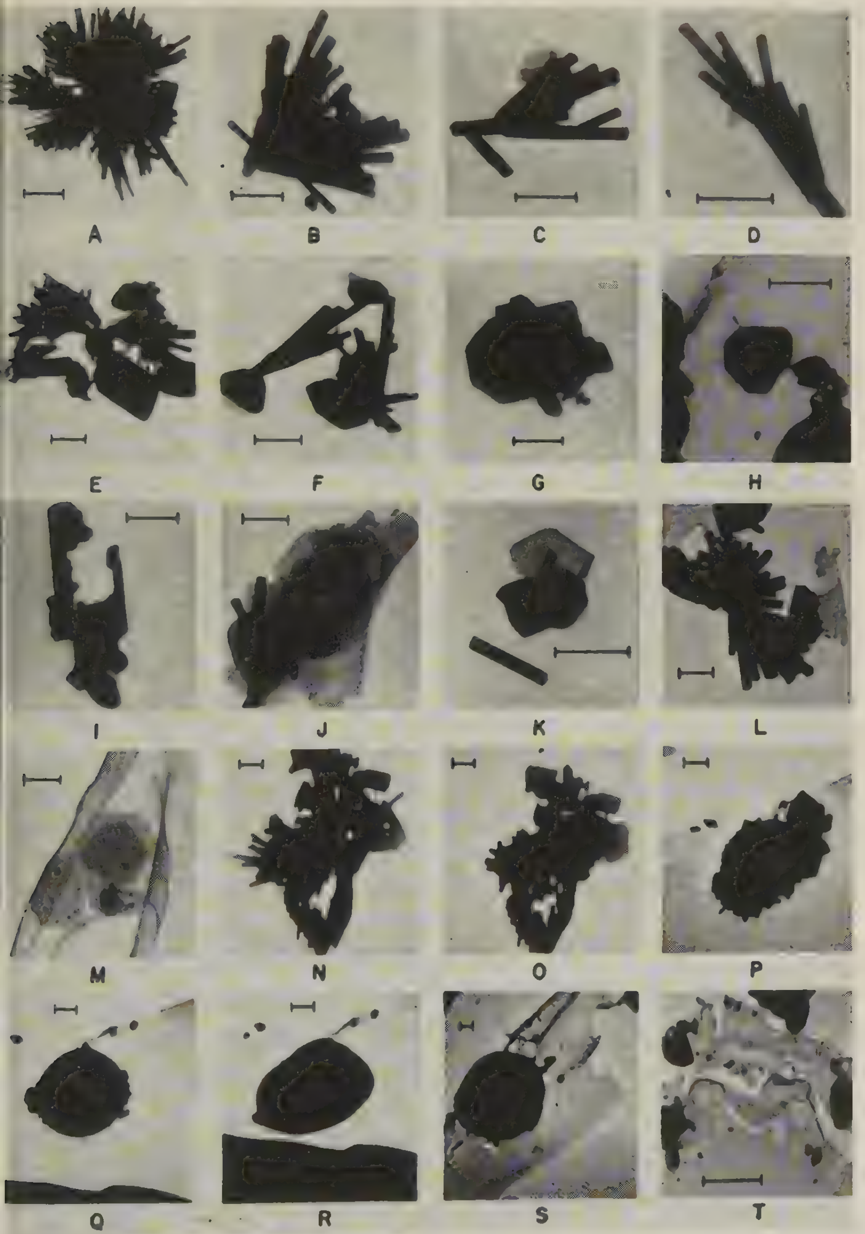

FIG. 1. Electron micrographs of synthetic tourmaline crystals.
(For explanation, see text.)

K, L, M. In addition to the isolated prismatic crystal in Fig. 1 K, the irregular dark and light patches represent thick and thin sheets of the micaceous material, the former partially wrapped around a prism whose end is outlined against the lighter sheet. (It should be mentioned that the disc that appears as a possible hole in the darker sheet of mica is due to the visible light from the electron gun filament; it will also be observed in the center of Fig. 1 J.)

In appearance, the micaceous material varies from heavily spotted, as in the sheets in the folds of the broken and curled edge of the formvar film in Fig. 1 M to clear and beautifully formed, as in the example on the right hand side of Fig. 1 L. Under magnification, and particularly stereoscopically, the latter looks like muscovite. Basal cleavage, elastic deformation of the sheets and what appears to be ribbon parting have been observed in other photographs. A few cases of relatively thick masses of small fragments of this material have been noticed.

During examination of the tourmaline crystals on the fluorescent screen in the microscope many of the groups of crystals showed a tendency to fuse in the electron beam. The same effect has been observed with other materials. It can be controlled to some extent by manipulation of the beam current and intensity dials; it is most frequently observed with the electron beam highly concentrated on the specimen at cross-over and with the beam current turned up. Not all groups of the tourmaline crystals could be fused in the electron beam but the phenomenon seemed to be more frequent with radiating clusters of long narrow prisms. Larger aggregates generally were more susceptible than smaller ones and very rarely were attempts to melt individual crystals successful. In most cases of fusion the formvar film ruptured either at the crystals or very close to them. Aggregates touching or near the wire of the specimen screen appeared to be the most vulnerable. In some cases plastic bending of the crystals occurred prior to melting.

Under favorable conditions it was possible to arrest the fusion process at successive stages. Thus in Fig. 1, N shows a group of crystals that has just started to shrink under the electron bombardment; its initial appearance can be deduced (at least in the original negative) from the marks on the formvar film. In O the group has become further consolidated and the rounded outlines of some fused crystals can be seen. Subsequent stages, including rupture of the supporting film, are illustrated in P, Q and R. The black region across the bottom of the last two plates is the image of the edge of the specimen screen wire towards which the broken formvar screen tends to draw.

The molten mass frequently behaves in a very dramatic way under continued bombardment; it seethes and bubbles, due presumably to the escape of water vapor, oxygen and fluorine, from the release of OH^- and F^-. Frequently, small particles of molten material are ejected from the mass and move around on the formvar film leaving tracks in their wake as shown in Fig. 1 S.

Since tourmaline melts between about 1050° and 1200° C. for iron-rich types to above 1725° C. for lithia-tourmaline (Frondel, Hurlbut & Collette, 1947, p. 680), the present observations are in qualitative agreement with Watson's conclusion (1948, p. 718) "that local temperatures of at least the order of 1600° C. can be achieved in electron microscopes, using a biased gun."*

Usually there is no change in the appearance of the thin formvar supporting film other than rupture and the marks left by the passage of these molten particles. An unusual film, however, appears in Fig. 1 T where the formvar has a grainy, brittle appearance due possibly to light shadow casting by evaporation from the molten tourmaline. Watson has noted a similar effect in his study of "pseudo-structures." Stereoscopically the two clear particles on the northwest edge of the globule in the upper left corner of the photograph appear to be transparent crystals with well-defined faces. This is observed in a less striking manner with the clear section that forms the upper part of the black mass on the right hand edge of the field. These are the only definite indications of possible recrystallization of the molten material observed during the investigation. Admittedly, however, it is more probable that the effect is caused by peculiar convolutions of the broken formvar film.

I am indebted to Miss Helen Jago and to Miss Ivy Michel for technical assistance in the preparation of specimens and the processing of the plates and prints.

REFERENCES

Frondel, C., Hurlbut, C. S. & Collette, R. C. (1947): Synthesis of tourmaline—*Am. Mineral.*, **32,** 680–681.

Frondel, C. (1948): Tourmaline pressure gauges—*Am. Mineral.*, **33,** 1–17.

Watson, J. H. L. (1948): Pseudostructures in electron microscope specimens—*J. App. Phys.*, **19,** 713–720.

---

* In Watson's paper (1948, p. 718), SiO_2 should read TiO_2. At the melting point, (1640° C.), titanium dioxide, in the form of rutile, decomposes and part of the activity of the molten material observed by Watson probably was due to the evolution of oxygen.

A ROENTGENOGRAPHIC METHOD FOR DETERMINING PLAGIOCLASES*

Fernand Claisse
Department of Mines, Quebec, Canada.

Abstract

A new x-ray diffraction method is described which permits the measurement of the Ab-An percentage composition of plagioclases to 1 or 2 per cent. The determination of line separation instead of absolute line position eliminates several sources of error, and enables the same calibration curves to be used by any laboratory. Several plagioclases of known composition were analyzed in this manner, and calibration curves are given. They indicate that plagioclases do not constitute a single isomorphic series, but rather two such series, with a transition point in the vicinity of Ab_2An_1.

Plagioclases may be considered as solid solutions of albite ($NaAlSi_3O_8$) and anorthite ($CaAl_2Si_2O_8$) the composition of which may vary from $Ab_{100}An_0$ to Ab_0An_{100}. This composition may be determined by various optical methods, but these are not accurate when the sample crystals have been altered, or when the sample is finely powdered.

Since the physical properties of solid solutions vary with their composition, a study of the latter by x-ray diffraction is theoretically possible and would overcome the difficulties of the optical methods. The positions of corresponding lines in the diffraction patterns of Ab and An (which crystallize in the same system and with unit cells which have approximately the same dimensions) will be shifted in complementary fashion as the composition of the plagioclase changes. However accurate measurement of these line positions is very difficult, and is subject to several errors, such as those due to eccentricity of the sample in the powder camera, and to film shrinkage during processing. Even when these are corrected the resulting accuracy is usually too low to make the determinations useful, and in general the calibration curves so obtained may not be of any use with other instruments.

In this laboratory, we have analyzed the composition of such solid solutions by measuring the distance between two adjacent lines in the diffraction pattern, instead of the absolute position of one line. This has resulted in much greater accuracy, and eliminates the errors due to sample eccentricity and film shrinkage. In addition, the calibration curves obtained with the powder camera are identical with those obtained with the spectrometer.

Procedures

The percentage compositions of the eight plagioclases examined were first determined by various optical methods to about 1 per cent. The results are given in Table 1.

---

* Published by permission of the Deputy Minister, Department of Mines, Quebec.

TABLE 1. MINERALOGICAL ANALYSIS OF THE PLAGIOCLASES

Plagioclase	Mineralogical Collection	Locality	Composition	Optical Method
Albite	I.I.A.	Amelia Court House, Virginia,	$Ab_{99-100}An_{1-9}$ (a)	(a) Double variation
Pericline	Ward's	Teufelsmühle, Habachtal, Salzburg	$Ab_{91}An_{9}$ (b)	(b) Extinction angle on (010), α':[100]
Oligoclase	I.I.A.	Buckingham, Quebec	$Ab_{82}An_{18}$ (b)	(c) Fedorov
Oligoclase	....	Unknown	$Ab_{69-71}An_{31-29}$ (b)	
Andesine	Ward's	Kragerö, Norway	$Ab_{57}An_{43}$ (b, c)	
Labradorite	Ward's	Near Nain, Labrador	$Ab_{45}An_{55}$ (b)	
Bytownite	Ward's	Crystal Bay, Minnesota	$Ab_{22}An_{78}$ (c)	
Anorthite	I.I.A.	Miakejima, Japan	$Ab_{1-2}An_{99-98}$ (b)	

I.I.A. = Institute of Industrial Arts, Gardenvale, P.Q.

Diffraction patterns of the samples were then obtained in various ways. Three patterns of each sample were taken with a Norelco x-ray Diffraction Spectrometer, where the detection is performed by a Geiger-Müller counter with scaling circuit and mechanical register. Tube current and voltage for a copper target were 6 ma and 35 kv respectively. The source slit was 1.5×6 mm. while the detector slit was 0.25×6 mm. The first pattern was drawn by taking readings (counts/min.) every 0.01° as the counter was displaced. The second pattern was taken for 0.05° displacements. For the third pattern, the counter was displaced automatically at the rate of 1° per minute, while its output was recorded on a Brown Electronik potentiometer. Two additional diffraction patterns were taken of each sample using a Norelco 114.59 mm. diameter powder camera. Both copper (20 ma and 35 kv) and iron (15 ma and 30 kv) targets were used.

In examining the diffraction patterns taken of each sample, it was necessary to choose lines satisfying several requirements. They must be (a) prominent so as to be observable even when the sample is diluted; (b) easily recognizable; (c) in a high dispersion region of the pattern for accuracy of measurement; and (d) selected in at least two groups in case one should be masked by impurities. Such conditions are met by the two groups of lines chosen as indicated in Figs. 1 to 8. They are identified as follows:

	LINE	POSITION	RECOGNIZABLE CHARACTERISTIC
Group I	1	2.64 A	Strong line between two weak lines
	2	2.55–2.49 A	
	3	2.51–2.44 A	
Group II	4	1.83–1.82 A	Weak line between two strong lines.
	5	1.79 A	
	6	1.78–1.76 A	

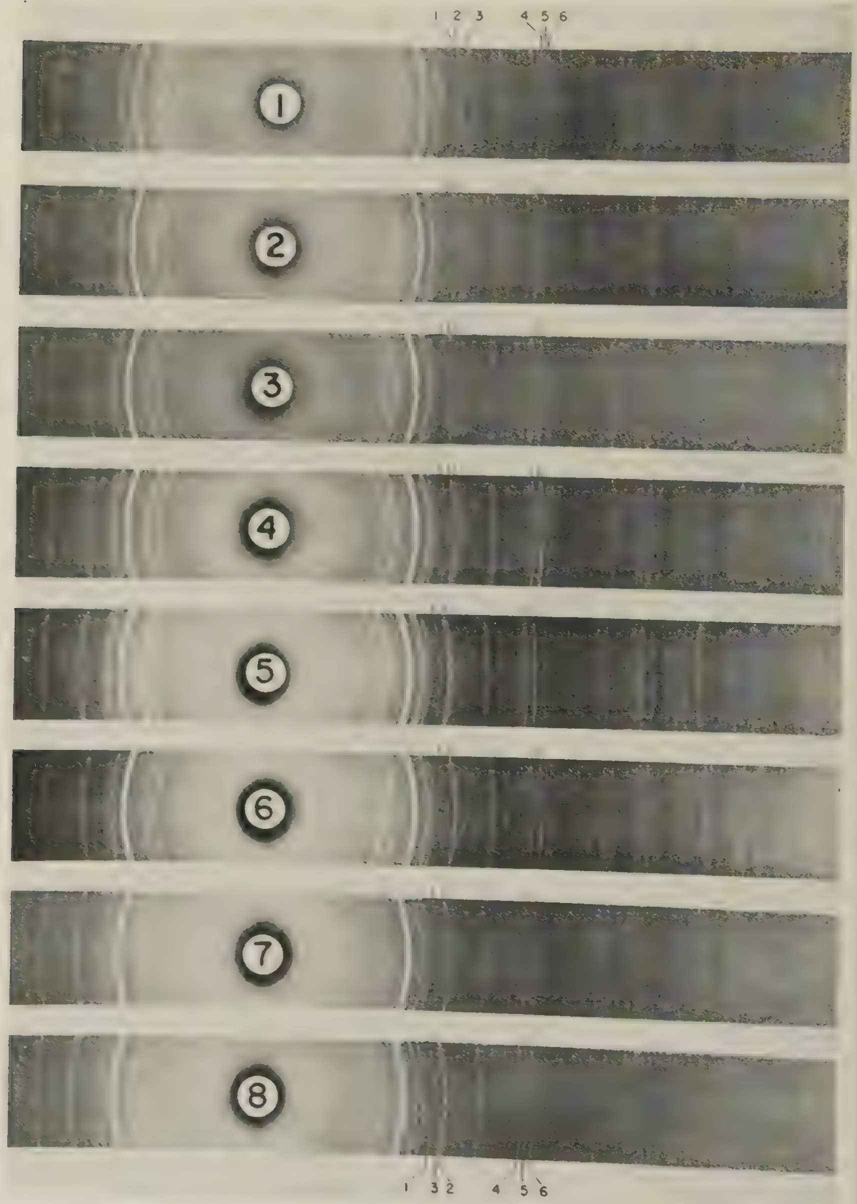

Fig. 1–8. X-ray diffraction pattern (FeKα) of a few plagioclases showing positions of the two groups of lines chosen. The inversion in the position of lines 2 and 3 in Fig. 8, following the overlapping of the same two lines in Fig. 7, is to be noted. 1. Albite. 2. Pericline. 3. Oligoclase. 4. Oligoclase. 5. Andesine. 6. Labradorite, 7. Bytownite, 8. Anorthite.

TABLE 2. DISTANCE* BETWEEN THE LINES 1, 2, AND 3 AS OBTAINED BY DIFFERENT MEANS

Plagioclase	Lines	Powder camera			Spectrometer			Average		
		FeKα	FeKα / 1.31†	CuKα	Motor 1°/m.	Manual .05 deg.	Manual .01 deg.	1–2	2–3	1–3
$Ab_{1-2}An_{99-98}$	1–2	2.75	2.10	(1.95)	2.10	2.08	2.11	2.10		
	2–3	−.38	−.29	(.00)	−.25	−.27	−.27		−.27	
	1–3	2.37	1.81	(1.95)	1.85	1.81	1.84			1.83
$Ab_{22}An_{78}$	1–2	2.50	1.91	1.88	1.90	1.87	1.86	1.88		
	2–3	.00	.00	.00	.00	.00	.04		.01	
	1–3	2.50	1.91	1.88	1.90	1.87	1.90			1.89
$Ab_{45}An_{55}$	1–2	2.23	1.70	1.69	1.80	1.70	1.69	1.72		
	2–3	.55	.42	.48	.45	.38	.38		.42	
	1–3	2.78	2.12	2.17	2.25	2.08	2.07			2.14
$Ab_{57}An_{43}$	1–2	2.08	1.59	1.62	1.55	1.57	1.57	1.58		
	2–3	.80	.61	.65	.60	.59	.57		.61	
	1–3	2.88	2.20	2.27	2.15	2.16	2.14			2.18
$Ab_{69-71}An_{31-29}$	1–2	2.00	1.53	1.52	1.60	1.53	1.55	1.55		
	2–3	1.00	.76	.80	.70	.73	.75		.75	
	1–3	3.00	2.29	2.32	2.30	2.26	2.29			2.30
$Ab_{82}An_{18}$	1–2	1.75	1.34	1.37	1.35	1.31	1.32	1.34		
	2–3	1.40	1.07	1.15	1.25	1.20	1.19		1.17	
	1–3	3.15	2.40	2.52	2.60	2.51	2.51			2.51
$Ab_{91}An_9$	1–2	1.60	1.22	1.18	1.20	1.20	1.20	1.20		
	2–3	1.90	1.45	1.45	1.35	1.42	1.44		1.42	
	1–3	3.50	2.67	2.63	2.55	2.62	2.64			2.62
$Ab_{99-100}An_{1-0}$	1–2	1.42	1.08	1.02	1.10	1.05	1.05	1.06		
	2–3	2.25	1.72	1.83	1.70	1.77	1.76		1.76	
	1–3	3.67	2.80	2.85	2.80	2.82	2.81			2.82

* The readings are in degrees 2θ.

† Ratio of the dispersion of iron radiation to that of copper radiation in this region.

The distances between the lines in each group were then accurately measured. For the first two diffraction patterns taken with the spectrometer, the counting rate was plotted as a function of counter position, and the distance between line peaks measured in degrees. For the third

Table 3. Distance* between the Lines 4, 5, and 6 as Obtained by Different Means

Plagioclase	Lines	Powder camera			Spectrometer		Average		
		$\mathrm{Fe}K\alpha$	$\frac{\mathrm{Fe}K\alpha}{1.35}$†	$\mathrm{Cu}K\alpha$	Motor 1°/m.	Manual .05 deg.	4–5	5–6	4–6
$Ab_{1-2}An_{99-98}$	4–5	1.58	1.17	1.15	1.20	1.15	1.17		
	5–6	1.25	.93	.98	1.00	.86		.94	
	4–6	2.83	2.10	2.13	2.20	2.01			2.11
$Ab_{22}An_{78}$	4–5	1.45	1.07	1.20	1.20	1.10	1.14		
	5–6	1.00	.74	.73	.70	.75		.73	
	4–6	2.45	1.81	1.93	1.90	1.85			1.87
$Ab_{45}An_{55}$	4–5	1.35	1.00	1.05	1.05	.99	1.02		
	5–6	.98	.73	.66	.70	.71		.70	
	4–6	2.33	1.72	1.71	1.75	1.70			1.72
$Ab_{57}An_{43}$	4–5	1.35	1.00	.97	.95	.87	.95		
	5–6	.80	.59	.62	.60	.65		.61	
	4–6	2.15	1.59	1.59	1.55	1.52			1.56
$Ab_{69-71}An_{31-29}$	4–5	1.29	.95	.95	.85	.89	.91		
	5–6	.80	.59	.55	.60	.59		.58	
	4–6	2.08	1.54	1.50	1.45	1.48			1.49
$Ab_{82}An_{18}$	4–5	1.10	.81	.83	.80	.82	.81		
	5–6	.85	.63	.55	.60	.59		.59	
	4–6	1.95	1.44	1.38	1.40	1.41			1.41
$Ab_{91}An_{9}$	4–5	1.00	.74	—	.75	.70	.73		
	5–6	.67	.50	—	.55	.55		.53	
	4–6	1.67	1.24	1.30	1.30	1.25			1.27
$Ab_{99-100}An_{1-0}$	4–5	.95	.70	—	.60	.65	.66		
	5–6	.70	.52	—	.60	.52		.54	
	4–6	1.65	1.22	1.22	1.20	1.17			1.20

* The readings are in degrees 2θ.

† Ratio of the dispersion of iron radiation to that of copper radiation in this region.

pattern, the distance between lines was measured directly on the Brown potentiometer chart. The films of the powder camera patterns were measured with a Norelco measuring box without magnification. The camera used was such that 1 mm. of film corresponded to 1° 2θ, so that conversion to degrees was simple. The distance between the lines for the two groups are given in Tables 2 and 3.

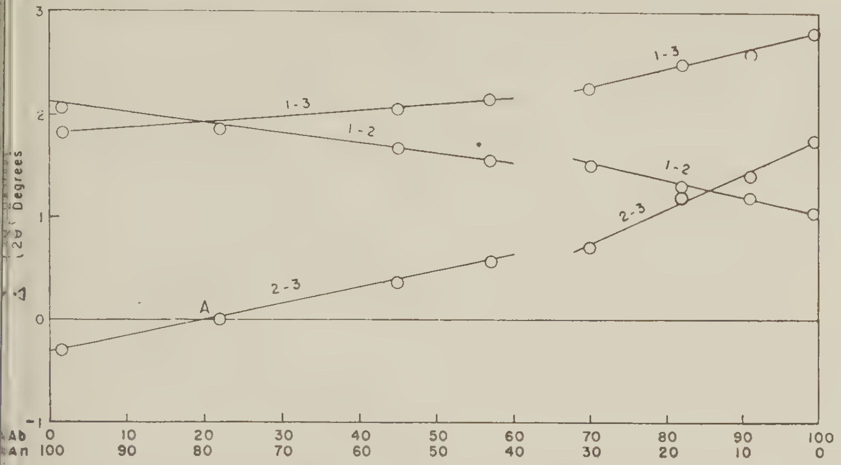

FIG. 9. Distance between lines 1, 2, and 3. These readings are those obtained by using the spectrometer and measuring the intensity of the diffracted rays every 0.05 degree 2θ. The other methods give essentially the same curves.

RESULTS

When the averages of the five measurements of the distances between the lines are plotted as a function of percentage composition, we obtain the curves such as those in Fig. 9 for the first group, and those of Fig. 10 for the second group. It is immediately obvious that the first set may be used to determine percentage composition with far more accuracy than is possible by absolute line position measurement. In particular, the dis-

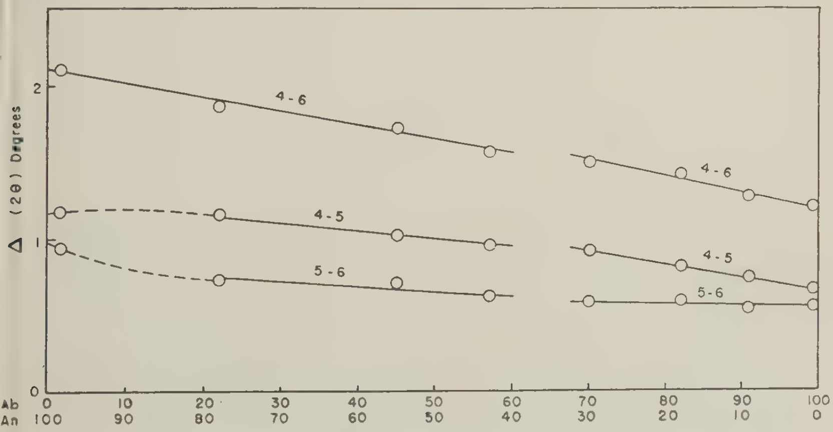

FIG. 10. Distance between lines 4, 5, and 6. These readings are the average of those obtained by different methods and given in Table 3.

tance between the lines 2 and 3 provides a very accurate index which may be obtained quite rapidly with any type of diffraction apparatus. The displacements are given in degrees, and hence these curves may be used in any laboratory.

TABLE 4. ACCURACY EXPECTED IN ANALYSING PLAGIOCLASES USING THE CURVES OF FIG. 1

Method	Absolute error	Curve	Accuracy*	
			$Ab_{100} \rightarrow Ab_{65}$	$Ab_{65} \rightarrow Ab_0$
	degrees		Percentage†	Percentage†
Powder camera, Cu target	±0.05	1–2	±2.9	±8.0
		1–3	3.1	5.3
		2–3	1.5	3.1
Powder camera, Fe target	.05	1–2	2.2	5.4
		1–3	2.6	4.1
		2–3	1.2	2.5
Spectrometer, manual, readings every 0.01 deg.	$.01_5$	1–2	0.9	2.4
		1–3	0.9	1.6
		2–3	0.5	0.9
Spectrometer, manual, readings every 0.05 deg.	.03	1–2	1.7	4.8
		1–3	1.9	3.3
		2–3	0.9	1.9
Spectrometer, motor 1° pm.	.05	1–2	2.9	8.0
		1–3	3.1	5.3
		2–3	1.5	3.1

* The accuracy is given for one measurement; it is greater when three measurements are made.

† Last figure uncertain.

Should lines 2 or 3 be masked by an impurity then one of the other curves of Fig. 9 will also give accurate composition data. However, since the lines 2 and 3 cross each other, the operator may not always be certain which one he is measuring, and consequently may have to choose between two accurate but ambiguous points equidistant from A for samples containing less than 40 per cent Ab (the minority). In this case the ambiguity is easily resolved by the curves of Fig. 10, which permit somewhat less accuracy but immediately indicate in which region of Fig. 9 the sample is located.

PRECISION

From Tables 2 and 3 it is seen that the results obtained by the five recording methods tested agree very well. The spectrometer is seen to be somewhat more accurate, and is also to be preferred for reasons of ease and rapidity of analysis. The greater slope of the curves in the high Ab content region, and the fact that most plagioclases are of this type is a fortunate coincidence. In our tests, the least precise results were obtained in measuring low Ab content samples with Cu$K\alpha$ radiation in the powder camera.

Summarized in Table 4 are the accuracies which may be expected from the measurement of the distance between two lines by different methods, for two different parts of the percentage range. Should more than one distance be measured, the accuracy will be correspondingly greater, and in general it is possible to make a composition analysis to 1 per cent by this simple and rapid method.

NOTE ON PLAGIOCLASES

It has been pointed out by Taylor, Darbyshire & Strunz (1934) that plagioclases probably do not form a single isomorphous series from $Ab_{100}An_0$ to Ab_0An_{100}, but rather two such series. They base this on their observation that the *c*-axis of low Ab content plagioclases is twice that of high Ab content samples. They explain this by remarking that the dominant Na ion of albite is surrounded by only 6 oxygen atoms, while the dominant Ca ion of anorthite is probably surrounded by 7 or 8 oxygen atoms. This in turn leads them to believe that the transition point between the series will be around the Ab_1An_1 point, where the nature of the dominant atom changes.

However, if their explanation is correct, it seems to us that albite would more easily replace anorthite than vice versa, since the Na atom would find its 6 oxygen atoms in the anorthite structure more easily than the Ca atom could find 7 or 8 in the albite structure. In other words albite will be more soluble in anorthite than the reverse. By the same token the transition point of the two isomorphous series—from albite solutions to anorthite solutions—should not be at the Ab_1An_1 point, but rather displaced so as to show more albite solutions.

The lines of Figs. 9 and 10 all show breaks in the vicinity of 60–70 per cent albite. This supports the theory that two isomorphous series exist, and that their transition point is displaced towards albite.

Acknowledgments. The writer is glad to express his gratitude to Mr. A. O. Dufresne, deputy minister of Mines, for permission to publish this paper. He also gratefully acknowledges the assistance furnished by Mr.

J. Girault who made the optical analyses of the plagioclases used in this work.

REFERENCES

BUHLER, J. S. (1945*a*): Engineering-design development of *x*-ray spectrometer—*Electrical Manufacturing*, **35,** No. 6.

—— (1945*b*): Process quality control with *x*-ray spectrometer –*Instrumentation*, **1,** No. 6.

FRIEDMAN, G. (1945): Geiger-counter spectrometer for industrial research –*Electronics*, **18,** 132–137.

TAYLOR, W. H., DARBYSHIRE, J. A. & STRUNZ, H. (1934): An x-ray investigation of the feldspars—*Zeits. Krist.*, **87,** 482–487.

A NEW METHOD FOR MEASURING THE REFRACTIVE INDICES IN MICACEOUS MINERALS*

J. P. Girault

Department of Mines, Quebec, Canada

Abstract

A narrow strip of the mineral to be studied is cut and set vertically in a small cup containing a liquid of suitable refractive index; the whole is then placed on a temperature cell (heating stage) which is attached to a microscope and coupled to a thermostat and a refractometer. The refractive index of the mineral is measured by varying the temperature and consequently the refractive index of the liquid medium. The method outlined also permits measurement of the birefringence of chlorites.

The complete study of a mica sample is often necessary, either for purely scientific information or when its industrial utilization is contemplated. This study is facilitated by the fact that the members of the mica group have some characteristic properties in common. A similar statement can be made concerning the chlorites, though this group is less homogeneous and less well known.

Winchell (1925, 1933, 1935) has proposed a classification showing rather close relations between the chemical composition and some of the optic properties of micas (γ, α, and $\gamma-\alpha$). The measurement of the indices of refraction is necessary for knowing the position occupied by a mica in Winchell's classification. At the same time, these measurements give a fair idea of the chemical composition of the mica. It has been thought that, for both reasons, the publication of a new method for measuring α would be of interest.

Previous Methods

The measurement of γ presents no great problem, since for the micas Z is always in the (001) plane. It can therefore be determined by the classical immersion method. The index normal to (001) is more difficult to measure.

Marie Louise Lindbergh (1946) has proposed a method which consists in introducing several cleavage flakes into a sirupy sodium silicate solution. In this medium, these fragments take up all possible orientations and one may be found having its (001) plane vertically disposed. Index α can thus be determined in the usual way.

Ferguson & Peacock (1943) have proposed another procedure. The index γ of the cleavage flake is measured and the lamella is then placed between the two hemispheres of a Fedorov universal stage in a liquid, the index N of which is such that $\alpha < N < \gamma$. The preparation is then tilted about the optical direction Y, on the E.-W. axis, until the Becke line disappears. Knowing the angle of rotation necessary to bring this about, an equation permits the evaluation of α.

---

* Published by permission of the Deputy Minister, Department of Mines, Quebec.

It has, however, seemed useful to devise a method allowing the measurement of α on a selected fragment without recourse to the Fedorov universal stage, since a number of laboratories do not yet possess this instrument. The proposed method is simple, rapid, and its degree of precision is good.

PROCEDURE

Using a razor blade, a narrow strip of mica 0.2 mm. or less in width is cut perpendicularly to (001). With the aid of a blowpipe, a pellet of lead about 2 mm. in diameter is fused on a supporting block of plaster or metal in such a way that the pellet presents a flat base. This pellet is then detached and, again with the aid of a razor blade, a vertical nick is cut on its top. Using a needle, one end of the mica strip is introduced into the gap in the fused lead pellet in such a way that its plane of cleavage rests vertically, and following this the groove is closed with the aid of fine forceps. Because of the malleability of lead, a slight error can be easily corrected. These operations can be accurately and rapidly carried out under a binocular microscope.

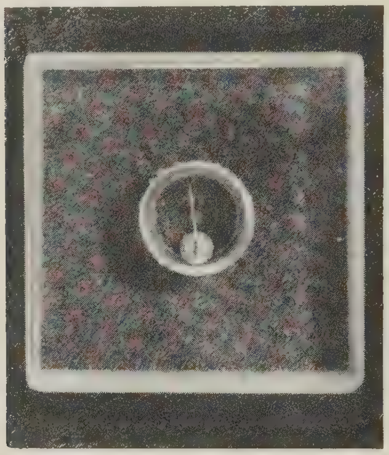

FIG. 1

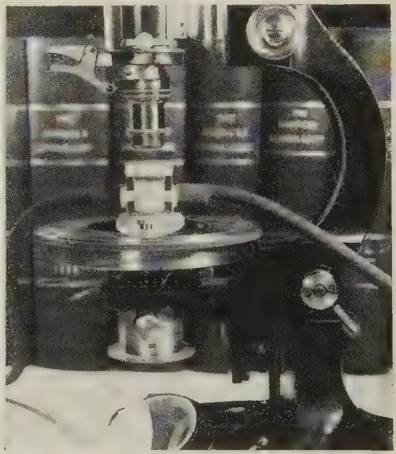

FIG. 2

The lead pellet is then introduced into a small cylindrical cavity bored in a glass block (Fig. 1). This cup is filled with a liquid of suitable index and the whole is placed on a temperature cell fixed to a microscope (Fig. 2); a drop of oil assures good contact and facilitates heat transfer. Details of the temperature cell are shown in Fig. 3.

The set-up for the measurement of the refractive index is of the current type, the heating stage being connected at one end to a thermostat and at the other end to an Abbe refractometer To regulate the temperature, a Hoeppler Ultra-thermostat characterized by its great precision (0.02° C.) and by the speed of circulation of water (6 litres/min.) has been used by the author. The latter characteristic is of great value, since it assures perfect equality of temperature throughout the whole apparatus.

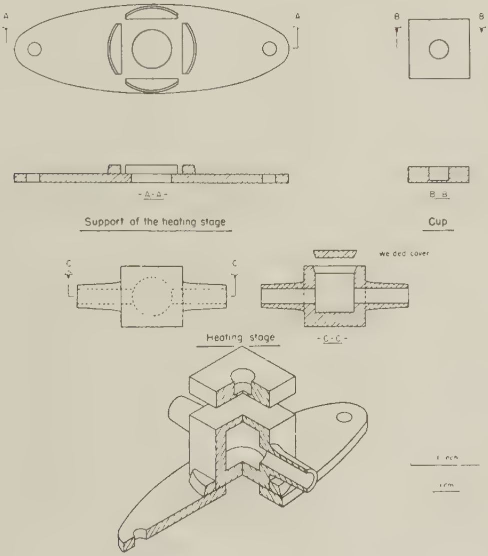

FIG. 3

The temperature of the water is varied till the Becke line disappears. At this point, the refractive index of the liquid is equal to that of the mica and it can be read on the refractometer drum.

The cup temperature has been checked with products of known melting points (beeswax and paraffin waxes), and found to be equal to that indicated by the refractometer and thermostat thermometers. To avoid differences in temperature between the various parts of the apparatus, it is necessary to vary the temperature slowly. The precision of the refractive index measurements made thus far is of the order of 0.002, but the use of a powerful monochromator would doubtless improve this.

APPLICATION AND LIMITATIONS OF THE METHOD

Because of its principle, the method applies to all minerals possessing a perfect micaceous cleavage and having one of their indices in a direction normal to this cleavage. In the micas and most of the chlorites α is the index normal to the cleavage; in some other chlorites it is γ and in these cases the method permits the measurement of the larger index. In a few minerals of the chlorite group, the direction of the index makes too large an angle with the normal to the plane of perfect cleavage, and in this instance the method does not apply. The flakes must be of sufficient size (a few millimeters is ample) and their optical orientation must be uniform.

MEASUREMENT OF THE BIREFRINGENCE OF CHLORITES

The method provides a means of measuring directly the birefringence $\gamma-\alpha$ of oriented sections of chlorites. This birefringence is usually weak and seldom exceeds 0.010. Consequently, by placing the chlorite section at 45° from the cross-hairs and in a position of substraction, the retardation Γ can be measured by means of a Berek compensator. If the breadth d of the section has been previously determined with a micrometer, one has $\gamma-\alpha=\Gamma/d$.

The majority of chlorites have birefringence values within the range of the Berek compensator. Using a section 0.2 mm. wide, birefringence up to 0.012 can be measured, which is large enough for all practical purposes.

This method does not apply to the micas, at least when using the standard compensator, because their birefringence $\gamma-\alpha$ is too high.

Acknowledgments. The present work was carried out in the Laboratories of the Department of Mines of the Province of Quebec, during the month of February 1948, under the guidance of the Director, Dr. Maurice Archambault, whose criticism and counsel have been most helpful. The author is also indebted to Dr. M. A. Peacock, of the University of Toronto, who critically revised this paper and made useful suggestions for its improvement. Mr. Laurent Bedard, of the Laboratories of the Department of Mines constructed the cup and the heating stage; his aid is much appreciated.

REFERENCES

FERGUSON, R. B. & PEACOCK, M. A. (1943): Measurement of the three principal indices of refraction in micaceous minerals by immersion on a tilting stage—*Am. Mineral.*, **28**, 563–570.

LINDBERGH, M. L. (1946): Measurement of the alpha index of refraction in micaceous minerals—*Am. Mineral.*, **31**, 317-320.

WINCHELL, A. N. (1925): Studies in the mica group—*Am. Jour. Sci.*, **9**, 309–327, 415–430.

—— (1933): *Elements of optical mineralogy. Part 2. Descriptions of minerals.* Ed. 3—New York.

—— (1935): The biotite system—*Am. Mineral.*, **20**, 773–779.

ON PARKERITE AND SHANDITE AND THE CRYSTAL STRUCTURE OF $Ni_3Pb_2S_2$*

M. A. Peacock and John McAndrew†
University of Toronto, Toronto, Canada.

Abstract

By quantitative spectrographic analysis parkerite from Sudbury carries 1.5±0.1 per cent Pb, giving the composition $Ni_3Bi_{1.95}Pb_{0.05}S_2$. If the composition $Ni_3Bi_{1.2}Pb_{0.8}S_2$ attributed to the original parkerite from Insizwa should be verified, it would be proper to use the name parkerite for the natural equivalent of the isostructural α-phase $Ni_3Bi_2S_2$ $-Ni_3BiPbS_2$, of the artificial system, and to distinguish the Canadian and South African examples as bismuthian and plumbian varieties.

Shandite (Ramdohr, 1950) from Trial Harbour, Tasmania, gives the distinctive x-ray powder pattern of pure $Ni_3Pb_2S_2$, the artificial β-phase which will hold almost no Bi in solid solution. In keeping with a face-centered "cubic" lattice and strong optical antisotropism $Ni_3Pb_2S_2$ has the following structure (rhombohedral description): $R\bar{3}m$; $r=5.565$ kX, $\alpha=60°$; $Z=1$. Pb I at 0 0 0. Pb II at $\frac{1}{2}\,\frac{1}{2}\,\frac{1}{2}$. 3 Ni at $\frac{1}{2}\,0\,0$; $0\,\frac{1}{2}\,0$; $0\,0\,\frac{1}{2}$. 2 S at $x\,x\,x$; $\bar{x}\,\bar{x}\,\bar{x}$; with $x=0.285$.

Since the original description of parkerite by Scholtz (1936, p. 186) on scanty material from Waterfall Gorge, Insizwa, East Griqualand, South Africa, and the description of a structurally identical mineral from Sudbury, Ontario, by Michener & Peacock (1943), our attention has been recalled to this mineral by certain relevant spectrographic, thermal, and roentgenographic studies which have been made in South Africa, and by the discovery by Ramdohr (1950) of a closely related new mineral, shandite, at Trial Harbour, Tasmania. As the South African publications are not generally available, and Professor Ramdohr's paper on shandite is in press at the time of writing, a brief summary of the previous work will be needed for the present contribution.

Owing to limitations of material the first description of parkerite was rather tentative and incomplete. In particular, the suggested composition, Ni_2S_3 or NiS_2, was misleading and subsequent occurrences of the mineral might not have been referred to parkerite except for the x-ray powder data supplied by Niggli in Scholtz' paper. Previous to 1940 Michener found an apparently new nickel bismuth sulphide in nickel ore from Sudbury, and subsequent detailed study by Michener & Peacock (1943) showed that this mineral is identical in all determinable crystallographic, physical, and chemical properties with artificial $Ni_3Bi_2S_2$, a compound previously prepared by Schenck & von der Forst (1939); practical identity of the *x*-ray powder pattern of the Sudbury mineral with that of the mineral from South Africa, and general compatability of their observed properties, showed that the Canadian mineral is at least structurally identical with the South African mineral and decided the authors to refer the new occurrence to parkerite rather than to propose a new name.

---

* Contributions to Mineralogy from the Department of Geological Sciences, University of Toronto, 1950, No. 2.

† Holding a Studentship of the Commonwealth Scientific & Industrial Research Organization (of Australia).

Subsequently Scholtz re-investigated the composition of the Insizwa parkerite with the aid of the spectrograph. Two microsamples were obtained from a polished ore specimen and submitted to Dr. Strasheim for qualitative spectrochemical analysis. Naudé (1945) reported that the two samples gave identical spectra showing lines of Ni, Bi, and also Pb, and from this he inferred that Pb is an important constituent of the South African mineral. From this qualitative spectrographic work, perhaps supported by other evidence which we cannot find in print, Dr. Scholtz appears to have decided that the composition of the South African parkerite is close to $Ni_3Bi_2S_2:Ni_3Pb_2S_2=6:4$, or $Ni_3Bi_{1.2}Pb_{0.8}S_2$ (du Preez, 1945; Cormack, 1948). This suggested that Pb, reported only as a chemical trace in Canadian parkerite, might actually be present in substantial amount.

Du Preez (1945) made a thermal study of a series of melts covering the whole range, $Ni_3Bi_2S_2-Ni_3Pb_2S_2$, which was called the "Parkerite series" with end-members "Bismuth-Parkerite, Bp" and "Lead-Parkerite, Lp." He found that Bp (mp 686° C.) forms a complete series of solid solutions with Lp (mp 717° C.) from pure Bp to practically $Bp_{50}Lp_{50}$, giving homogeneous products composed of large twinned crystals, like those of parkerite. The solid solution at $Bp_{60}Lp_{40}$, the supposed composition of South African parkerite, is distinguished by congruent melting at 707° C. Rapidly cooled melts from $Bp_{60}Lp_{40}$ to $Bp_{10}Lp_{90}$ are inhomogeneous, being composed of unmixed solid solutions and homogeneous twinned crystals of different composition, in various proportions. Pure Lp shows an unexplained deflection of the cooling curve at 543° C. and it will apparently hold less than 4 per cent Bp in solid solution at equilibrium.

Cormack (1948) made *x*-ray powder photographs of samples from du Preez' preparations, using unfiltered Cu-radiation and apparently strong exposures, and reporting the results by glancing angles and visual intensities. Cormack obtained a practically invariant parkerite pattern, substantially identical with those of Niggli and Michener & Peacock, from crystals (α-phase) in the range $Ni_3Bi_2S_2$ to $Ni_3Bi_{0.7}Pb_{1.3}S_2$. From samples in the range $Ni_3Bi_{0.6}Pb_{1.4}S_2$ to $Ni_3Bi_{0.2}Pb_{1.8}S_2$ he obtained a weakening pattern of the α-phase with a strengthening pattern of

$Ni_3Pb_2S_2$ (β-phase), which is similar to the pattern of the α-phase but distinct from it. Pure $Ni_3Pb_2S_2$ of course gave the pattern of the β-phase alone. These results can be reconciled with du Preez' thermal work and they show that the composition of Bp−Lp solid solutions, Bp_{100} to $Bp_{50}Lp_{50}$, cannot be determined by x-ray powder patterns. Cormack points out that Scholtz' supposition that his parkerite has the composition $Ni_3Bi_{1.2}Pb_{0.8}S_2$ is not at variance with the powder data, and he repeats the suggestion that the composition of the Canadian material should be examined again for Pb.

PARKERITE

As pointed out by Cormack, there is an inconsistency in the chemical composition of the Sudbury parkerite reported by Michener & Peacock (1943), who gave Ni and Bi and traces of Cu and Sn by spectrographic analysis, while the chemical analysis gave the composition $Ni_3Bi_2S_2$ with a trace of Pb. It was therefore decided to check the presence of Pb in our material and if possible to measure its proportion by quantitative spectrographic procedure.

The sample of parkerite used for quantitative spectrographic analysis was part of the material which had been prepared and used for the chemical analysis in Michener & Peacock (1943). This material still contained a few grains of sperrylite and other minerals which were removed as far as possible by hand.

For comparison the following series of $Ni_3(Bi, Pb)_2S_2$ solid solutions were prepared by fusion of the elements in evacuated silica glass bulbs: $Ni_3Bi_2S_2$, $Ni_3Bi_{1.5}Pb_{0.5}S_2$, Ni_3BiPbS_2, $Ni_3Pb_2S_2$. Subsequently, for closer comparison in the range $Bi_2Pb_0-Bi_{1.5}Pb_{0.5}$, the following additional fusions were made: $Ni_3Bi_{1.9}Pb_{0.1}S_2$, $Ni_3Bi_{1.8}Pb_{0.2}S_2$, $Ni_3Bi_{1.7}Pb_{0.3}S_2$. In the range $Ni_3Bi_2S_2-Ni_3BiPbS_2$ the products show the excellent broad cleavage surfaces of parkerite unlike the product $Ni_3Pb_2S_2$ which lacks this appearance.

To obtain a first approximation of the Pb content in our parkerite, ground samples of 10 mg. of parkerite and of the first four artificial preparations were arced for 60 seconds at 10 amps. in a 2 meter A.R.L. grating spectrograph. This treatment was sufficient to volatilize Bi and Pb completely, as shown by the fact that no Bi or Pb lines were obtained on re-arcing. By inspection of the spectrogram it was clear that the composition of parkerite lies between $Ni_3Bi_2S_2$ and $Ni_3Bi_{1.5}Pb_{0.5}S_2$.

To fix the composition more closely the spectra from 10 mg. samples of the first two and the additional three fusion products and parkerite were recorded on one film, and the intensities of the Bi line (I_{Bi}) at 2730.5 A and the Pb line (I_{Pb}) at 2663.2 A were obtained from measurements with a photometer, corrected for background. The ratio I_{Pb}/I_{Bi}. for each sample was then plotted against the known Pb contents on log.-log. paper giving a straight line which determined the Pb content of parkerite as 1.6 per cent.

An independent determination of Pb in parkerite was obtained by using 10 mg. of the same five materials with 5 mg. of Bi added to each; this reduced the variation of Bi in the samples. Using the Bi line at 2524.5 A and the Pb line at 2663.2 A, with the same procedure, the Pb content of parkerite was found to be 1.4 per cent (Figs. 1, 2).

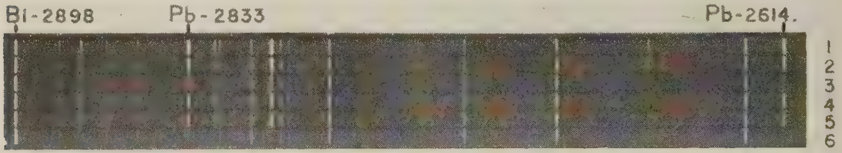

FIG. 1. Part of spectrograms of artificial $Ni_3(Bi, Pb)_2S_2$ compounds and parkerite from Sudbury. 1—$Bi_{1.5}Pb_{0.5}$; 2—$Bi_{1.7}Pb_{0.3}$; 3—parkerite; 4—$Bi_{1.8}Pb_{0.2}$; 5—$Bi_{1.9}Pb_{0.1}$; 6—Bi_2Pb_0. It can be seen that the Pb lines in 3 are weaker than in 5.

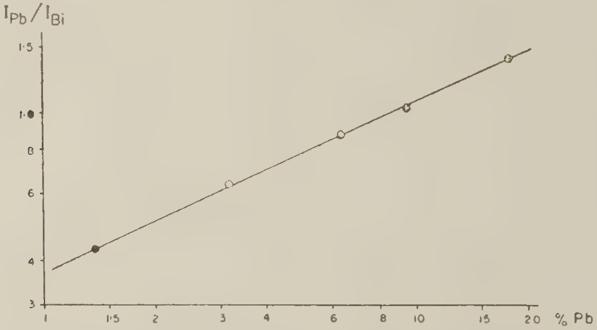

FIG. 2. Plot of spectrographic I_{Pb}/I_{Bi} against wt. percent Pb for artificial compounds (blank points) and parkerite (filled point).

The foregoing work shows that Pb is actually present in Sudbury parkerite to the extent of 1.5 ± 0.1 per cent, in keeping with the previous chemical work, and showing that the previously reported spectrographic Sn was probably based on a misreading of Pb lines. The Canadian mineral is thus practically $Ni_3Bi_2S_2$ and therefore, in a sense, it is not identical with the South African mineral, if we accept the supposed composition, $Ni_3Bi_{1.2}Pb_{0.8}S_2$, of the latter mineral. However, the tendency today is to identify a mineral species with an isostructural phase and, if necessary, to distinguish members of such a series as varieties with suitable adjectival qualifiers. Thus the natural equivalent of the isostructural α-phase extending from $Ni_3Bi_2S_2$ to about Ni_3BiPbS_2 would be named parkerite, and the Bi-rich and Pb-rich members could be described as bismuthian parkerite and plumbian parkerite respectively.

It should be emphasized, however, that the Pb content of the Insizwa mineral remains to be determined by quantitative means and that, therefore, the existence of a natural parkerite series is not yet proved. Actually there are some reasons for doubting the high Pb content attributed to the South African mineral. Both at Sudbury and at Insizwa, parkerite is intimately associated with galena; since nearly pure $Ni_3Bi_2S_2$ formed in the former deposit we might expect the same in the latter. Again, the association of parkerite with galena inevitably raises the suspicion that microsamples extracted from polished sections of parkerite might be contaminated with PbS, in spite of careful manipulation. Finally, it is a curious fact that the x-ray powder patterns of parkerite from both localities and of pure artificial $Ni_3Bi_2S_2$, given by Niggli, Michener & Peacock, and Cormack, all run to $\theta=69°$ as the last legible line, whereas Cormack's pattern for artificial $Ni_3Bi_{1.2}Pb_{0.8}S_2$, the supposed composition of Insizwa parkerite, gives out at $\theta=45.6°$, indicating the less perfect crystallinity of this solid solution. We propose, therefore, that the specific name parkerite be used for natural $Ni_3(Bi, Pb)_2S_2$ in which as yet only a minor proportion of Pb (1.5 per cent) has been actually proved by a quantitative method. If the existence of a natural parkerite series should be clearly established, the name parkerite will still be appropriate in the range $Ni_3Bi_2S_2-Ni_3BiPbS_2$.

Shandite

In May, 1949, the senior author received from Professor P. Ramdohr, then stationed in Melbourne, a polished specimen of ore from Trial Harbour, Tasmania. The specimen is mainly serpentine in which Dr. Ramdohr had noted pentlandite, heazlewoodite, and other sulphides, and also a few minute grains of an ore mineral which he believed to correspond to the artificial compound $Ni_3Pb_2S_2$, hitherto unknown in nature. Dr. Ramdohr had located these grains on the polished surface with characteristic marks, and he asked if his presumption regarding their identity could be tested by x-ray powder photographs. Doubting his ability to obtain samples from such minute areas, the senior author sent the specimen to his skillful former student, Dr. R. M. Thompson, Vancouver, B. C., who kindly undertook the delicate task of excavating and x-raying samples from the grains in question. From two areas Dr. Thompson obtained identical x-ray powder photographs, and a list of observed intensities and spacings which was found to correspond to Cormack's data (1948) for pure artificial $Ni_3Pb_2S_2$ and to differ distinctly from the

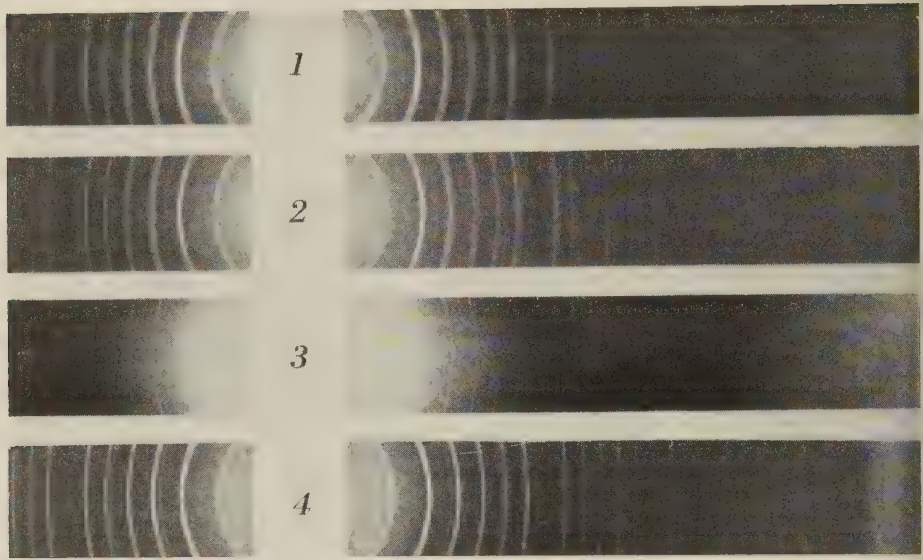

FIG. 3. *X*-ray powder patterns; Cu/Ni radiation; camera radius 90/π mm.; contact prints, full size. 1—Artificial $Ni_3Bi_2S_2$; 2 Parkerite, Sudbury; 3 –Shandite, Trial Harbour, Tasmania (sample with impurities scraped from minute grains in polished section); 4—Artificial $Ni_3Pb_2S_2$ (print somewhat stretched).

similar data for parkerite, $Ni_3Bi_2S_2$ (Michener & Peacock, 1943) or members of the artificial series $Ni_3(Bi, Pb)_2S_2$ (Cormack, 1948). Thus it was proved that the mineral from Tasmania is indeed the natural form of $Ni_3Pb_2S_2$, and Dr. Ramdohr's remarkable prediction was confirmed (Fig. 3).

On receiving this result Dr. Ramdohr intimated in a private communication (Nov., 1949) that he proposed to name the new mineral *shandite*, after Professor S. J. Shand, the distinguished Scottish petrologist who had suggested to Dr. D. L. Scholtz the study of the Insizwa nickel ores which led to the discovery of parkerite. At the same time Dr. Ramdohr stated that his paper on shandite was nearly ready for publication; and therefore we venture to use the new name which should be in print by the time this work is published.[1] Our subsequent observations on $Ni_3Pb_2S_2$ are confined to the artificial compound whose structural properties can be taken to supplement those of shandite, since the mineral is structurally identical with the laboratory compound.

Two lots of artificial shandite were prepared by fusing charges of 1 gm. and 2 gm. of the powdered elements in the proportions 3Ni:2Bi:2S in evacuated silica glass bulbs of about 2 cc. capacity. The first of these was allowed to cool in air; the second was cooled overnight in a furnace. The compact metallic products are similar to galena in colour; when broken they show bright metallic lustre and a compact fine to medium grained aggregation of crystals with good cleavage. Unlike artificial parkerite which shows broad (001) cleavage plates traversed by (111) twin lamellae (orthorhombic indices), fragments of artificial shandite show discontinuous cleavage in four directions which give distinct reflections on the two-circle goniometer proving octahedral relationship.

---

[1] Since this was written Dr. Ramdohr has sent us a copy of his MS on shandite with the information that the work is in press (Feb., 1950).

Polished sections from these preparations are compact, cream-white, with noticeable reflection pleochroism and fairly strong anisotropism giving grey-blue and yellow-brown as maximum polarization colors. Crossed nicols reveal a mosaic of angular to irregular grains which are not in random arrangement but in several sets of optically parallel individuals which give simultaneous extinction sometimes over large areas. The Talmage hardness is C and the highest specific gravity by the Berman balance is 8.72.

CRYSTAL STRUCTURE OF $Ni_3Pb_2S_2$

Table 1 compares the *x*-ray powder patterns of shandite and our artificial $Ni_3Pb_2S_2$. Except for some weak extra lines in the pattern of shandite, no doubt due to unavoidable contamination in sampling minute grains in a polished section, the glancing angles, spacings, and intensities are identical within the limits of observation. The pattern of shandite is markedly similar to that of parkerite in spacings and intensities, but it differs in having certain single lines in place of double lines in parkerite (Fig. 3). This is due to the fact that parkerite has a pseudo-cubic sub-structure with edges 3.97 and 4.02 kX (Peacock, 1947, p. 68); in shandite the corresponding sub-structure is, metrically, exactly cubic with the edge $c' = 3.935$ kX. This cube-edge serves to index all but a few weak lines in $Ni_3Pb_2S_2$; to index the pattern completely the double value, $c = 7.87$ kX, is required. This gives indices which show the missing spectra of the *F*-lattice, and no others, and calculated spacings which agree with the values observed on natural and artificial material. The sharp shandite pattern shows no evidence of splitting of cubic lines, even in the sensitive back reflections, and therefore the lattice has strictly equal rectangular periods. With $4[Ni_3Pb_2S_2]$ or $Ni_{12}Pb_8S_8$ in the cube with edge c the calculated density is 8.86 as compared to the highest measured specific gravity 8.72. The cubelet with edge c' thus contains $\frac{1}{2}[Ni_3Pb_2S_2]$.

These results obtained from good powder photographs were verified by rotation and Weissenberg photographs on a fragment of artificial

TABLE 1. SHANDITE AND ARTIFICIAL $Ni_3Pb_2S_2$: *X*-RAY POWDER PATTERN

"Cubic", *F*; $a = 7.87$ kX

Shandite*			Artificial $Ni_3Pb_2S_2$†			(*hkl*)	*d*(calc.)
I	θ(Cu)	*d*(meas.)	*I*	θ(Cu)	*d*(meas.)		
1	6.2°	7.12	—	—	—	—	—
2	9.75	4.54	2	9.75°	4.54	(111)	4.544
8	11.25	3.94	7	11.2	3.96	(002)	3.935
½	12.05	3.68	—	—	—	—	-
½	12.9	3.44	—	—	—	—	—
½	14.3	3.11	—	—	—	—	—
10	16.05	2.78	10	16.0	2.79	(022)	2.782
1	17.85	2.51	—	—	—	—	—
1	18.9	2.37	2	18.85	2.38	(113)	2.373
7	19.8	2.27	8	19.8	2.27	(222)	2.272
6	22.95	1.971	6	23.0	1.969	(004)	1.968
½	23.65	1.916	—	—	—	—	—
½	25.05	1.816	2	25.25	1.803	(133)	1.805
5	25.9	1.760	5	25.9	1.760	(024)	1.760
½	27.45	1.668	—	—	—	—	—
7	28.5	1.611	7	28.55	1.609	(224)	1.606
—	—	—	½	30.7	1.506	(115) (333)	1.515
4	33.55	1.391	4	33.55	1.391	(044)	1.391
3	35.9	1.311	3	35.95	1.309	(006) (244)	1.312
3	38.2	1.243	3	38.15	1.244	(026)	1.244
5	40.3	1.189	5	40.35	1.187	(226)	1.186
1	42.6	1.136	2	42.65	1.135	(444)	1.136
1	44.9	1.089	2	44.9	1.089	(046)	1.091
3	47.0	1.051	4	46.95	1.052	(246)	1.052
½	48.7	1.023	½	48.65	1.024	(137) (355)	1.025
½	51.5	0.982	2	51.45	0.983	(008)	0.984
2	53.6	0.955	3	53.65	0.954	(028) (446)	0.954
1	56.0	0.927	3	56.1	0.926	(228) (066)	0.927
1	58.4	0.903	3	58.35	0.903	(266)	0.903
2	61.0	0.879	3	60.85	0.880	(048)	0.880
½	63.6	0.858	3	63.6	0.858	(248)	0.859
½	66.1	0.841	½	66.2	0.840	(466)	0.839
2	72.6	0.806	2	72.95	0.804	(448)	0.803
—	—	—	1	78.0	0.786	(0.0.10) (068)	0.787

* Observations by R. M. Thompson (Vancouver, B.C.) on a sample from minute grains marked as shandite by P. Ramdohr in a polished section of ore from Trial Harbour, Tasmania.

† Intensities visually estimated by R. M. Thompson; spacings measured by J. McA.

shandite showing interrupted octahedral cleavage. These also led to a simple cubic pseudo-cell with $c'=3.935$ kX and a face-centered cubic real cell with $c=2c'=7.87$ kX. This real cell was indicated by a very weak first layer line in the rotation photograph about an axis of apparent 4-fold symmetry. There are no systematically missing spectra beyond those of the cubic F-lattice.

In view of the apparently normal cubic diffraction effects, the incompatible optical behavior was at first set aside and an attempt was made to find a cubic-F structure for shandite. Since the structure of adjacent cubelets must be nearly alike the 8 Pb atoms are probably at the corners of the cubelets; but no reasonable arrangement of 12 Ni and 8 S could be found within the limitations of the F-lattice.

In keeping with the optical anisotropism tetragonal structures were then sought in a face-centered cell with $a=c=7.87$ kX or a body-centered cell with $a'=c/\sqrt{2}$. One plausible tetragonal structure was found with Pb atoms at the corners of the cubelets, Ni atoms distributed over the centers of their vertical faces, and S atoms paired along vertical 4-fold axes and about the centers of horizontal faces of the cubelets. However, certain interatomic distances for this structure and the calculated intensities were not satisfactory, and therefore the idea of a tetragonal structure was abandoned.

A face-centered rhombohedral structure with $r'=c=7.87$ kX, $\alpha'=90°$, containing $4[Ni_3Pb_2S_2]$, or a simple rhombohedral structure with $r=c/\sqrt{2}=5.565$ kX, $\alpha=60°$, containing Ni_3Pb2S_2, next came into consideration; and a single structure was soon found that gave entirely satisfactory distances and calculated intensities and a good explanation of the optical behavior and cleavage appearance of the crystal. The structure has the symmetry of the centrosymmetrical space group $R\bar{3}m$, and the atoms in the 60° cell are placed as follows (rhombohedral coordinates):

Pb I in (a): $0\,0\,0$. Pb II in (b): $\frac{1}{2}\,\frac{1}{2}\,\frac{1}{2}$
3 Ni in (d): $\frac{1}{2}\,0\,0;\ 0\,\frac{1}{2}\,0;\ 0\,0\,\frac{1}{2}$
2 S in (c): $x\,x\,x;\ \bar{x}\,\bar{x}\,\bar{x}$, with $x=0.285$ ($\sim 2/7$)

The correctness of this structure is shown by the comparison of calculated and observed powder intensities in Table 2. For each cubic-F structural form (with the number of equivalent sets of planes, n), are given the equivalent rhombohedral ($\alpha=60°$) and hexagonal structural form or forms (with the numbers of equivalent sets of planes, n). The cubic indices, in all significantly different permutations having $h\leqq k\leqq l$ (algebraically) are related to the rhombohedral indices with $h\geqq k\geqq l$ by the transformations:

Cubic to rhombohedral: $0\frac{1}{2}\frac{1}{2}/\frac{1}{2}0\frac{1}{2}/\frac{1}{2}\frac{1}{2}0$
Rhombohedral to cubic: $\bar{1}11/1\bar{1}1/11\bar{1}$

TABLE 2. $Ni_3Pb_2S_2$ (SHANDITE): CALCULATED AND OBSERVED X-RAY POWDER INTENSITIES

Cubic F	n	Rhombohedral	n	Hexagonal	I (calc.)		I(obs.)	
							M.A.P.*	J.McA.†
(111)	4	(111)	1	(0003)	0.73	0.96	1	0.3
		(100)	3	(10$\bar{1}$1)	0.23			
(002)	3	(110)	3	(01$\bar{1}$2)	5.48	5.48	4	3
(022)	6	(211)	3	(10$\bar{1}$4)	4.71	10.00	10	10
		(10$\bar{1}$)	3	(11$\bar{2}$0)	5.29			
(113)	12	(221)	3	(01$\bar{1}$5)	0.00	1.06	1	0.5
		(11$\bar{1}$)	3	(02$\bar{2}$1)	0.71			
		(210)	6	(11$\bar{2}$3)	0.35			
(222)	4	(222)	1	(0006)	1.68	6.07	6	6
		(200)	3	(20$\bar{2}$2)	4.39			
(004)	3	(220)	3	(02$\bar{2}$4)	3.99	3.99	5	5
(133)	12	(322)	3	(10$\bar{1}$7)	0.12	0.61	$\frac{1}{2}$	0.5
		(311)	3	(20$\bar{2}$5)	0.42			
		(20$\bar{1}$)	6	(21$\bar{3}$1)	0.03			
(024)	12	(321)	6	(11$\bar{2}$6)	1.62	2.87	3	2
		(21$\bar{1}$)	6	(12$\bar{3}$2)	1.25			
(244)	12	(332)	3	(01$\bar{1}$8)	0.62	3.14	4	4
		(11$\bar{2}$)	3	(03$\bar{3}$0)	0.90			
		(310)	6	(21$\bar{3}$4)	1.62			
(115)	12	(331)	3	(02$\bar{2}$7)	0.057	0.22	$<\frac{1}{2}$	0.1
		(22$\bar{1}$)	3	(03$\bar{3}$3)	0.041			
		(320)	6	(12$\bar{3}$5)	0.000			
(333)	4	(333)	1	(0009)	0.078			
		(300)	3	(30$\bar{3}$3)	0.041			
(044)	6	(422)	3	(20$\bar{2}$8)	1.10	2.48	3	3
		(20$\bar{2}$)	3	(22$\bar{4}$0)	1.38			
(135)	24	(432)	6	(11$\bar{2}$9)	0.000	0.20	—	—
		(31$\bar{1}$)	6	(22$\bar{4}$3)	0.104			
		(21$\bar{2}$)	6	(13$\bar{4}$1)	0.011			
		(421)	6	(21$\bar{3}$7)	0.080			
(006)	3	(330)	3	(03$\bar{3}$6)	0.311	1.52	2	2
(244)	12	(433)	3	(1.0.$\bar{1}$.10)	0.413			
		(411)	3	(30$\bar{3}$6)	0.311			
		(30$\bar{1}$)	6	(31$\bar{4}$2)	0.482			
(026)	12	(431)	6	(12$\bar{3}$8)	0.574	1.28	2	2
		(321)	6	(13$\bar{4}$4)	0.706			
(335)	12	(443)	3	(0.1.$\bar{1}$.11)	0.021	0.09	—	—
		(3$\bar{1}\bar{1}$)	3	(40$\bar{4}$1)	0.071			
		(410)	6	(31$\bar{4}$5)	0.000			
(226)	12	(442)	3	(0.2.$\bar{2}$.10)	0.634	2.42	3	2.5
		(22$\bar{2}$)	3	(04$\bar{4}$2)	0.538			
		(420)	6	(22$\bar{4}$6)	1.250			
(444)	4	(444)	1	(0.0.0.12)	0.164	0.85	1	1
		(400)	3	(40$\bar{4}$4)	0.681			
(117)	12	(441)	3	(03$\bar{3}$9)	0.024	0.24	—	—
		(33$\bar{1}$)	3	(04$\bar{4}$5)	0.084			
		(430)	6	(13$\bar{4}$7)	0.047			
(155)	12	(533)	3	(2.0.$\bar{2}$.11)	0.074			
		(522)	3	(30$\bar{3}$9)	0.000			
		(30$\bar{2}$)	6	(32$\bar{5}$1)	0.006			

TABLE 2, *Continued*

Cubic F	n	Rhombo-hedral	n	Hexagonal	I (calc.)		I(obs.) M.A.P.*	J.McA.†
(046)	12	(532)	6	(2.1.$\bar{3}$.10)	0.475	0.75	1	1
		(31$\bar{2}$)	6	(23$\bar{5}$2)	0.275			
(246)	24	(543)	6	(1.1.$\bar{2}$.12)	0.191	1.59	2	2.5
		(21$\bar{3}$)	6	(14$\bar{5}$0)	0.502			
		(521)	6	(31$\bar{4}$8)	0.341			
		(41$\bar{1}$)	6	(32$\bar{5}$4)	0.557			
(137)	24	(531)	6	(22$\bar{4}$9)	0.145	0.24	½	0.2
		(542)	6	(1.2.$\bar{3}$.11)	0.025			
		(32$\bar{2}$)	6	(14$\bar{5}$3)	0.028			
		(42$\bar{1}$)	6	(23$\bar{5}$5)	0.000			
(355)	12	(544)	3	(1.0.$\bar{1}$.13)	0.002			
		(511)	3	(40$\bar{4}$7)	0.017			
		(40$\bar{1}$)	6	(41$\bar{5}$3)	0.028			
(008)	3	(440)	3	(04$\bar{4}$8)	0.443	0.44	1	0.5
(337)	12	(553)	3	(0.2.$\bar{2}$.13)	0.048	0.09	—	—
		(22$\bar{3}$)	3	(05$\bar{5}$1)	0.005			
		(520)	6	(32$\bar{5}$7)	0.039			
(028)	12	(541)	6	(1.3.$\bar{4}$.10)	0.415	1.40	3	1.5
		(43$\bar{1}$)	6	(14$\bar{5}$6)	0.314			
(446)	12	(554)	3	(0.1.$\bar{1}$.14)	0.233			
		(4$\bar{1}\bar{1}$)	3	(50$\bar{5}$2)	0.123			
		(510)	6	(41$\bar{5}$6)	0.314			
(228)	12	(552)	3	(0.3.$\bar{3}$.12)	0.126	0.98	2	1.5
		(330)	3	(03$\bar{3}$6)	0.160			
		(530)	6	(23$\bar{5}$8)	0.327			
(066)	6	(633)	3	(3.0.$\bar{3}$.12)	0.126			
		(30$\bar{3}$)	3	(33$\bar{6}$0)	0.239			
(157)	24	(643)	6	(2.1.$\bar{3}$.13)	0.004	0.16	—	—
		(31$\bar{3}$)	6	(24$\bar{6}$1)	0.093			
		(632)	6	(3.1.$\bar{4}$.11)	0.026			
		(41$\bar{2}$)	6	(33$\bar{6}$3)	0.025			
(555)	4	(555)	1	(0.0.0.15)	0.015			
		(500)	3	(50$\bar{5}$5)	0.000			
(266)	12	(644)	3	(2.0.$\bar{2}$.14)	0.599	1.56	3	1.5
		(622)	3	(4.0.$\bar{4}$.10)	0.556			
		(40$\bar{2}$)	6	(42$\bar{6}$2)	0.406			
(048)	12	(642)	6	(2.2.$\bar{4}$.12)	0.819	1.94	3	1.5
		(42$\bar{2}$)	6	(24$\bar{6}$4)	1.124			
(119)	12	(551)	3	(0.4.$\bar{4}$.11)	0.026	0.20	—	—
		(44$\bar{1}$)	3	(05$\bar{5}$7)	0.021			
		(540)	6	(14$\bar{5}$9)	0.000			
(357)	24	(654)	6	(1.1.$\bar{2}$.15)	0.001			
		(621)	6	(41$\bar{5}$9)	0.000			
		(51$\bar{1}$)	6	(42$\bar{6}$5)	0.154			
		(4$\bar{1}\bar{2}$)	6	(51$\bar{6}$1)	0.002			
(248)	24	(52$\bar{1}$)	6	(33$\bar{6}$6)	0.380	1.29	3	1.5
		(653)	6	(1.2.$\bar{3}$.14)	0.566			
		(32$\bar{3}$)	6	(15$\bar{6}$2)	0.296			
		(631)	6	(3.2.$\bar{5}$.10)	0.050			

* By inspection.

† By visual comparison with a standard film of Al.

The resulting hexagonal indices then have $hk{*}l$ all positive, which is required. The intensity for each structural form was most conveniently computed from the rhombohedral indices, with the usual formula:

$$I = kn\,\frac{1+\cos^2 2\theta}{\sin^2\theta\cos\theta}\left\{\sum f_0 \cos 2\pi(hx+ky+lz)\right\}^2$$

where k is a constant chosen to reduce the intensities for convenient comparison with the observed values, n is the number of equivalent sets of planes, and f_0 are scattering factors taken from the *International Tables for the Determination of Crystal Structures*, vol. 2. The sum of the calculated intensities of all rhombohedral forms contributing to a single "cubic" powder ring is thus directly comparable with two independent sets of readings on a good powder film. The qualitative, even quantitative, agreement in Table 2 is satisfactory. The observed intensities in Table 1 show qualitative agreement with the calculated values.

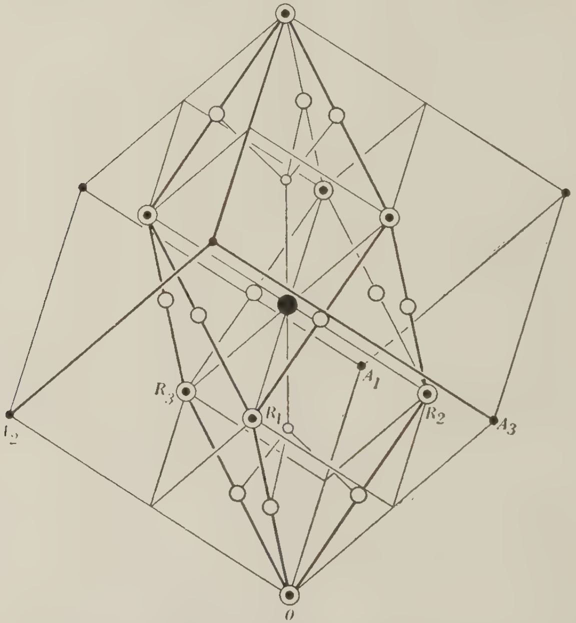

FIG. 4. $Ni_3Pb_2S_2$ (shandite): Atomic arrangement in the primitive (60°) rhombohedral cell, OR_1, OR_2, OR_3, in relation to the face-centered (90°) rhombohedral (cubic) cell, OA_1, OA_2, OA_3, and two of the eight contained cubelets. Large circles at F-lattice points; PbI; large filled circle, PbII; medium circles, Ni; small circles S.

As shown in Fig. 4, which gives the structure of $Ni_3Pb_2S_2$ in one 60° cell in relation to the face-centered 90° cell—the large cube, which is best seen with the edge OA_2 vertical—PbI is at the origin and face-centers of the large cube, PbII is at the body-centre, 3 Ni are at non-opposite face-centers of a cubelet, and 2 S are on a body diagonal, resting between 3 Ni and PbII.

The atomic positions in the face-centered 90° rhombohedron (or cube) with identical points 000; $0\frac{1}{2}\frac{1}{2}$; $\frac{1}{2}0\frac{1}{2}$; $\frac{1}{2}\frac{1}{2}0$; are:

4 Pb I: 0 0 0; 4 Pb II: $\frac{1}{2}\frac{1}{2}\frac{1}{2}$
12 Ni: $0\frac{1}{4}\frac{1}{4}$; $\frac{1}{4}0\frac{1}{4}$; $\frac{1}{4}\frac{1}{4}0$;
8 S: $x\,x\,x$; $\bar{x}\,\bar{x}\,\bar{x}$.

The entire structure in the 90° cell is shown in Fig. 5. 4 PbI and 4 PbII are in NaCl arrangement and the 12 Ni occupy half the 24 face-centers of the 8 cubelets; it is this arrangement of Pb and Ni atoms which presumably determines the cubic form of the large cell. PbI is surrounded by 6 Ni at the corners of two equilateral triangles, one above and one below; Pb II is at the center of an hexagonal bipyramid made by 6 Ni and 2 S. S is surrounded by 3 Ni at the corners of an equilateral triangle, above or below, and on the opposite side by PbII. Since the S-parameter could hardly be determined by the intensities, it has been chosen to give

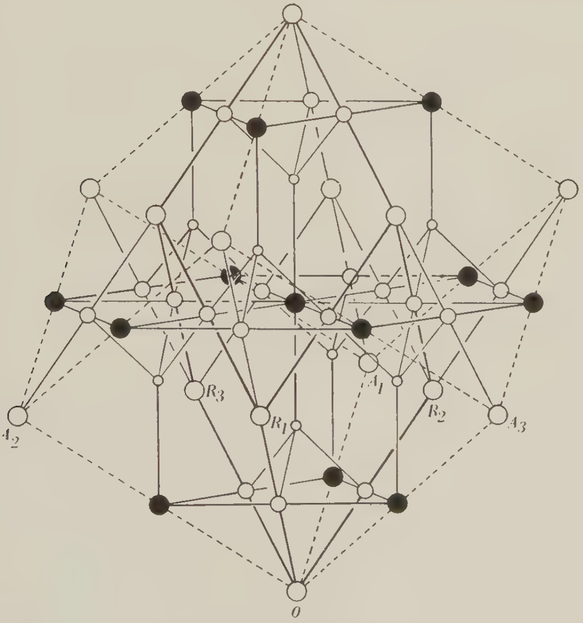

FIG. 5. $Ni_3Pb_2S_2$ (shandite): Atomic arrangement in the face-centered (90°) rhombohedral cell. Cell edges and scheme of atoms as in Fig. 4. The unbroken lines show only the shortest atomic connections.

the S−Ni distance 2.28 kX, as in Ni_3S_2 (heazlewoodite) (Peacock, 1947). The shortest interatomic distances in this structure are: Ni−Pb=2.78 kX, Ni−S=2.28 kX, Pb−S=2.93 kX. Comparable distances are Ni−S=2.3 in NiS (millerite); Pb−S=2.96 in PbS (galena). A Ni−Pb distance was not found.

The rhombohedral structure of $Ni_3Pb_2S_2$ is in keeping with the optical anisotropism of the compound and it explains the peculiar mosaic texture and the apparent cubic symmetry and octahedral cleavage of single fragments. With a metrically cubic lattice we would expect the crystal to form complementary twins on all the elements of symmetry of the cube which are not elements of symmetry of the structure. These are the cube faces, the 4-fold axes, etc., which can altogether give rise to four orientations in which the singular 3-fold axis of the structure is brought into the four directions of the body-diagonals of the cube while the twinned complex is still pervaded by the undeviated face-centered cubic lattice. In twinning of this sort (twinning by merohedry of Friedel) the twinned parts will fit on any composition surface and thus they could give rise to the observed angular to irregular mosaic with several groups of optically parallel grains. A fragment of such a twinned complex large enough for single crystal reflection and *x*-ray measurements would therefore show cubic symmetry by twinning. The interrupted octahedral cleavage of such a fragment is therefore most likely the result of a single cleavage, namely (111) (basal rhombohedral) repeated by twinning to give the four directions of the octahedron; and the cubic appearance of the "single" crystal *x*-ray photographs is no doubt due to the same cause.

Finally, the structure of $Ni_3Pb_2S_2$ (shandite) shows again how unsatisfactory it is to define the crystal systems by the metrical relations of their lattice elements or axes. With equal rectangular cell edges shandite cannot be placed in the cubic system, in view of the symmetry of the structure and optical anisotropism; and even the stipulation that cubic crystals must have equal rectangular cell edges *at all temperatures*, fails in this case and is generally impracticable. The face-centered lattice of shandite very probably retains its cubic form from room temperature up to the deflection noted by du Preez at 543° C., where, by analogy with other crystals, the structure may invert to a truly cubic disordered arrangement. But, in any case, it is impossible to measure cell dimensions at all temperatures, and therefore it may often be impossible to assign a crystal to its metrical crystal system. Actually, working crystallographers have always assigned crystals to their systems on the basis of symmetry, accepting the systems in effect as groups of crystal classes. The crystal systems have lattices with certain typical metrical relations; but by specialization of lengths and angles the lattice in any symmetry system may occasionally assume the metrical relations typical of any higher symmetry system, even over a range of temperature.

Acknowledgment. The spectrographic work described in this paper was done by the junior author in the laboratories of the Ontario Department of Mines (Toronto), by the courtesy of Mr. H. C. Rickaby, Deputy Minister of Mines, and Mr. D. A. Moddle, Provincial Assayer, and with the instructive co-operation of H. G. Taylor, Spectrographer.

REFERENCES

Cormack, A. M. (1948): *X*-ray powder data of the parkerite series $Ni_3Bi_2S_2$—$Ni_3Pb_2S_2$ —*Trans. Geol. Soc. South Africa*, **50** (for 1947), 17–22.

Du Preez, J. W. (1945): A thermal investigation of the parkerite series—*Ann. Univ. Stellenbosch*, **22,** A (for 1944), 97–104.

Michener, C. E. & Peacock, M. A. (1943): Parkerite ($Ni_3Bi_2S_2$) from Sudbury, Ontario: redefinition of the species—*Am. Mineral.*, **28**, 343–355.

Naudé, S. M. (1945): Spectrochemical analysis and its application in science and industry —*South African J. Sci.*, **41,** 10–32.

Peacock, M. A. (1947): On heazlewoodite and the artificial compound Ni_3S_2—*Univ. Toronto Studies*, Geol. Ser. **51** (for 1946), 59–69.

Ramdohr, P. (1950): Ueber das Vorkommen von Heazlewoodit Ni_3S_2 und über ein neues ihn begleitendes Mineral: Shandit $Ni_3Pb_2S_2$—*in press.*

Schenck, R. & von der Forst, P. (1939): Gleichgewichtsstudien an erzbildenden Sulfiden. II—*Zeits. anorg. Chem.*, **241,** 145–157.

Scholtz, D. L. (1936): The magmatic nickeliferous ore deposits of East Griqualand and Pondoland—*Trans. Geol. Soc. South Africa*, **39,** 81–210.

HAUCHECORNITE*

M. A. Peacock, *University of Toronto, Toronto, Canada*

Abstract

Study of a specimen (Harvard Mineralogical Museum, 89710) from the original locality, Friedrich mine, Hamm a. d. Sieg, Westphalia, confirms the individuality of hauchecornite. Tetragonal, $a : c = 1 : 0.7404$ (goniometric and *x*-ray), with *c*(001), *a*(010), *m*(110), *q*(011), *p*(021), *e*(111); tabular on *c* and bipyramidal. Laue symmetry $4/mmm$; $a = 7.28$, $c = 5.39$ kX (λ Cu$K\alpha_1 = 1.5374$ kX); allowable space groups, $P\bar{4}2m$, $P42$, $P4/mmm$ (not $P4_22$). Unit cell content, $Ni_9(Bi, Sb)_2S_8$ (not $Ni_8(Bi, Sb)_2S_8$). G = 6.36 (on crystal weighing 17 mg.). Strongest *x*-ray powder lines for identification: 2.79 kX (10), 2.39 (6), 2.30 (6), 4.34 (5), 1.861 (5). Associated with millerite, ullmannite (or kallilite), and gersdorffite (or corynite), with quartz.

Our continuing Toronto studies of rare and doubtful ore minerals often show that a substance originally thought to be a new mineral consists in fact of one or more already known species; and in this event we can do a service to mineralogy by striking the worthless name from the nomenclature. Occasionally, however, we find that a substance in question is composed, wholly or in part, of a mineral with clearly distinctive properties; and in such circumstance we have the pleasanter task of confirming the individuality of a mineral which was hitherto in disrepute, owing perhaps to an inadequate original description, or to later unfavourable but superficial observations or suggestions, or merely to lack of the eventual substantiating work by which the validity of most good mineral species is finally placed beyond all doubt.

Hauchecornite is a mineral of the second sort. Originally described in detail, with full goniometric, physical, and chemical information, and a careful account of associations and paragenesis, hauchecornite was never examined again except in polished sections of massive ore showing an intergrowth of several minerals. Thus the mineral has been condemned as "a mixture," a verdict by which many supposed new ore minerals and a few good species have been hustled to oblivion.

Since many may have access only to brief note in Dana (1944, p. 242) a more detailed summary of the work on hauchecornite will be useful. The mineral was first mentioned by Scheibe (1888) and later named after W. Hauchecorne (Director of the Geological Survey and the Mining Academy, Berlin) and fully described by Scheibe (1893). Crystals tetragonal, $a{:}c = 1{:}1.05215$ (8 crystals), with *c*(001), *a*(100), *m*(110), *e*(101), *s*(112), *o*(111), and vicinals, mostly tabular on *c*, also bipyramidal to short prismatic (14 figures). No cleavage; fracture flat conchoidal; H = 5; G = 6.4; light bronze-yellow, tarnishing darker; lively metallic lustre on a fresh break; streak grey-black. Four generally concordant analyses (quoted later) by three chemists, interpreted as (Ni, Co, Fe)$_7$(S, Bi, Sb, As)$_8$ or $Ni_{14}SbBi_2S_{13}$. Found in a pocket opened in 1884, containing about 5 tons of ore in siderite gangue, in the Friedrich mine, near Wissen a. d. Sieg. The upper part of the pocket carried mainly millerite (NiS) and hauchecornite, the lower part kallilite (bismuthian ullmannite, Ni(Sb, Bi)S). Some specimens showed siegenite (Co, Ni)$_3$S$_4$ and zincblende and in cavities bismuthinite and quartz. Small crystals of hauchecornite perched on idiomorphic millerite proved the order of deposition of these minerals.

---

* Contributions to Mineralogy from the Department of Geological Sciences, University of Toronto, 1950, no. 3.

Polished sections of ore specimens containing hauchecornite from the original and only proved locality have been described by Schneiderhöhn & Ramdohr (1931, p. 372), Short (1940, p. 140), and Harcourt (1942, p. 105). Although differing in some details these notes describe hauchecornite as similar to pyrrhotite in colour, moderately to strongly anisotropic; hardness E; contains Ni, Bi, S; etch tests: HNO_3 brown, HCl, KOH, $FeCl_3$, KCN, $HgCl_2$, negative; associated with millerite and ullmannite. Harcourt obtained a distinctive *x*-ray powder pattern from hauchecornite. Short also noted a second unknown mineral, containing Ni, As, Sb, S; grey with yellow tinge; strongly anisotropic; hardness and etch-tests like those of hauchecornite. We have found nothing corresponding to this substance in our material.

Professor Clifford Frondel kindly provided a typical specimen and polished section of hauchecornite (Harvard Mineralogical Museum, 89710, Friedrich mine, Hamm a. d. Sieg, Westphalia) for the study of this mineral, and Professor R. M. Thompson (Vancouver, B. C.) assisted in the study of the polished section.

The hand specimen shows an open intergrowth of well crystallized, hauchecornite in bronze-colored squarish tables, up to 5 mm. wide and 3 mm. thick, showing good basal and truncating faces, and groups of brassy radiating prismatic crystals of millerite up to 5 mm. long, which sometimes penetrate the hauchecornite tables. These well crystallized minerals pass into massive tarnished ore with a little quartz gangue. The physical properties of hauchecornite agree well with the original description. A clean crystal (17 mg.) gave $G=6.36$ on the Berman balance, as compared to $a=6.35-6.47$ in Scheibe (1893).

The polished section from a piece of compact ore shows idiomorphic sections of tabular hauchecornite crystals, pinkish white, and distinctly anisotropic, giving parallel extinction and sometimes a blue polarization colour in the 45° position. Against the hauchecornite the millerite prisms are yellowish white and more anisotropic. Rounded blebs of a grey isotropic mineral occur with the hauchecornite. These give the ullmannite type of *x*-ray powder pattern, with $a=5.91$ kX. The mineral could be ordinary ullmannite ($a = 5.89 - 5.91$ A, Peacock & Berry, 1940) or the bismuthian ullmannite, kallilite ($a = 5.915$, Peacock & Berry, 1940) originally described from the Friedrich mine. In addition there are pinkish white isotropic subhedral grains in the gangue. These give the same type of x-ray powder pattern with $a = 5.71$ kX; this value compares with $a = 5.68 - 5.72$ for gersdorffite from German localities and it is near $a = 5.724$ for the antimonian variety, corynite (Peacock & Berry, 1940). By rough estimate the amount of millerite associated with hauchecornite is 10–30 per cent while the amount of ullmannite or kallilite might be 5–10 per cent.

Among the crumbs from the specimen of hauchecornite was found a small well-formed crystal which was suitable for reflection and x-ray goniometry as well as a measurement of specific gravity with the Berman balance. The crystal is 0.5 mm. in greatest dimension and it shows fair faces of all the common forms reported by Scheibe. The two-circle measurements obtained on this crystal are compared with calculated angles based on the tetragonal ratio:

$$a : c = 1 : 0.7404$$

which was derived from reflection and subsequent x-ray measurements. For comparison Scheibe's more numerous measurements of the angles *cs*, *co*, *ce*, are given (Table 1). The adopted setting corresponds to a tetragonal *P*-cell; it is related to Scheibe's setting by the transformation formulae:

Scheibe to Peacock: $\frac{1}{2}\overline{\frac{1}{2}}0/\frac{1}{2}\frac{1}{2}0/00\frac{1}{2}$
Peacock to Scheibe: $110/\bar{1}10/002$

In the absence of a general form (*hkl*) there is no direct morphological indication of the crystal class. But since the forms *s*(011), *o*(021), *e*(111), are apparently tetragonal bipyramids, the class is probably $\bar{4}2m$, 422, or $4/mmm$.

TABLE 1. HAUCHECORNITE: MEASURED AND CALCULATED ANGLES
Tetragonal; $a:c = 1:0.7404$

Forms	Measured		No. of Faces	Calculated		Forms	Scheibe (1893) Measured	No. of Faces
	ϕ	ρ		ϕ	ρ		$c:(hkl)$	
c (001)	—	0° 00′	1	—	0° 00′	*c* (001)		
a (010)	0° 00′	89 53	3	0° 00′	90 00	*m* (110)		
m (110)	45 02	90 28	1	45 00	90 00	*a* (010)		
s (011)	0 00	36 28	4	0 00	36 31	*s* (112)	35° 36′—38°13′	13
o (021)	0 00	54 55	4	0 00	55 58	*o* (111)	54 57½—56 29	13
e (111)	45 02	46 24	2	45 00	46 19	*e* (011)	45 25½—46 46	31

The crystal of hauchecornite gave sharp rotation and Weissenberg photographs with [001] and [100] as rotation axes, leading to the cell dimensions:

$$a=7.28,\ c=5.39 \text{ kX}$$

using Cu$K\alpha_1$ with $\lambda=1.5374$ kX. The Laue symmetry is $4/mmm$ (classes $\bar{4}2m$, $4mm$, 422, $4/mmm$), but the bipyramidal crystal forms exclude $4mm$. Strictly, there are no systematically missing spectra and the probable space-groups are thus $P\bar{4}2m$, $P42$, $P4/mmm$. The space group $P4_22$ mentioned in an abstract of this paper (1950) was later found to be excluded by an exception, (003) *vvw*, to the condition $(00l)$ present only with l even.

The *x*-ray powder pattern (Table 2) is distinctive and unlike any other in our collection. The observed intensities and spacings agree well with those given by Harcourt (1942).

For the determination of the unit cell content of hauchecornite we have the four original analyses, given in the upper part of Table 3 with explanatory notes taken from Scheibe (1893).

In view of the care which was evidently given to the preparation and analysis of the samples, especially 2 and 3, it seems proper first to calculate the empirical cell contents form each analysis, using the given measured specific gravities (6.36, M.A.P., for analysis 4) and the appropriate mass factor, 1.650. In this calculation it is assumed that all the elements—except the trifling amounts of Zn, Pb, and Cu, which have been removed as the common sulphides—are contained in hauchecornite. This is in keeping with the composition of the ullmannite group in which the same elements, Ni, Co, Fe, Bi, Sb, As, S, are all found in various amounts in varieties from Siegen (Dana, 1944, p. 301). In the lower part of Table 3, especially under column A which gives the averages for the two most reliable analyses, 2 and 3, it is clear that (Bi, Sb, As) amounts to 2 atoms per unit cell while S evidently tends to 8 atoms. On the other hand, (Ni, Co, Fe) persistently and considerably exceeds 8 atoms, which was the number assumed in the cell content $Ni_8(Bi, Sb)_2S_8$ proposed in the abstract (1950), to suit the supposed space group $P4_22$ in which there are only 2-fold, 4-fold, and 8-fold positions.

A reconsideration of the problem of the cell content of hauchecornite now suggests $Ni_9(Bi, Sb)_2S_8$ as the ideal formula. This formula gives the calculated composition (column B) which agrees well with the analyses, and the best average cell content (column A) gives $(Ni, Co, Fe)_{8.98}(Bi, Sb, As)_{2.01}S_{8.00}$ when increased by 1.7 per cent. This corresponds to an increase of density from 6.47 to 6.58. Such a difference between measured and calculated densities is not uncommon; for ullmannite, for

TABLE 2. HAUCHECORNITE—$Ni_9(Bi, Sb)_2S_8$: *X*-RAY POWDER PATTERN
Tetragonal, *P*4/*mmm*; $a=7.28$, $c=5.39$; $Z=1$

I	θ(Cu)	*d*(meas.)	(*hkl*)	*d*(calc.)	*I*	θ(Cu)	*d*(meas.)	(*hkl*)	*d*(calc.)
1	8.5°	5.20	(110)	5.148	½	28.5°	1.611	(232)	1.616
5	10.2	4.34	(011)	4.332				(023)	1.611
½	10.65	4.16	—	—	2	29.25	1.573	(123)	1.573
4	12.2	3.64	(020)	3.640	1	30.7	1.506	(042)	1.508
4	13.7	3.25	(120)	3.256	½	32.0	1.451	(332)	1.447
1	14.7	3.03	(021)	3.017	½	33.1	1.408	(051)	1.406
10	16.0	2.79	(121)	2.787				(341)	1.406
1	17.6	2.54	(012)	2.527	1	33.5	1.393	(242)	1.393
6	18.75	2.39	(112)	2.388	2	34.7	1.350	(004)	1.348
6	19.5	2.30	(221)	2.323	2	35.8	1.314	(251)	1.311
			(130)	2.302	1	36.9	1.280	(052)	1.281
½	20.4	2.21	(031)	2.213				(342)	1.281
½	20.8	2.16	(022)	2.166				(043)	1.279
1	21.7	2.08	(122)	2.076	3	37.5	1.263	(024)	1.264
5	24.4	1.861	(222)	1.861				(152)	1.262
3	25.0	1.819	(040)	1.819	½	38.0	1.249	(350)	1.249
3	25.3	1.799	(032)	1.803				(124)	1.245
1	26.0	1.754	(132)	1.751	1	39.3	1.214	(351)	1.216
			(013)	1.744				(060)	1.213
2	26.6	1.717	(330)	1.716	2	41.3	1.165	(161)	1.168
1	27.25	1.679	(141)	1.678				(442)	1.161

I	θ(Cu)	*d*(meas.)	*I*	θ(Cu)	*d*(meas.)	*I*	θ(Cu)	*d*(meas.)
½	41.8°	1.153	1	52.9°	0.964	½	59.5°	0.892
1	42.7	1.134	1	53.4	0.958	½	61.2	0.877
2	45.3	1.082	½	55.7	0.931	1	65.5	0.845
2	46.45	1.061	1	56.7	0.920	1	71.7	0.810
1	48.2	1.031	2	58.4	0.903	2	79.6	0.782
1	49.7	1.008						

example, Dana (1944, p. 301) gives $G=6.65\pm0.04$ (measured), 6.793 (calculated). Also, there is now no structural objection to 9 Ni atoms in the unit cell, since the probable space groups, $P\bar{4}2m$, *P*42, *P*4/*mmm*, all have 1-fold positions as well as positions with 2, 4, and 8 equipoints. And finally, metallic sulphides, especially those of Fe, Co, and Ni, are prone to give defective or complex compositions: one recalls pyrrhotite $Fe_{1-x}S$, smaltite $NiAs_{3-x}$, maucherite $Ni_{11}As_8$ or $4Ni_{3-x}As_2$, and most cogently, pentlandite, for which the composition $(Fe, Ni)_9S_8$ is established not only by chemical analyses but by successful synthesis and determination of the atomic arrangement.

The cell formula $Ni_9(Bi, Sb)_2S_8$ was not adopted for hauchecornite

TABLE 3. HAUCHECORNITE: ANALYSES AND CELL CONTENTS

	1	2	3	4	A	B
Ni	41.08	45.054	45.883	45.26	45.47	46.17
Co	2.83	0.704	0.82	—	0.76	—
Fe	0.89	0.271	0.17	trace	0.22	—
Zn	0.12	—	—	—	—	—
Pb	0.64	0.03	—	—	—	—
Cu	—	—	—	0.09	—	—
Bi	24.06	24.508	23.72	24.74	24.11	24.36
Sb	5.69	6.738	6.226	3.14	6.48	7.10
As	1.96	0.895	0.45	3.04	0.67	—
S	22.71	22.879	22.625	22.71	22.75	22.37
	99.98	101.079	99.894	98.98	100.46	100.00
Ni	7.77	8.51	8.77	8.59	8.64	9
Co	0.53	0.13	0.16	—	0.15	—
Fe	0.18	0.05	0.03	—	0.04	—
	8.48	8.69	8.96	8.59	8.83	9
Bi	1.28	1.30	1.27	1.32	1.29	4/3
Sb	0.52	0.61	0.57	0.29	0.59	2/3
As	0.29	0.13	0.07	0.45	0.10	—
	2.09	2.04	1.91	2.06	1.98	2
S	7.80	7.91	7.82	7.88	7.87	8

1. Anal. Fischer, after withdrawing 1.59 per cent quartz. G=6.35 after withdrawing quartz; made on carefully picked crystals and massive ore.

2, 3. Anal. Hesse, on material composed wholly of crystal fragments with bright fracture surfaces and no trace of impurities or alteration. G=6.47.

4. Anal. Fraatz, on a small sample of material carefully picked in Clausthal.

A. Average composition and cell content from analyses 2 and 3.

B. Composition calculated for the ideal cell content $Ni_9(Bi, Sb)_2S_8$, with Bi : Sb=2 : 1.

without searching for a simpler formula on the assumption that the analyzed samples did contain significant amounts of the observed associated minerals, millerite NiS, and kallilite Ni(Sb,Bi,)S. Since Ni and S are present in equal or nearly equal proportions in these minerals, and in the analyses of hauchecornite, the assumption that either millerite or kallilite was present even in considerable amounts in the analysed samples has mainly the effect of raising or lowering the proportion of (Bi, Sb) relation to Ni and S. Trial quickly shows that (Bi,Sb) is thus displaced away from the reasonable value of 2 atoms toward 1 or 3, and that even improbably large admixtures give no satisfactory alternative cell content.

On the other hand, since the inferred composition of hauchecornite is roughly $3NiS+Ni(Sb, Bi)S$, admixture of 3 parts of millerite and 1 part of kallilite produces practically no change of composition. In the polished section the proportions of millerite and kallilite were estimated at 10–30 per cent and 5–10 per cent respectively. Even if such amounts were actually included in the analyzed hauchecornite, which can hardly be admitted in view of Hesse's statement regarding the preparation of his samples, the inferred composition of hauchecornite would be almost unchanged. From the appearance of the hand specimen and the polished section I am inclined to believe that, despite all reasonable care in picking, some smaller amounts of millerite and kallilite were inevitably included in analysed samples; but that, for the reasons just given, these admixtures have practically no effect on the inferred composition and cell content. The cell formula $Ni_9(Bi, Sb)_2S_8$ is therefore retained for hauchecornite. It will be interesting if this cell content should be confirmed by synthesis and structural analysis; so far these have not been attempted.

REFERENCES

DANA, J. D., AND E. S. (1944): *The system of mineralogy,* ed. 7, **1,** by C. PALACHE, H. BERMAN & C. FRONDEL—New York.

HARCOURT, G. A., (1942): Tables for the identification of ore minerals by *x*-ray powder patterns—*Am. Mineral.,* **27,** 63–113.

PEACOCK, M. A. (1950): Hauchecornite—*Am. Mineral.,* **35,** p. 287 (abstract).

——— & BERRY, L. G. (1940): Röntgenographic observations on ore minerals—*Univ. Toronto Studies,* Geol. Ser., **44,** 47–69.

RAMDOHR, P. (1931): *Lehrbuch der Erzmikroskopie,* **2**—Berlin.

SCHEIBE, R. (1888): *Zeits. deutsche geol. Ges.,* **40,** 611.

——— (1893): Ueber Hauchecornit, ein Nickelwismuthsulfid von der Grube Friedrich (Bergrevier Hamm a. d. Sieg)—*Jb. preuss. geol. Landesanst.,* **12**C (for 1891), 91–125.

SHORT, M. N. (1940): Microscopic determination of the ore minerals—*U. S. Geol. Surv.,* Bull. **914.**

CRYSTAL PROPERTIES OF COPPER (II) AND NICKEL (II) CHLORIDE COORDINATION COMPLEXES WITH DIETHYLENETRIAMINE

A. G. Brook*

University of Toronto, Toronto, Canada.

Abstract

The crystal properties of the complexes of copper (II) and nickel (II) chloride with diethylenetriamine (dn) indicate that the complex $[Cudn_2]Cl_2 \cdot H_2O$ is isostructural with the analogous nickel compound $[Nidn_2]Cl_2 \cdot H_2O$ and that in each case the metal ion is probably in 6-fold covalent coordination. The complex $[CudnCl]Cl \cdot \frac{1}{2}H_2O$ was also studied.

Considerable interest has been shown in recent years in the complexes formed by metallic ions such as Cu^{++} and Ni^{++} with various organic compounds of basic character. This paper reports the crystal properties (morphology, optics, and unit cell dimensions) of three of these complexes formed from copper (II) or nickel (II) chloride and the organic base diethylenetriamine ($dn = NH_2\text{-}CH_2\text{-}CH_2\text{-}NH\text{-}CH_2\text{-}CH_2\text{-}NH_2$). These compounds, reported by Breckenridge (1948) have the formulae $[Cudn_2]Cl_2 \cdot H_2O$, $[Nidn_2]Cl_2 \cdot H_2O$ and $[CudnCl]Cl \cdot \frac{1}{2}H_2O$.

In complexes of this type it has been well established that nickel is in 6-fold covalent coordination (Mann & Pope, 1926; Mann, 1934; Haendler 1942). On the other hand, copper is more commonly in 4-fold coordination. However, since both metals form complexes of similar formulae, it might be expected that the coordination number of the metal ion would be the same in each compound.

A study of the crystal properties of these two complexes does indeed show that the complexes $[Cudn_2]Cl_2 \cdot H_2O$ and $[Nidn_2]Cl_2 \cdot H_2O$ are isostructural and hence that the states of coordination are identical. From chemical considerations, it seems probable therefore that both the copper and nickel ions are in 6-fold covalent coordination.

The complex $[CudnCl]Cl \cdot \frac{1}{2}H_2O$ has quite different crystal properties from the above complexes. It seems probable that the copper ion in this complex is in 4-fold covalent coordination.

Crystalline samples of these three complexes were donated by Dr. J. G. Breckenridge of the Department of Chemical Engineering of this University. These crystals were regrown from 95% ethanol to a size suitable for morphological, optical and *x*-ray studies (1–2 mm.). The complex $[\mathrm{CudnCl}]\mathrm{Cl}\cdot\frac{1}{2}\mathrm{H_2O}$ would not crystallize from this solvent until acetone was added, which caused its rapid precipitation as fine needle-like prisms. *X*-ray powder photographs established the identity of these needles with the original material.

---

* Teaching Assistant, Department of Chemistry. The morphological and optical observations were made in the Mineralogical Laboratory, Department of Geological Sciences, under the supervision of Professor M. A. Peacock.

An examination with a two-circle reflecting goniometer was first made of each of the compounds. Since the crystal faces were in most cases very poor, the morphology was determined graphically with reference to the unit cells later found by *x*-ray measurements. Typical crystals of the three complexes (Figs. 1–3) show the similarity between the copper and nickel complexes of similar formulae.

An investigation of the optical properties of the compounds was made with the polarizing microscope and the universal stage using immersion technique (Table 1).

TABLE 1. CRYSTAL PROPERTIES OF COPPER AND NICKEL COMPLEXES WITH DIETHYLENETRIAMINE

$[\mathrm{Cudn_2}]\mathrm{Cl_2}\cdot\mathrm{H_2O}$

Monoclinic, $P2_1/a$
$a=13.96$, $b=8.80$, $c=13.62$ A, $\beta=102°\ 40'$, Z=4
$a{:}b{:}c=1.586{:}1{:}1.548$ (*x*-ray)
Forms: *c*(001), *a*(100), *m*(110). Habit: tabular *c*
Physical Properties: m.p. 197°. $d=1.459$—1.467 (meas.), 1.460 (calc.)

Optical Properties:	*n*(Na)	
X (light blue): $c=+84°$	1.582 ± 0.001	Positive
Y (purplish blue): $c=-6°$	1.592 ± 0.001	$2V=81\frac{1}{2}°$ (meas.)
Z (dark blue) $=b$	1.607 ± 0.001	$r>v$ perceptible

$[\mathrm{Nidn_2}]\mathrm{Cl_2}\cdot\mathrm{H_2O}$

Monoclinic, $P2_1/a$
$a=13.91$, $b=8.67$, $c=13.50$ A, $\beta=102°\ 15'$, Z=4
$a{:}b{:}c=1.604{:}1{:}1.557$ (*x*-ray)
Forms: *c*(001), *a*(100), *m*(110), *d*(011). Habit: tabular *c*
Physical Properties: m.p. 232°. $d=1.468$ (meas.), 1.478 (calc.)

Optical Properties:	*n*(Na)	
X (reddish): $c=-65°$	1.591 ± 0.001	Positive
Y (purplish): $c=+25°$	1.596 ± 0.001	$2V=89°$ (meas.)
Z (bluish) $=b$	1.601 ± 0.001	Dispersion not perceptible

$[\mathrm{CudnCl}]\mathrm{Cl}\cdot\frac{1}{2}\mathrm{H_2O}$

Monoclinic, $P2/m$
$a=7.32$, $b=10.27$, $c=6.72$ A, $\beta=95°\ 56'$, Z=2
$a{:}b{:}c=0.713{:}1{:}0.654$
Forms: *c*(001), *a*(100), *b*(010), *m*(110), $p(\bar{1}11)$. Habit: prismatic [001]
Physical Properties: m.p. 205° (decomposed). $d=1.633$ (meas.), 1.628 (calc.)

Optical Properties:	*n*(Na)	
X (bluish): $c=-54°$	1.555 ± 0.002	Negative
Y (bluish purple) $=b$	1.600 ± 0.002	$2V=66°$ (meas.)
Z (reddish purple): $c=+36°$	1.625 ± 0.002	$r>v$ perceptible

The unit cell dimensions were found using a Weissenberg camera and copper radiation ($CuK\alpha_1 = 1.5405$ A). In each case rotation and Weissenberg photographs were taken about the *b*-axis and one other direction of the crystal. The space groups were derived from a consideration of the systematically missing reflections on the zero and first layer-line Weissenberg exposures. Table 1 summarizes the observed crystallographic data of the three compounds in the form recently proposed by Peacock (1945, p. 558).

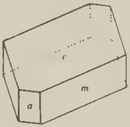

1

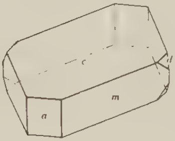

2

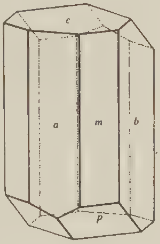

3

FIG. 1. $[Cudn_2]Cl_2 \cdot H_2O$; forms *c* (001), *a* (100), *m* (110).
FIG. 2. $[Nidn_2]Cl_2 \cdot H_2O$; forms *c* (001), *a* (100), *m* (110), *d* (011).
FIG. 3. $[CudnCl]Cl \cdot \frac{1}{2}H_2O$; forms *c*(001), *a* (100), *b* (010), *m* (110), *p* ($\bar{1}11$).

TABLE 2. OBSERVED INTENSITIES AND SPACINGS (A) OF POWDER PATTERNS

$[Cudn_2]Cl_2 \cdot H_2O$				$[Nidn_2]Cl_2 \cdot H_2O$				$[CudnCl]Cl \cdot \frac{1}{2} H_2O$			
I	*d*	*I*	*d*	*I*	*d*	*I*	*d*	*I*	*d*	*I*	*d*
1	8.19	1	2.57	10	7.37	2	2.47	5	8.43	1	2.34
10	7.31	1	2.47	9	6.66	2	2.37	10	7.31	1	2.30
9	6.71	1	2.39	1	6.19	1	2.30	10	6.71	1	2.21
1	6.19	1	2.32	3	5.64	1	2.21	10	5.44	1	2.15
2	5.61	1	2.20	5	5.33	1	2.19	3	5.13	2	2.12
5	5.31	2	2.09	3	4.67	3	2.08	1	4.53	1	2.05
3	4.67	1	2.02	2	4.37	1	2.03	4	4.42	1	1.982
2	4.29			2	4.13	½	2.01	2	4.25		
1	4.15			2	3.90	1	1.941	3	3.63		
1	3.87			2	3.72	½	1.906	1	3.45		
1	3.74			2	3.68	½	1.848	2	3.34		
1	3.66			2	3.45	½	1.762	1	3.20		
1	3.49			3	3.27	1	1.692	8	3.10		
3	3.29			10	3.15	½	1.664	1	3.04		
10	3.15			2	3.02	½	1.634	1	2.94		
1	3.02			3	2.85	½	1.595	1	2.70		
3	2.85			3	2.67	½	1.570	2	2.53		
2	2.68			1	2.56	½	1.441	1	2.43		

Table 2 lists the principal interplanar spacings and visually estimated intensities of the x-ray powder patterns of the three complexes, using filtered copper radiation, CuKα = 1.5418 A.

REFERENCES

Breckenridge, J. G. (1948): Copper (II) and nickel (II) coordination compounds with diethylenetriamine and hydroxyethylethylenediamine—*Can. J. Research*, **26**B, 11–19.

Haendler, H. M. (1942): Copper (II) and nickel (II) complex ions of ethylenetriamine—*J. Am. Chem. Soc.*, **64**, 686–688.

Mann, F. G. (1934): The constitution of complex metallic salts. Part II. The platinum derivatives of β,β'-diaminodiethylamine—*J. Chem. Soc.*, 466–474.

—— & Pope, W. J. (1926): The configuration of the bistriaminopropane metallic complexes—*J. Chem. Soc.*, 2675–2681.

Peacock, M. A. (1945): Determination of crystal form—*Physical methods of organic chemistry*, ed. 1, **1**—New York.

NOTES AND NEWS

MINERAL OCCURRENCES IN WESTERN CANADA

R. M. Thompson
University of British Columbia, Vancouver, B. C.

These notes reporting some of the less common minerals from Western Canada continue the series of notes the last of which appeared in *Am. Mineral.*, **34,** 458, 1949. All identifications were established or confirmed by *x*-ray powder photographs. The writer wishes to thank Dr. H. V. Warren for his assistance in many ways during the course of this work. The following students at the University of British Columbia also assisted in collecting and examining ores: A. C. Taplin, A. E. Aho, A. M. Patterson, A. N. Bahan, W. L. Brown, M. M. Menzies, J. A. Roddick, and P. W. Richardson.

Bismuth. Highet Creek, Mayo District, Y. T. Small rounded yellow oxide coated nuggets with the characteristic pink tinge on a freshly broken surface were found in the heavy minerals from a placer operation on this creek.

Haggart Creek, Mayo District, Y. T. Nuggets similar to the above and up to 10 mm. were found in the heavy sands from the placer operations of Mr. E. Barker.

Bismuthinite. Divided Mineral Claim, extreme head of the Klaza River, near Carmacks, Y. T. Samples of white vein quartz submitted by Mr. G. Dickson show only sparse amounts of a massive gray metallic mineral which proved to be bismuthinite.

Dividend Lakeview Mine, Osoyoos, M. D., B. C. This property is located one mile north of the International Boundary and two miles southwest of the town of Osoyoos. Bismuthinite was noted as a minor constituent of the ore which consists of massive pyrite, pyrrhotite, arsenopyrite, and accessory chalcopyrite, magnetite, tetrahedrite, and gold. Erratic high gold values suggest that tellurides may be present but as yet none has been identified.

Boulangerite. Great Britain Property, Lardeau M. D., B. C. This is one of a number of claims located about 1894 on Sable Creek in the remote Trout Lake district. A specimen donated by Mr. J. M. Turnbull consists of a fine grained somewhat feathery solid compact mass of a silvery gray metallic mineral which gave the combined *x*-ray patterns of boulangerite and galena.

Erickson-Ashby Property, Atlin M. D., B. C. These claims are situated on the north end of Erickson Mountain about 3 miles from the settlement of Tulsequah. Mr. C. S. Ney donated massive sulphides consisting of galena, pyrite, sphalerite, pyrrhotite, arsenopyrite, tetrahedrite, and silvery-gray fibrous masses of boulangerite.

Bournonite. Allco Silver Mines Limited, Revelstoke M. D., B. C. This property is situated at the head of Silver Creek, 20 miles northwest of Revelstoke. Specimens of white quartz with tetrahedrite were examined and bournonite was found to occur as thin selvages on tetrahedrite and galena.

Pelly Creek, Cassiar District, Omineca M. D., B. C. A sample collected by Mr. E. Bronlund from a vuggy quartz vein in the Ingenika Group quartzite on a ridge on the northeast side of Pelly Creek about 5 miles northwest of Pelly Lake, contains disseminated grains of a black metallic mineral which gave the *x*-ray powder pattern of bournonite. Mr. Bronlund believes that there are other occurrences of bournonite in this area.

Galenobismutite. Dublin Gulch, Mayo District, Y. T. This rare mineral was found surrounding a small nugget of gold from the placer workings of Mr. F. Taylor.

Hessite. Hebson Property, Surel Lake, Tweedsmuir Park, Omineca M. D., B. C. Vuggy limonite stained quartz veins up to 14 inches in width occur in greenstone close to a granite contact near the southeast end of Surel Lake. Altaite, hessite, and galena were identified in the field and subsequently confirmed by *x*-ray powder photographs. The above show mutual boundary relationships in polished sections. This property is about 10 miles southeast of the Harrison Group described earlier in these studies and is similar geologically and mineralogically, both being on the eastern contact of the coast range batholith.

Jamesonite. Polaris Taku Mine, Atlin M. D., B. C. This mine is located between elevations of 100 and 1000 feet on the west bank of the Tulsequah River about 6 miles from its confluence with the Taku River. Specimens of milky white quartz calcite vein material show radiating needles of a silvery gray mineral up to 20 mm., in length. Both on these needles and in more compact areas a cleavage perpendicular to the elongation was noticed. This feature suggested jamesonite and the identity of this mineral was confirmed by an *x*-ray powder photograph.

Giant Mine, Yellowknife, N. W. T. Samples donated by Mr. G. Pinsky from the 306 stope of this mine consist of quartz calcite vein material with large compact areas of jamesonite in contact with brown sphalerite and minor amounts of pyrite. Here again the cleavage perpendicular to the elongation of the mineral is well developed.

Joseite A. Highet Creek, Mayo District, Y. T. An examination of the heavy minerals from a placer operation on this creek showed a few small flexible plates of a bismuth telluride (2×2 mm.) which an *x*-ray powder photograph proved to be joseite A (*Am. Mineral.*, **34**, 365, 1949).

Clear Creek, McQuesten District, Y. T. An examination of the heavy minerals from a dredge operating on this creek showed an occasional plate of a bismuth telluride which also proved to be joseite A.

Linnaeite. Shell Property, near Aiken Lake, Omineca M. D., B. C. This property is located in north central British Columbia, about 13 miles north of Aiken Lake. Polished sections from a chalcopyrite vein in andesitic tuffs show corroded crystals of magnetite and pyrite in a groundmass of chalcopyrite which contains small areas (up to 1 mm.) of a pinkish-cream mineral with no relief against chalcopyrite. The mineral is very weakly anisotropic in gray to mauve and negative to all reagents. An x-ray powder photograph places this mineral in the linnaeite group.

Owyheeite. Sherwood Mine, Della Lake, Alberni M. D., Vancounver Island. This property is located on the headwaters of Drinkwater Creek approximately 9 miles by road and trail northwest of the upper end of Great Central Lake. Samples submitted by Dr. D. F. Kidd show somewhat vuggy quartz with bands of dark sphalerite and minor amounts of disseminated galena, tetrahedrite, and needles of arsenopyrite. The vugs are occupied by a capillary mineral which looks like a keg of nails under the binocular microscope. These extremely fine hairs were carefully selected and ground with difficulty. An x-ray powder photograph identified them as owyheeite (*Am. Mineral.*, **34**, 398, 1949), thus making a fourth occurrence of this rare mineral in British Columbia.

Polybasite. Silver Horde Mine, Vernon M.D., B. C. This is one of a number of claims situated on Bromide Mountain between the north and south forks of Cherry Creek some 47 miles east of Vernon. Polished sections of ore show polybasite in microscopic amounts in galena and associated with chalcopyrite, sphalerite, tetrahedrite, silver, pyrite, and magnetite.

Skutterudite. Hazelton View Mine, Omineca M. D., B. C. (O'Neill, *Geol. Sur. Canada*, Mem. **110**, 20, 1919). This mine is on the northwest slope of Rocher Déboulé Mountain, 4 miles south of South Hazelton. The workings are between 5,100 and 6,025 feet. The main vein occupies a strong fault fissure in coarsely crystalline granodiorite and in surrounding sediments (greywacke and garnetiferous argillite) and is reported to contain arsenopyrite, safflorite, loellingite, molybdenite, native gold, chalcopyrite, and probably some electrum or telluride carrying silver.

Samples kindly provided by Mr. Franc Joubin and Mr. W. Holyk, show massive to euhedral crystals of arsenopyrite and skutterudite with much erythrite coating in a gangue of actinolite and quartz. Polished sections show massive to euhedral crystals of cobaltian arsenopyrite with minor amounts of irregular remnants and laths of cobaltian loellingite which appears smooth bluish-white against the somewhat pitted pinkish-white of the former. Skutterudite was determined on the basis of a specific gravity of 6.71, microchemical tests for Co, Fe, and As, and a cell edge of 8.19 kX which is in exact agreement with skutterudite from the Agaunico Mine, Cobalt, Ontario. Skutterudite shows cubic outlines or massive areas with a good polish and a distinct cleavage. It appears to replace both arsenopyrite and loellingite. Chalcopyrite, molybdenite and gold are accessory although locally abundant.

Stannite. Rose Pass Prospect, Ainsworth M. D., B. C. (Rice, *Geol. Surv. Canada*, Mem. **228**, 73, 1941). This prospect and the nearby Humbolt Claim are situated near the summit of Rose Pass close to the Crawford Bay-Rose Pass trail, 5 miles from the end of the Crawford Bay (on Kootenay Lake) road. The deposits consist of quartz veins in closely folded black slates. The principal minerals reported are galena, sphalerite, chalcopyrite, pyrite, and probably stannite or a mineral closely resembling it.

Polished sections of material from the Rose Pass prospect kindly supplied by Dr. H. M. A. Rice show the suspected stannite with its usual microscopic properties, intergrown with sphalerite, chalcopyrite, pyrite and galena. The identity of the stannite was confirmed by comparing the *x*-ray powder photograph with that of stannite from type localities.

Tellurbismuth. Jeep Mine, Bissett, Manitoba. A small hand specimen kindly supplied by Dr. M. H. Frohberg shows somewhat smoky quartz contacting greenstone, with gold embedded in the quartz and along the quartz-greenstone contact in grains up to 3 mm. Gold is also present as a film on one flat surface of the greenstone. A bismuth telluride which proved to be tellurbismuth occurs in the quartz as plates up to 10 mm. and and is closely intergrown with gold. Gold is also visible as very fine films parallel to the eminent cleavage of the tellurbismuth.

Tetradymite. Reno Placer Property, Canadian Creek, Y. T. Mr. A. J. Hadden kindly supplied a number of solid compact nuggets of tetradymite up to $1 \times 1 \times \frac{1}{4}$ inch which were thought to contain values in precious metals. Polished sections show clean areas of tetradymite with much secondary alteration along the cleavage planes. The mineral contains a few small inclusions of a pinkish gray isotropic mineral which proved to be coloradoite. Minor amounts of gold were observed along the cleavage planes of the tetradymite.

Wehrlite. Ajax Claim, Wavell Group, Clinton M. D., B. C. (*Am. Mineral.*, **34**, 458, 1949). Superpanning of limonitic carbonate vein material containing scant sulphides revealed small amounts of a brilliant metallic mineral in the tip which gave the *x*-ray powder pattern of wehrlite (*Am. Mineral.*, **34**, 369, 1949).

Wittichenite. Best Chance, Carlisle, Copper Cliff, and Rabbit's Foot Claims, near Whitehorse, Y.T. Microscopic examination of polished sections from these pyrometasomatic deposits in the Whitehorse Copper Belt show minute stringers and blebs of wittichenite in intimate association with bornite, chalcocite, and chalcopyrite. The occurrence here is similar to that described by Watson from the Maid of Erin Claim in the Rainy Hollow area some 90 miles to the southwest. Very small grains of a mineral tentatively identified as linnaeite by its x-ray powder pattern were observed as inclusions in bornite from both the above mentioned areas.

Wurtzite. Fairview Mine, Osoyoos M.D., B.C. (Cockfield, *Geol. Surv. Canada*, Mem. **179**). This mine is situated about 5 miles northwest of Oliver, B.C. A highway connecting with Similkameen valley and joining the transprovincial highway at Oliver, passes through the camp.

The veins, which occur in partly silicified schist and in granitic rocks, are mainly quartz mineralized with small amounts of pyrite, galena, and sphalerite. The small gold content of these ores is largely associated with the galena and sphalerite and not with the pyrite. The veins are mined for use as a flux at the Trail smelter.

Samples submitted by Mr. G. E. Clayton show galena, pyrite, chalcopyrite, pyrrhotite, dark brown sphalerite and minor amounts of a translucent cinnamon-brown mineral with a resinous lustre, occupying small fractures in milky-white quartz. The galena, pyrite, chalcopyrite, sphalerite, and pyrrhotite are readily visible by eye and occur in veinlets and patches up to 10 mm. and sometimes larger. The cinnamon-brown mineral occurs as very thin films and anhedral grains which occasionally reach 1 mm. in size.

In polished section this mineral is grey in colour with strong reddish-brown internal reflection. It fills minute fractures in quartz and is rarely seen in contact with other sulphides. An insufficient number of sections were examined to determine its paragenetic relationships. No evidence was found to indicate that sphalerite was altering to wurtzite. An x-ray powder photograph identified this mineral as wurtzite whose cell dimensions, $a=3.91$, $c=6.39$ kX, differ somewhat from those of Fuller in Dana (1944, 227). This is believed to be the first authenticated occurrence of this mineral in British Columbia.

THE PROBABLE NON-EXISTENCE OF ALASKAITE

R. M. Thompson
University of British Columbia, Vancouver, B. C.

Alaskaite of Koenig (*Am. Phil. Soc.*, **19**, 472, 881) is an ill-defined sulphide of Pb, Ag, and Cu, which was classed as a silver-bearing variety of galenobismutite in Dana (1892) but was revived as a distinct species with the uncertain composition $PbS \cdot (Ag,Cu)_2S \cdot 2Bi_2S_3$ in Dana (1944). The mineral is described as massive, compact or foliated, with cleavage in one (or two) directions; brittle; $H=2$ (or $3\frac{1}{2}$); $G=6.8$ (or 6.2); metallic, gray (with bronzy tarnish?); white in polished section, distinctly anisotropic. Further details are given in Dana (1944). To test the individuality of this substance the following five specimens, including three from the type locality, were examined with the aid of polished sections; the identities of all the minerals noted below were confirmed by *x*-ray powder photographs.

1. Alaskaite, Alaska vein, Poughkeepsie Gulch, San Juan Co., Colorado (UT E2942).
2. Alaskaite, Poughkeepsie Gulch, San Juan Co., Colorado (R. E. MacKay, No. 387).
3. Alaskaite, Alaska Mine, Silverton, Colorado (HMM 80239).
4. Alaskaite, 75 km SSW. of Esmoraca, Bolivia (HMM, Ahlfeld).
5. Alaskaite, Cerro Bonete, Bolivia (ROM M21003).

Materials 1 and 5 were kindly loaned by Dr. V. B. Meen of the Royal Ontario Museum; 3, 4, from the Harvard Mineralogical Museum, were obtained from Dr. Frondel through the courtesy of Dr. M. A. Peacock; Mr. R. E. MacKay of Seattle kindly supplied no. 2.

Material 1 is a small hand specimen showing pyrite and a gray metallic mineral embedded in a gangue of dark quartz and pink feldspar. A polished section shows large areas of a grayish-white anisotropic mineral (matildite) intergrown in part with a creamy-white strongly anisotropic mineral (aikinite). These areas are traversed by small stringers of sphalerite and chalcopyrite. Subhedral crystals of pyrite corroded by chalcopyrite occur free from the intergrowth.

Material 2 is a single specimen, 4×3 in., of massive dark quartz coated with limonite and containing appreciable sulphides. A broken surface shows masses of a gray-black lustrous mineral and disseminated pyrite. An *x*-ray powder photograph of the dark mineral proved it to be a mixture of tetrahedrite and galena. Several polished sections were made which showed the above minerals in intimate association together with an occasional lath of a white anisotropic mineral which gave an *x*-ray powder pattern identical with that of aikinite from the type locality.

Material 3 is a piece of white vuggy quartz, $1 \times \frac{1}{2}$ in., with disseminated patches and streaks of a mineral resembling tetrahedrite, and minor amounts of chalcopyrite. A polished section shows large irregular areas of tetrahedrite with inclusions of chalcopyrite. Larger areas of chalcopyrite contain corroded crystals of pyrite. Tetrahedrite appears to be contemporaneous with chalcopyrite.

In polished section, the Ahlfeld specimen, material 4, shows abundant coarse laths of bismuthinite, contacting and intergrown with bent, twisted, and shredded laths of franckeite. Sphalerite, with small lath-like inclusions of a weakly anisotropic tan coloured mineral, possibly stannite, and finely disseminated chalcopyrite are accessory. Apparently this specimen is not typical of the Bolivian occurrence.

The specimen from Cerro Bonete, Bolivia, material 5, is a compact mass of silvery-gray ore, $2\times1\times1$ in., lacking visible cleavage and coated with a partial film of limonite. Polished sections show a homogeneous white mineral with distinct twinning, weak pleochroism in cream to gray, and strong anisotropism in yellowing-white, blue, green, and brown. The microscopic properties and an *x*-ray powder photograph of this material are identical with those of benjaminite from the type locality, Round Mountain, Nye County, Nevada.

These observations suggest that previous workers were dealing with non-homogeneous material which consisted of such minerals as matildite, aikinite, benajminite, tetrahedrite, with chalcopyrite, sphalerite, pyrite, and galena. An intergrowth of matildite ($Ag_2S\cdot Bi_2S_3$) and aikinite ($2PbS\cdot Cu_2S\cdot Bi_2S_3$) roughly accounts for the composition and physical properties of the original material from Colorado, while the properties of benjaminite $Pb(Cu,Ag)Bi_2S_4$(?), which gives a distinctive *x*-ray powder pattern, agree reasonably with those of the reported alaskaite from Bolivia. Unless others can support the individuality of typical alaskaite from Colorado by microscopic and *x*-ray observations, the above notes must lead to the disqualification of this supposed species.

HYDROCARBON WITH CINNABAR IN BRITISH COLUMBIA

K. DeP. Watson
University of British Columbia, Vancouver, B.C.

Hydrocarbons, although occurring as minor constituents in many mercury deposits in various parts of the world (Halse, *Imp. Inst.*, Monog. Min. Res., 40–90, 1923; Ross, *Econ. Geol.*, **37**, 453, 1942), have been recorded from only one deposit in British Columbia (Cairnes, *Geol. Surv. Canada*, pap. **43–15**, 37, 1943) and have not been described. This note describes an occurrence of hydrocarbon with cinnabar observed by the writer at the Phillips' prospect near the Manitou mercury mine in the Tyaughton Lake Area of southwestern British Columbia.

Phillips' main cinnabar showing, described by Stevenson (*B.C. Dept. Mines*, Bull. **5**, 84, 1940) and by Cairnes (1943), is exposed in a large open cut on the eastern side of Tyaughton Creek valley about one-half mile south of Mercury Creek. The deposit occurs in rocks of the Fergusson Group of pre-Upper Triassic age, consisting mainly of chert, argillite, and greenstone. The eastern contact of a large body of serpentine and carbonatized serpentine lies about 250 feet west of the deposit. In the vicinity, small bodies of feldspar porphyry of probable Tertiary age intrude the serpentine and the rocks of the Fergusson Group.

The open cut exposes mineralized greenstone which dips eastward at 60 degrees, flanked on its hanging wall by highly contorted argillite and ribbon-chert. The greenstone is a rusty weathering, slightly amygdaloidal rock consisting of fine-grained ferruginous carbonate, albite, chlorite, and iron ores. The cinnabar occurs disseminated in this rock in places, in small calcite amygdules, and in irregular veinlets composed mainly of white calcite and smaller amounts of grey quartz, black hydrocarbon, and sericite cutting the greenstone. These veinlets range from 1 to 5 mm. wide and are generally crustified with calcite margins and quartz centers. Hydrocarbon occurs in places within these quartz centers as lenses that reach a maximum width of 4 mm. and a length of 20 mm.

The hydrocarbon is a very brittle, jet-black substance with a brilliant vitreous lustre and a perfect conchoidal fracture. Its hardness is approximately 3 and its specific gravity, determined from three samples, ranges from 1.364 to 1.398 and averages 1.376. The substance does not soften when heated in air, but ignites and loses more than 95% of its weight. A spectrographic analysis made with graphite electrodes, which of course could not detect C, H, or O, revealed no other major constituents and only traces of Si, Mg, Fe, Al, Ca, and Cu.

The crustification shows that the calcite, accompanied by cinnabar in places, was deposited early and was followed by quartz and then by hydrocarbon. It was seen microscopically that deposition of most of the sericite occurred after most of the quartz and before most of the hydrocarbon. It was also seen microscopically that slight overlap in deposition of calcite and quartz, of quartz and sericite, and of hydrocarbon and quartz had occurred and that minute amounts of quartz, cinnabar, calcite and sericite had been deposited in lunate contraction fractures in the hydrocarbon.

The widespread occurrence of bitumens as minor constituents of cinnabar deposits presents a problem. According to Schuette (*T.A.I.M.M.E.*, 410, 1931):

> "Generally, where bitumen is found in a quicksilver mine the underlying rocks are sedimentaries containing organic matter. Heat developed in these rocks by proximity of the mineralizing magma, by the strain attendant on fissuring or by the hot ascending ore-bearing solutions, no doubt initiates distillation and stimulates migration of organic bituminous matter. This ascends in the same fissure with the ore-bearing solutions and is trapped and deposited in the same horizon as the cinnabar."

Ross (*Econ. Geol.*, **36**, 140, 1941), however, considers this to be unsatisfactory as a general explanation. He has observed that:

> "In the Terlingua region bituminous material is perceptible only within the lodes and is almost everywhere present irrespective of the character or stratigraphic position of the wall rocks."

Although information pertinent to the problem of the genesis of hydrocarbon in Phillips' mercury deposit is meagre, it seems to favor Schuette's hypothesis. The black argillite of the Fergusson Group at the deposit, at the adjacent Manitou mine where Cairnes (1943) noted "a little unidentified hydrocarbon mineral" and at other places in the region, is distinctly carbonaceous (Cairnes, *Geol. Surv. Canada, Mem.* **213,** 10, 1937; Stevenson, 79, 1940). Moreover, it may be significant that methane issues from drill holes in some gold mines in the vicinity of Fergusson Group sediments in the nearby Bridge River Area.

RED GOLD FROM THE SAN ANTONIO GOLD MINE, BISSETT, MANITOBA

R. B. Ferguson
University of Manitoba, Winnipeg, Canada

Two specimens of quartz-carbonate-sulphide ore submitted to the author by Mr. J. Gordon Bragg, assistant geologist of the San Antonio Gold Mine, Bissett, Manitoba, contain splotches of a coppery-red metallic mineral which, except for its colour, resembles gold; in one of the specimens, typical yellow gold is very close to the red metal. In both specimens the metals are in contact with or closely adjacent to pyrite and less abundant chalcopyrite. The mine geologists concluded from the colour alone that the red metal is cuprian gold. With the idea of checking this conclusion and, if it proved correct, of determining the approximate Au:Cu ratio, the author took x-ray powder photographs of a few small fragments of the red mineral from both specimens and of the yellow gold from the one specimen. During preparation of the powder samples, the unexpected observation was made under the binocular microscope that the red metal is red only on the surface; a gouge with the needle shows that the interior is golden yellow. A cursory search of the literature brought to light no previous description of a red-coated native gold, and therefore attempts were made to discover the nature of the present material.

Since the red surface coating is very thin, it is impossible to select it alone for x-ray or other analysis, and consequently the two above-mentioned powder samples of the red mineral consisted of the red coating with, of necessity, a much larger proportion of the yellow interior. The x-ray powder patterns of all three samples, the two red-surfaced metals and the all-yellow one, are identical with that of pure gold and with each other. Thus all three metals consist essentially of gold. A closer examination of the powder patterns of the red gold showed no additional lines which might have helped in identifying the red coating. Nor was a polished section of any assistance: no rims could be discovered around the gold, all of which appeared typically yellow. Etch tests of the red gold in the hand specimens were then made using the standard $FeCl_3$ and $HgCl_2$ etching solutions, but both gave negative results. Finally, spectrographic analyses were carried out on fragments of both the red and the yellow gold which had been picked visibly free from sulphides. These analyses were kindly carried out by Dr. Wm. Leach, Professor of Botany and Chairman of the Department in this University. The yellow gold spectrum showed prominent Au, Ag, Cu, and Fe, and the red gold spectrum prominent Au, Ag, and Cu but no Fe.

These results suggest that the yellow gold sample, containing both Cu and Fe, was contaminated by chalcopyrite although the presence of one or both of these elements within the gold is not entirely impossible. In the case of the red gold, however, the absence of Fe is proof that no chalcopyrite was present in the sample, and that the Cu must be a part of the red gold. The logical conclusion is that the Cu makes up the red coating, either as the more or less pure metal or, because of the negative etch tests, more likely as a Cu-Au alloy. Such a coating must be very thin since its quantity in the x-ray samples was less than the method can detect.

If, as the results indicate, the red coating is copper or Cu-Au, why its unusual occurrence on yellow gold? Perhaps the copper has been "naturally electroplated" on the gold as a result of some electrochemical action occurring in the crystallizing solution at the time of deposition. Whatever the explanation, the existence of copper-plated gold is unusual, and especially so when it occurs as it does in places, within millimetres of ordinary yellow gold.

WALKER MINERALOGICAL CLUB*

OFFICERS 1949

Honorary President, A. L. Parsons, *President,* M. H. Frohberg, *Past President,* G. E. Steel, *Secretary-Treasurer,* W. M. Tovell, *Editor,* M. A. Peacock, *Councillors,* F. Ebbutt, R. B. Ferguson, I. H. Milne, E. W. Nuffield, L. G. Smith.

ABSTRACT OF PROCEEDINGS, 1949

February 10, 1949. Dr. V. B. Meen, Associate Director, Royal Ontario Museum of Geology and Mineralogy, addressed the Club on the subject "Fundy's Minerals." Dr. Meen described and illustrated with specimens and coloured slides mineral occurrences of Nova Scotia, emphasizing the zeolite localities where he collected along the shores of the Bay of Fundy. Two specimens of stilbite from Nova Scotia were offered as door prizes.

April 21, 1949. Dr. F. G. Smith, Assistant Professor in the Department of Geological Sciences, University of Toronto, spoke to the Club on the subject "Determining the Temperature of Mineral Formation." The talk was illustrated by experiments devised in collaboration with P. A. Peach. Following Dr. Smith's address, W. H. Gross, G. D. Springer, H. S. Scott, and L. G. Phelan spoke briefly on the application of the temperature of mineral formation to the solution of particular geological and mineralogical problems.

September 30–October 2, 1949. On the occasion of the annual mineral collecting trip, the Club met at Drag Lake Lodge, Haliburton County, Ontario. Dr. V. B. Meen and Mr. G. E. Steel acted as guides. The highlight of the trip was the visit to the Fission Mines property at Wilberforce, where good specimens of uraninite, apatite, fluorite and calcite were obtained. At other localities, serpentine, wilsonite, tremolite, peristerite, and cancrinite were collected.

December 8, 1949. Mr. F. Ebbutt spoke to the Club on the subject "Some Mineral Caves in Conjunction with the Lead Mines of Chihuahua, Mexico." Before describing the various minerals and their genesis, Mr. Ebbutt reviewed the mining history of the area, and described the occurrence and formation of the caves. The talk was illustrated with coloured slides, and many fine specimens collected by the speaker were on display.

The Council of the Walker Club wishes to acknowledge the courtesy of the Council of the Mineralogical Society of America in again making possible the publication of a Canadian number of *The American Mineralogist.*

Walter M. Tovell
Secretary-Treasurer

---

* Founded in 1938 and named in honour of the late Professor T. L. Walker (1867–1942), then Professor Emeritus of Mineralogy and Petrography in the University of Toronto and Director of the Royal Ontario Museum of Mineralogy. The by-laws of the Club were published in *Am. Mineral.,* **34,** 469, 1949.

CIPEA NO. 2

FOUTH INTERNATIONAL CONGRESS OF SOIL SCIENCE

This Congress is to be held in Amsterdam on July 24 to August 1, 1950, with a post-Congress excursion (15 days) through Holland and Belgium. The programme includes a "Section of Clay Minerals" with the following subjects for discussion:

		Invited:
General lecture:	The Electrochemistry of clay minerals in relation to pedology	Prof. Dr. C. E. Marshall
Subjects:	1. The structure of clay minerals	Dr. G. W. Brindley
	2. Genesis and synthesis of clay minerals and their mutual transformation	(Prof. Dr. I. D. Sedletzky)
	3. a) Interstratified clay minerals	Dr. W. F. Bradley
	b) Influence of shape and interstratification on *X*-ray diagrams of clay minerals	Prof. J. Mering
	4. Differential thermal analysis of clay minerals	R. C. Mackenzie
	5. Crystal structure and ion exchange	(Dr. S. B. Hendricks)
	6. Solvation of clay minerals in relation of crystal structure	Dr. D. M. C. MacEwan

In addition to the "Section of Clay Minerals" the following subject occurs under the heading of "Section of Soil Chemistry":

"2. Determination of Exchange Capacity and Exchangeable Ions
a) Clay minerals in Soils."

There is also to be a meeting of an informal group on the "Technology of Clay Minerals," with the following provisional programme:

General lecture: General review of the technology of clay minerals by Dr. R. E. Grim.
Subjects: Fixation of organic matter on clay minerals

Changes which occur on heating clays
Changes which occur on firing clay minerals
Clay minerals as catalysts.

Members wishing to contribute papers should contact Dr. Favejee (Geological Laboratory, Duivendaalse laan 2, Wageningen, Holland).

THIS INFORMAL MEETING ONLY will be open to all members without the necessity of paying the Congress Fee. Members wishing to attend the "Section of clay Minerals" and/or any other Section of the Congress will be required to pay their Congress Fee.

The Congress Fee is 15 U.S. dollars or its equivalent in Dutch guilders for a member; 4 U.S. dollars or its equivalent for an accompanying relative. Prospective members are requested to pay this fee by obtaining through a bank and by remitting to the Amsterdamsche Bank in The Hague (Netherlands) in favour of the Treasurer of the Organising Committee of the Fourth Intern. Congress of Soil Science, a draft made payable to the Amsterdamsche Bank in The Hague.

Further details regarding accommodation etc., may be secured from Dr. P. A. Rowan, Secretary of the Organising Committee of the Fourth Congress of Soil Science, 3 van Hallstraat, Groningen (Netherlands).